

# Modeling a Semi-Submersible Floating Offshore Wind Turbine With Tuned Inerter Dampers Within the Platform

Ryan Okuda

Thesis submitted to the Faculty of the  
Virginia Polytechnic Institute and State University  
in partial fulfillment of the requirements for the degree of

Masters of Science  
in  
Mechanical Engineering

Lei Zuo, Chair  
Corina Sandu  
Biao Fang

May 5, 2023  
Blacksburg, Virginia

Keywords: Offshore Wind, Vibration Absorber, Energy Harvesting

Copyright 2023, Ryan Okuda

# Modeling a Semi-Submersible Floating Offshore Wind Turbine With Tuned Inerter Dampers Within the Platform

Ryan Okuda

(ABSTRACT)

With growing awareness of climate change and an increased interest in renewable energy, resources like offshore wind are projected to grow in the near future. One key issue within offshore wind is how to stabilize the floating system when it experiences large wind and wave forces that impact its performance and shorten its operating life. Researchers have been exploring structural control methods and creating modeling tools to evaluate the performance of the control methods. One such tool is OpenFAST, the industry standard for modeling wind turbine dynamics, and the goal of this paper is to build upon the existing capabilities of OpenFAST. Inerter-based structural control methods offer arguably better performance than traditional vibration absorbers, and the configuration proposed in this paper also offers the ability to use a generator as an element in the structural controller. This allows extra energy to be generated along with the improvement in vibration absorption. Through this study, this inerter-based control method is explored through the lens of an established modeling tool to provide the validation for the model to explore which load cases the inerter performs best in and what design considerations must be made. In addition, the energy harvesting potential of the inerter system is evaluated and shown to increase the system's capabilities especially under stormy ocean conditions.

# Modeling a Semi-Submersible Floating Offshore Wind Turbine With Tuned Inerter Dampers Within the Platform

Ryan Okuda

(GENERAL AUDIENCE ABSTRACT)

With growing awareness of climate change and an increased interest in renewable energy, resources like offshore wind are projected to grow in the near future. One key issue within offshore wind is how to stabilize the floating system when it experiences large wind and wave forces which impact its performance and shorten its lifespan. Researchers have been exploring several methods and creating modeling tools to evaluate the performance of control methods. One such tool is OpenFAST, the industry standard for modeling wind turbine dynamics, and the goal of this paper is to build upon the existing capabilities of OpenFAST. Structural control methods based on an element called an inerter offer arguably better performance than traditional vibration absorbers. The design in this paper also offers the ability to use an electrical generator as an element in the structural controller. This allows extra energy to be generated along with the reduced vibrations. Through this study, this inerter-based control method is explored through the lens of an established modeling tool to provide validation for the model. Another goal is to explore which scenarios the inerter performs best and what design considerations must be made for future development. In addition, the energy harvesting potential of the inerter system is evaluated and shown to increase the system's capabilities.

# Dedication

*This work is dedicated to my family, friends, colleagues, and mentors who believed in me and supported me through the toughest of times. Also, to Virginia Tech, Let's Go! Hokies!*

# Acknowledgments

This work was completed with the support of the New York State Energy Research and Development Authority (NYSERDA) and the National Offshore Wind Research and Development Consortium (NOWRDC). This material is based upon work supported by the U.S. Department of Energy's Office of Energy Efficiency and Renewable Energy (EERE) under the Wind Energy Technologies Office Award Number DE-EE0008390.

# Contents

- List of Figures ix
  
- List of Tables xiii
  
- 1 Introduction 1**
  
- 2 Background 4**
  - 2.1 Floating Offshore Wind Turbines . . . . . 4
  - 2.2 Fatigue Life of Floating Offshore Wind Systems . . . . . 8
  - 2.3 Vibration Absorbers . . . . . 9
    - 2.3.1 Tuned Liquid Column Dampers . . . . . 9
    - 2.3.2 Tuned Mass Dampers . . . . . 10
    - 2.3.3 Tuned Inerter Dampers . . . . . 11
  - 2.4 Hybrid Energy Harvesting Systems . . . . . 13
  - 2.5 Modling FOWTs with Vibration Absorbers . . . . . 15
  - 2.6 Tuned Mass Dampers in OpenFAST . . . . . 16
    - 2.6.1 Defining the Coordinate System, Position, Velocity, and Acceleration 17
    - 2.6.2 Developing the Equations of Motion for the Tuned Mass Damper . . 20
    - 2.6.3 State Space Approach to Modeling The Tuned Mass Damper . . . . 22

<b>3</b>	<b>System Modeling</b>	<b>26</b>
3.1	Equations of Motion for Tuned Inerter Damper . . . . .	26
3.2	Programming the Tuned Inerter Damper in OpenFAST . . . . .	30
3.2.1	Modifications to StrucCtrl.f90 . . . . .	31
3.2.2	Modification to ServoDyn.f90 . . . . .	32
3.2.3	Modifications to StrucCtrl_Registry.txt . . . . .	33
3.2.4	Modifications to ServoDyn_IO.f90 . . . . .	33
3.3	Tuned Inerter Damper Parametric Study . . . . .	34
3.4	Evaluating Energy Harvesting Potential of the TID . . . . .	35
<b>4</b>	<b>Results &amp; Discussion</b>	<b>36</b>
4.1	Model Validation . . . . .	39
4.2	Tuned Inerter Damper Parametric Study . . . . .	42
4.2.1	Pitch Free Decay . . . . .	42
4.2.2	JONSWAP Wave Spectrum . . . . .	43
4.3	Pitch Free Decay Tests . . . . .	47
4.4	Wave Only Tests . . . . .	48
4.5	Wave and Wind Tests . . . . .	53
4.6	Energy Harvesting Potential of the Tuned Inerter Damper . . . . .	54
<b>5</b>	<b>Conclusions &amp; Future Work</b>	<b>58</b>

<b>Bibliography</b>	<b>61</b>
<b>Appendices</b>	<b>68</b>
<b>Appendix A OpenFAST Input Files</b>	<b>69</b>
A.1 Main OpenFAST Input File . . . . .	69
A.2 StC Input File . . . . .	72
A.3 ServoDyn Input File . . . . .	76
A.4 Elastodyn Input File . . . . .	82
A.5 HydroDyn Input File . . . . .	87
<b>Appendix B OpenFAST Modified Subroutines</b>	<b>97</b>
B.1 Calc_Output . . . . .	97
B.2 Calc_ConstStateDerivative . . . . .	98
B.3 SrvD_Init_Jacobian . . . . .	99

# List of Figures

- 2.1 Wind resource map of the United States with average annual wind speeds at a height of 100 meters above surface level [1]. . . . . 5
- 2.2 The three most popular types of platforms for FOWTs: Spar (left), Semisubmersible (middle), and Tension Leg Platform (Right) [2]. . . . . 6
- 2.3 Stability triangle demonstrating the method used by each of the three platform types to stabilize the wind turbine system [3]. . . . . 7
- 2.4 The global market share for each floating substructure both installed and announced [4]. . . . . 7
- 2.5 Diagram of a U-shaped Tuned Liquid Column Damper [5]. . . . . 10
- 2.6 Diagram of a Tuned Mass Damper with mass,  $m$ , spring stiffness,  $k$ , and damping coefficient,  $c$ . . . . . 11
- 2.7 Several concepts for inerters that could be used in TIDs [6]. . . . . 12
- 2.8 Comparison between TID configurations (IDVA in this figure) and a TMD (Spring-damper DVA) [6]. . . . . 12
- 2.9 Frequency domain results of tower side to side displacement of simulation with no control, a TMD, and a TID (called an RIDTMD in this study) [7]. . . . . 13
- 2.10 WindWaveFloat configurations: a.) Base case, b.) Oscillating water column, c.) Sphere point absorber, d.) Oscillating wave surge converter [8]. . . . . 14
- 2.11 Diagram of the OpenFAST modular framework [9]. . . . . 17

2.12	Diagram of the body-fixed reference frames and position vectors used to define the TMD position in OpenFAST. . . . .	18
3.1	Diagram of the Tuned Inerter Damper being studied. The parameters of the system (masses, spring stiffness, and damping coefficients) labeled. . . . .	27
3.2	Flowchart of the process to modify "StrucCtrl.f90." . . . . .	32
3.3	Flowchart of the process to modify "ServoDyn.f90." . . . . .	33
4.1	Diagram of the OC4 semisubmersible floating system used as the reference model for this study [10]. . . . .	37
4.2	Diagram of the semisubmersible platform for the DeepCwind platform used in the OC4 analysis [10]. . . . .	37
4.3	Comparison between OpenFAST results when the added mass from the absorber is and is not offset in the ballast water levels. . . . .	38
4.4	Time-domain data from OpenFAST for a pitch free decay test to display the settling position discrepancy. . . . .	39
4.5	Time domain results for the heave free decay test at an 8% mass ratio. . . . .	40
4.6	Frequency domain results for the heave free decay test at an 8% mass ratio. . . . .	41
4.7	Time domain results for the pitch free decay test at an 8% mass ratio. . . . .	41
4.8	Frequency domain results for the pitch free decay test at an 8% mass ratio. . . . .	42
4.9	RMS pitch values as a function of the stiffness and damping values in the TMD for a 2% mass ratio . . . . .	44

4.10	RMS pitch values as a function of the stiffness and damping values in the TMD for a 5% mass ratio. . . . .	44
4.11	RMS pitch values as a function of the stiffness and damping values in the TMD for an 8% mass ratio. . . . .	45
4.12	RMS pitch values as a function of the stiffness and damping values in the TID for a 2% mass ratio . . . . .	45
4.13	RMS pitch values as a function of the stiffness and damping values in the TID for a 5% mass ratio. . . . .	46
4.14	RMS pitch values as a function of the stiffness and damping values in the TID for an 8% mass ratio. . . . .	46
4.15	Time domain results for the 2 percent mass ratio case for the TMD and TID compared to the baseline free decay test. . . . .	48
4.16	Time domain results for the 5 percent mass ratio case for the TMD and TID compared to the baseline free decay test. . . . .	49
4.17	Time domain results for the 8 percent mass ratio case for the TMD and TID compared to the baseline free decay test. . . . .	49
4.18	Frequency domain results for the 2 percent mass ratio case for the baseline, TMD, and TID free decay test. . . . .	50
4.19	Frequency domain results for the 5 percent mass ratio case for the baseline, TMD, and TID free decay test. . . . .	50
4.20	Frequency domain results for the 8 percent mass ratio case for the baseline, TMD, and TID free decay test. . . . .	51

4.21	Time domain results for the baseline, TMD, and TID using a mass ratio of 3% with a JONSWAP wave with a period of 10 seconds and height of 3 meters.	52
4.22	Frequency domain results for the baseline, TMD, and TID using a mass ratio of 3% with a JONSWAP wave with a period of 10 seconds and height of 3 meters. . . . .	52
4.23	Diagram of the wind and wave alignment approach used. . . . .	54
4.24	Time domain results for the baseline, TMD, and TID using a mass ratio of 3% with a JONSWAP wave with a period of 10 seconds and height of 3 meters and a 9 meter per second wind input with an angle of incidence of 0 degrees.	55
4.25	Time domain results for the baseline, TMD, and TID using a mass ratio of 3% with a JONSWAP wave with a period of 10 seconds and height of 3 meters and a 9 meter per second wind input with an angle of incidence of 30 degrees.	55
4.26	Velocity plot of the primary (m) mass in the TID in column 1 of the platform with a JONSWAP wave input of 10 s and 3 m. . . . .	56
4.27	Velocity plot of the secondary (b) mass in the TID in column 1 of the platform with a JONSWAP wave input of 10 s and 3 m. . . . .	57

# List of Tables

2.1	LCOEs of mutlipte types of wind turbines [11]. . . . .	8
2.2	Overview of aero-servo-hydro-elastic numerical models for FOWTs with their capabilities [12]. . . . .	15
2.3	Definitions of the terms on the right hand side of Eq. 2.6. . . . .	20
3.1	Initial conditions for the parametric study of the TID parameters to minimize RMS pitch motion. . . . .	34
4.1	Optimized values from the parametric study to minimize the impact of pitch motion for the pitch free decay test. . . . .	43
4.2	Optimized values from the parametric study to minimize the impact of pitch motion for the JONSWAP wave spectrum. . . . .	47
4.3	Final results for pitch free decay test. . . . .	53

# List of Abbreviations

FEM Finite Element Methods

FOWT Floating Offshore Wind Turbine

HAWT Horizontal Axis Wind Turbine

LCOE Levelized Cost of Energy/Electricity

NOWRDC National Offshore Wind Research and Design Consortium

NREL National Renewable Energy Laboratory

NYSERDA New York State Energy Research and Development Authority

RMS Root Mean Squared

StC Structural Control

TID Tuned Inerter Damper

TLCD Tuned Liquid Column Damper

TMD Tuned Mass Damper

VAWT Vertical Axis Wind Turbine

# Chapter 1

## Introduction

As the world moves towards more sustainable and renewable energy sources, it is important to ensure that these sources still compete with traditional fossil fuel energy sources. Renewable energy technologies are beginning to mature to a point where they are becoming viable options for energy harvesting. Sources like wind and solar energy seem especially popular. Other methods of generating electricity will still need to fill the gaps in energy generation. One promising option is in floating offshore wind turbines (FOWTs). The United States is estimated to have a wind energy pipeline of 40,083 MW of capacity with the advancement of many offshore projects in 2022 [4].

Offshore wind consists of turbines located off of the coast of major lakes and oceans. These systems can take advantage of the higher wind speeds that occur over bodies of water as convective currents create consistently higher wind speeds than many onshore locations [1]. These systems are also attractive because most of the world's population lives near coastlines. This reduces the cost and electricity losses associated with transmitting electricity long distances.

One important issue that FOWTs are facing has to do with the large wind and wave loads they experience. Since FOWTs tend to be in deeper waters that are further offshore, the wind speeds and waves are much larger than what nearshore turbines face. In addition, their location makes it more difficult and more expensive to perform maintenance and repairs on these systems. Therefore, it is important to reduce the frequency of necessary repairs and

required maintenance on the system [13]. One option to address this is using some form of vibration absorber to minimize the system oscillations and, therefore, the system fatigue.

Several models have been developed to model the dynamics of wind turbines [12] and an important function of these models is to estimate the loads acting on the turbines. Some models are incorporating vibration absorbers. Vibration absorbers are well-studied in the civil engineering space as methods for reducing motion in tall buildings [14, 15]. These methods for controlling vibrations are now being studied for application to FOWTs [6, 7, 9, 16, 17]. One interesting concept for vibration absorbers is inerter-based absorbers. These types of systems seem to outperform more traditional vibration absorbers [6] and they present a unique opportunity in real-world application. A real world element that mimics an inerter well is an electric generator. If an inerter-based absorber were installed using a generator as one of its elements, then a portion of the energy dissipated by the absorber would be converted to electricity. Depending on the size of the electrical output, it could have several uses including supplementing electricity output of the turbine and operating active control systems onboard the turbine.

This paper details the process of integrating new design capabilities into the well-renowned software OpenFAST to model an inerter-based vibration absorber. Section 2 details the existing knowledge in the fields of floating offshore wind turbines, fatigue analysis of wind turbines, several types of vibration absorbers, hybrid energy harvesters, modeling floating wind turbines, and the existing theory behind modeling tuned mass dampers in OpenFAST. Section 3 details the theory being applied to the existing OpenFAST framework to allow it to model an inerter-based vibration absorber, the process of modifying the existing code, and a parametric study to optimize the performance of the inerter-based absorber in reducing platform motion as well as how the energy harvesting potential of the inerter-based absorber was evaluated. Section 4 discusses the results of running the code to validate the performance

of the new capabilities, the final results of the parametric study, free decay simulations in the pitch direction, results from simulations with wind and wave conditions, and the results of evaluating the energy harvesting potential of the system. Lastly, Section 5 details the conclusions of this work and presents options for future work on this matter.

# Chapter 2

## Background

### 2.1 Floating Offshore Wind Turbines

Offshore wind offers a unique opportunity for energy harvesting on a large-scale. Moving turbines onto the ocean removes real-estate restrictions that land-based turbines face and it harnesses the higher average wind speeds that occur out at sea. Fig. 2.1 displays a map of the average wind speeds in the United States both on land and at sea [1]. In addition, in many countries, the majority of the population is located near coastlines, so it benefits consumers to have wind resources closer to the coasts as it reduces costs and energy losses associated with transmitting the electricity long distances. When discussing offshore wind, there are several types of substructures depending on the depth of water where the turbine will be located. Near the shore, most turbines have substructures built into the sediment. However, in water depth greater than 50 meters, fixed-bottom substructures are not longer economically viable and floating substructures become more popular [13].

Floating offshore wind systems can be categorized by the type of substructure that they employ as shown in Fig. 2.2 [2]. Each type of substructure has its own approach to stabilizing the turbine as shown in Fig. 2.3 [3]. Spar platforms operate by primarily using the weight of the ballast water located in the platform to provide a counteracting moment to the mass of the turbine. The long, vertical substructure contains the ballast water and allows the system to have a good resistance to roll and pitch motion. The semisubmersible platform

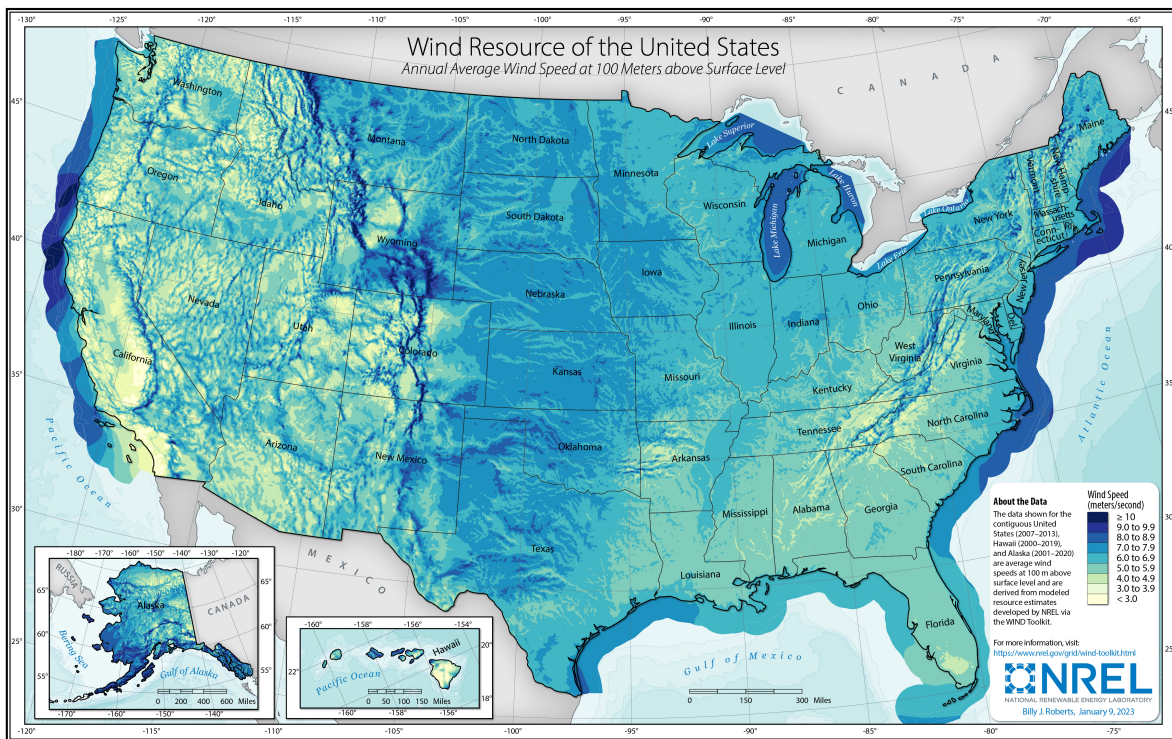


Figure 2.1: Wind resource map of the United States with average annual wind speeds at a height of 100 meters above surface level [1].

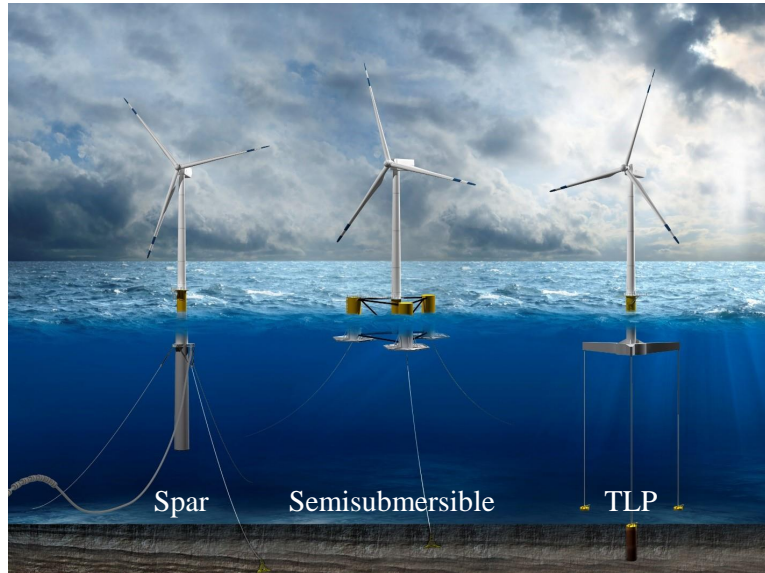


Figure 2.2: The three most popular types of platforms for FOWTs: Spar (left), Semisubmersible (middle), and Tension Leg Platform (Right) [2].

has a shallow draft but a large water plane area which allows it to counteract motion using the surface tension of the water. This type of substructure does tend to be more sensitive to wave-induced motion. Lastly, the tension leg platform stabilizes the platform by using mooring lines under constant tension instead of the traditional catenary approach [18, 19]. In addition, these stabilization approaches also play a role in which substructures are more popular. As shown in Fig. 2.4, the semisubmersible platform is the preferred substructure. This is attributed to the shallow draft and high hydrodynamic stability which allows the system to be assembled nearshore and towed to the site [4].

Currently, a major drawback to offshore wind energy is the high levelized cost of energy (LCOE). This is due to a high capital and operational expense compared to other forms of renewable energy. The substructure of an offshore wind system accounts for approximately 13% of the capital expense for a fixed-bottom offshore wind turbine and 37.5% for a FOWT [11]. Table 2.1 displays the LCOE for a land-based, fixed-bottom, and floating wind turbine. As shown, the FOWT has the highest LCOE which would make it the least attractive from

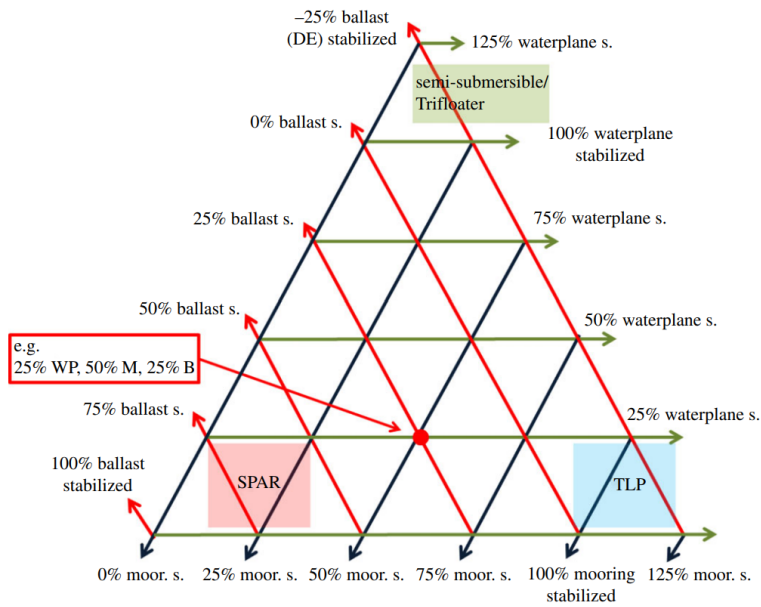


Figure 2.3: Stability triangle demonstrating the method used by each of the three platform types to stabilize the wind turbine system [3].

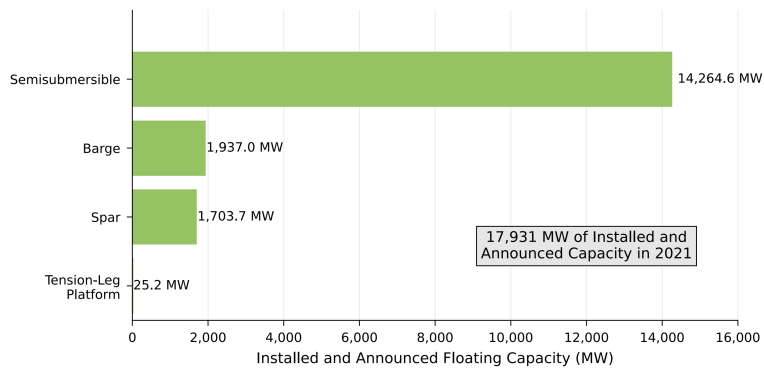


Figure 2.4: The global market share for each floating substructure both installed and announced [4].

an economics standpoint. One method to increase the LCOE of FOWTs is to increase the lifespan and decrease the maintenance costs which lowers the operational expense. This can be accomplished by minimizing the impacts of the fatigue loads acting on the system.

Table 2.1: LCOEs of mutlipte types of wind turbines [11].

Parameter	Onshore 3 MW	Fixed-Bottom 8 MW	Floating 8 MW	Units
Capital Expenditures	1,501	3,871	5,577	\$/kW
Operational Expenditures	40	111	118	\$/kW/yr
Net Annual Energy Production	3,775	4,295	3,336	MWh/MW/yr
Total LCOE	34	78	133	\$/MWh

## 2.2 Fatigue Life of Floating Offshore Wind Systems

Wind turbines are always subject to forces caused by the wind that they are designed to harness. However, offshore systems are also subjected to forces caused by ocean waves. Since FOWTs are suspended in the water column, they are subject to wind, wave, and hydrostatic forces. Therefore, FOWTs face larger fatigue loads than other types of turbines [20]. This is also reflected in the analysis presented in Sec. 2.1, where FOWTs have the largest operational expenditures meaning that they require more maintenance and repairs than the other types of turbines. In addition, the environmental conditions as well as the design of the wind farm impact the loads that the turbine experiences, so it is important to characterize the environmental conditions of the site [21]. For example, a turbine will experience higher fatigue loads under more turbulent wind conditions, so a turbine located in the wind shadow of another turbine will experience higher fatigue loads than the upstream turbine. In addition, higher average wind speeds correspond directly with a shorter fatigue life [22]. Furthermore, when comparing vertical axis wind turbines (VAWTs) with horizontal axis wind turbines (HAWTs), HAWTs experience higher fatigue loads caused by the larger

cross-section in the upwind direction [3]. There have also been analyses using Finite Element Methods (FEM) to evaluate the designs of FOWTs that concluded that current FOWTs have the highest stresses at locations like the tower base, blade roots, and other joints [23, 24, 25]. One way to decrease these fatigue loads is to use a vibration absorber to reduce the system's motion.

## 2.3 Vibration Absorbers

Vibration absorbers are used to mitigate the impact of unwanted vibrations acting on a system. These elements are meant to be attached to an existing system and tuned to transfer the vibrational energy from the primary system to the absorber. That way, the absorber will vibrate with the goal of dissipating the harmful vibrations that would otherwise be affecting the primary system. These types of systems can be either active or passive, meaning that they either require additional energy to dissipate the vibrations or they do this without any additional energy. Passive methods have the benefit that they work as soon as they are installed and do not require active control. There are several kinds of passive control methods that have been studied in minimizing the loads acting on the FOWT.

### 2.3.1 Tuned Liquid Column Dampers

One passive vibration absorber is called a Tuned Liquid Column Damper (TLCD) and utilizes the sloshing motion of water to absorb and dissipate vibrations. An example of this is the U-shaped TLCD shown in Fig. 2.5, where the movement of the primary system is transferred to the water causing it to move up the vertical columns. The restorative force from the difference in height between the vertical columns counteracts the motion of the



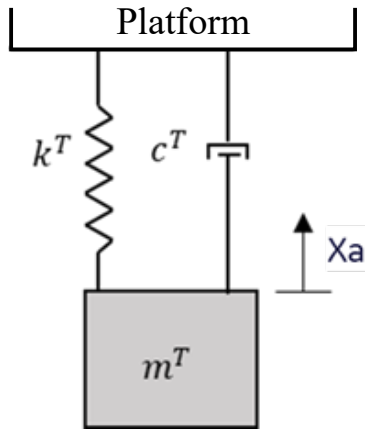


Figure 2.6: Diagram of a Tuned Mass Damper with mass,  $m$ , spring stiffness,  $k$ , and damping coefficient,  $c$ .

the primary frequency that is supposed to be reduced. This can be done using the natural frequency equation  $\omega_n = \sqrt{k/m}$  where  $k$  is the spring stiffness in the TMD and  $m$  is the mass. Several studies have proposed using TMDs to minimize the vibration of FOWT towers by placing one in the nacelle [22, 28, 29] while other proposed minimizing the motion of the entire system by placing the TMD in the substructure [30, 31]. These studies have shown that TMDs are a reliable passive method for reducing FOWT system motion.

### 2.3.3 Tuned Inerter Dampers

A modified version of the traditional TMD is the Tuned Inerter Damper (TID) which replaces the damper in the TMD with an element called an inerter. An inerter is an element that provides a force proportional to the relative acceleration between the two end nodes [32]. Fig. 2.7 displays several different possible configurations for TIDs. Several of these configurations were compared to a TMD and Fig. 2.8 displays the results of that analysis [6]. As shown, TIDs theoretically perform better than TMDs in reducing the frequency that they are tuned to and have a wider frequency band [33].

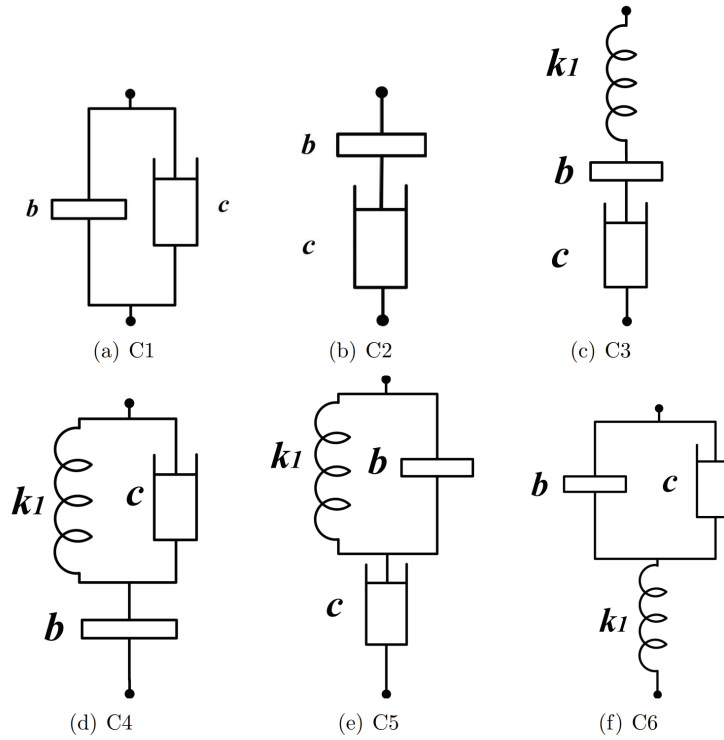


Figure 2.7: Several concepts for inerters that could be used in TIDs [6].

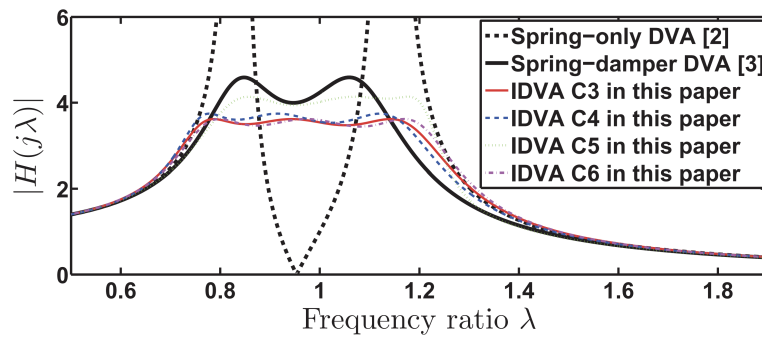


Figure 2.8: Comparison between TID configurations (IDVA in this figure) and a TMD (Spring-damper DVA) [6].

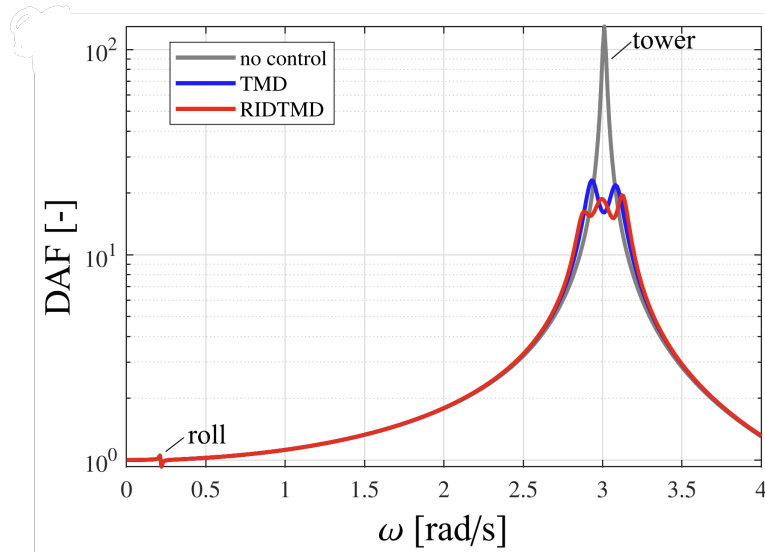


Figure 2.9: Frequency domain results of tower side to side displacement of simulation with no control, a TMD, and a TID (called an RIDTMD in this study) [7].

TIDs have been well studied in application to reducing seismic loads in buildings [14, 15] and vehicle suspensions [34], and they have also been studied for use in FOWTs [7, 32, 35, 36]. As shown in Fig. 2.9 [7], the TID performs very similarly to the theoretical result, as shown in Fig. 2.8. Comparing the two figures, the results from Zhang et al. [7] match well with the results presented in Hu et al. [6]. Many of the studies analyzing the performances of the TID in FOWTs use their own models that they developed and then later validate their models against a well-proven model like OpenFAST.

## 2.4 Hybrid Energy Harvesting Systems

As presented in Table 2.1, FOWTs have a larger LCOE than both land-based and fixed-bottom wind turbines. One way that researchers have tried to reduce this LCOE is to find ways to increase the electrical output of the system by adding additional energy harvesters to the FOWT. The concept is to increase the energy output in a low cost manner to decrease the

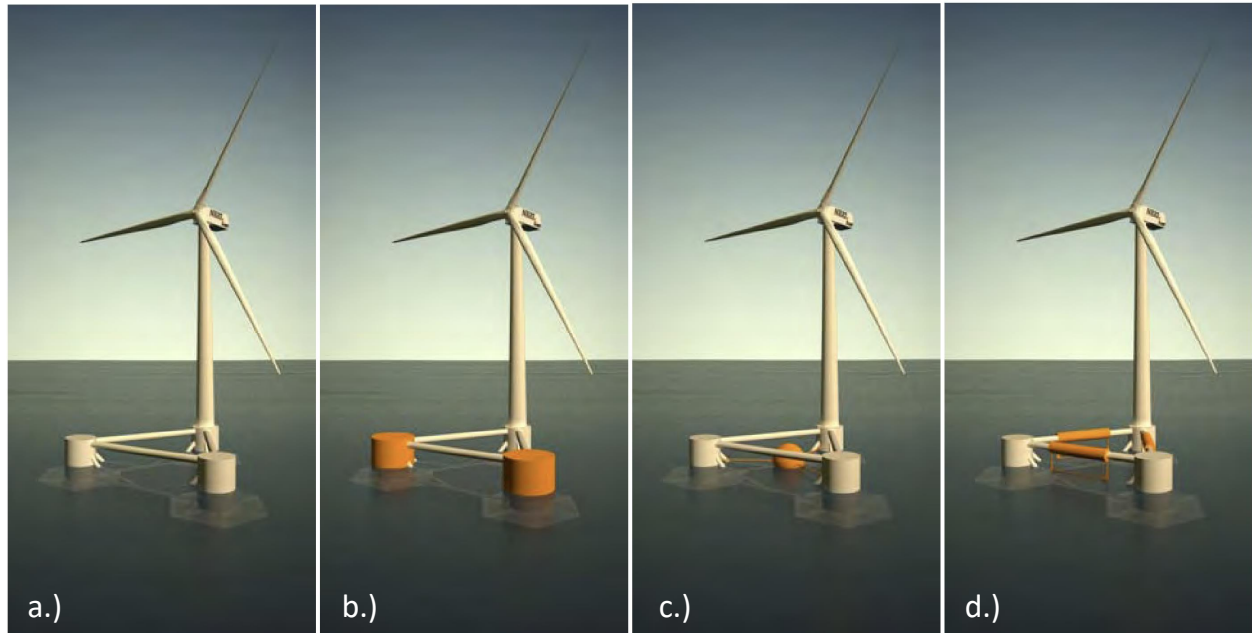


Figure 2.10: WindWaveFloat configurations: a.) Base case, b.) Oscillating water column, c.) Sphere point absorber, d.) Oscillating wave surge converter [8].

overall system's LCOE. Zhu et al. presented a concept where a semisubmersible platform would use three oscillating water columns to generate additional electricity. Through a scaled experiment, the system was able to reduce platform vibrations using both passive and active control methods for the oscillating surge devices. However, numerical results were not presented for energy harvesting or the reduction of platform motion when compared to a baseline system [37].

Principle Power, Inc. also released a series of reports discussing their study of using collocated wind and wave energy converters in the WindFloat platform. Fig. 2.10 displays the different concepts investigated in this study. They concluded that the reduced system motion did not significantly improve the energy output of the system, which was their main metric, and they concluded that the energy harvested from the wave energy converters was not significant enough to justify the cost. They did not examine the performance in increasing system life [8, 38, 39].

Table 2.2: Overview of aero-servo-hydro-elastic numerical models for FOWTs with their capabilities [12].

Code	Developer	Aerodynamics (aero)	Hydrodynamics (hydro)	Control (servo)	Structure (elastic)	Ice
Adams	MSC + NREL + LUH	BEM/GDW + DS	Airy <sup>8th</sup> /UD + ME, Airy + PF + ME	DLL, UD	T: MBS, M: QSCÉ, UDFD	None
ADCoS-Offshore [123]	ADC + IWES	BEM + DS	Airy <sup>8th</sup> /UD/Stream + ME	DLL, UD	FEM	None
ANSYS-WaveLoads [124,125]	ANSYS +LUH	None	Airy <sup>8th</sup> /UD/Stream + ME	None	FEM	None
BA-Simula [72,120]	BIT	BEM + UD	Airy/UD + ME	DLL, UD, SM	T: MBS, M: QSCÉ, UDFD	CRC, CC, FE, GM
BHaw <sup>c</sup>	Riso DTU + Siemens	BEM/GDW + DS	Airy <sup>8th</sup> /UD + ME	DLL, UD	MBS/FEM	None
Bladed [126]	GH	BEM/GDW + DS	Airy <sup>8th</sup> /UD + ME	DLL	T: FEM <sup>2</sup> + Modal/MBS, M: UDFD	None
Bladed Multibody	GH	BEM/GDW + DS	Airy <sup>8th</sup> /UD + ME	DLL	MBS	None
DeepInles Wind <sup>154</sup>	PRINCIPIA	BEM + DS	Airy + PF/UD + ME	DLL	T: FEM, M: FEM, QSCÉ	None
FAST [107,127,128]	NREL	BEM/GDW + DS	Airy <sup>8th</sup> , Airy + PF + ME	DLL, UD, SM	T: FEM <sup>2</sup> + Modal/MBS, M: QSCÉ	CRC, IC, LC, CC, FF
FLEX5	Riso DTU	BEM/GDW + DS	Airy <sup>8th</sup> /UD/Stream + ME	DLL, UD	FEM <sup>2</sup> + Modal/MBS	None
FLEX5-Poseidon [129,130]	Riso DTU + SWE + LUH	BEM/GDW + DS	Airy <sup>8th</sup> /UD/Stream + ME	DLL, UD	FEM + Modal/MBS	None
HAWC [131,132]	Riso DTU	BEM/GDW + DS	Airy <sup>8th</sup> /UD + ME	DLL, UD	FEM	None
HAWC2 [133]	Riso DTU	BEM/GDW + DS	Airy <sup>8th</sup> /UD + ME	DLL, UD, SM	T: MBS/FEM, M: UDFD	DLL
Ocaflex [134]	Orcina	BEM	Airy/UD + PF	DLL, UD	T: MBS, M: QSCÉ, UDFD	DLL
SESAM/DeepC [135]	DNV	None	Airy <sup>8th</sup> + ME/Airy + PF + ME	None	T: MBS, M: QSCÉ, FEM	None
Simo [136]	MARINTEK	BEM	Airy + PF + ME	DLL	T: MBS, M: QSCÉ, MBS	None
SIMPACT	SIMPACT	BEM/GDW + DS	None	DLL, UD	MBS	None
3Dfloat [137]	IFE-UMB	BEM/GDW	Airy + ME	UD	T: FEM, M: FEM, UDFD	None

## 2.5 Modling FOWTs with Vibration Absorbers

Modeling the dynamics of FOWTs is an important step in understanding the performance of a system for evaluating a design concept. In the offshore wind field, there are several models that have been developed with varying capabilities. Jonkman et al. describes the approach and methods used to develop their model, FAST [40, 41]. A list of this model and others is shown in Table 2.2 [12].

In addition, several studies that examine the impact of vibration absorbers also create their own simplified models. They do this so they can integrate their vibration absorber more easily since they create the structure of the model with the vibration absorber in mind. Tong et al. developed a model for a bidirectional TLCD and Wei et al. integrated this capability into the existing OpenFAST model, an open-source version of the FAST model listed in Table 2.2 [16, 17]. Yu et al. developed a model of their TLCD in the ANSYS AQWA framework to analyze the performance of different column shapes [27].

Lackner et al. developed a version of FAST, called FAST-SC, that allows the model to consider the dynamics of a tuned mass damper. They used Kane's dynamics to develop equations of motion to model the movement of a tuned mass damper. FAST-SC allows the user to place several TMDs anywhere on the turbine system [9]. Later, the capabilities were

added to FAST to also model TLCs and omni-directional TMDs as well.

Several studies have also been done on models created specifically for modeling the impacts of a TID on the dynamics of a turbine. Hu et al. presents a reduced-order model they developed to evaluate the impact of a TID in the nacelle of the turbine using a barge platform and validated it against Fast-SC [35]. Li et al. created a similar model for a monopile and spar foundation to evaluate the performance of placing a TID in the nacelle of the turbine and also validated their models against results from OpenFAST [36]. Zhang et al. also created a model for analyzing the impact of placing an inerter in the spar substructure of a turbine [7]. At this point, there have been no studies on adding these capabilities to established models such as OpenFAST.

## 2.6 Tuned Mass Dampers in OpenFAST

As described in Section 2.5, OpenFAST is an open-source modeling tool developed by the National Renewable Energy Laboratory (NREL) that models the aerodynamics, hydrodynamics, electrical systems, and structural dynamics of a wind turbine. It was originally developed to model onshore wind turbines, but NREL later added the capability to model offshore fixed-bottom and floating systems as well [40, 41, 42, 43]. OpenFAST is separated into submodules that handle specific functions within the model as shown in Fig. 2.11 [9]. An example would be that the ServoDyn module handles all electronics and controls within the system. These include structural controls such as TMDs. Each submodule also has its own designated input file with parameters the user can define for each simulation. Examples of these input files are provided in Appendix A.

The ServoDyn module in OpenFAST has a specific submodule called Structural Control (StC) that handles the modeling of the TMD or other form of structural control in the

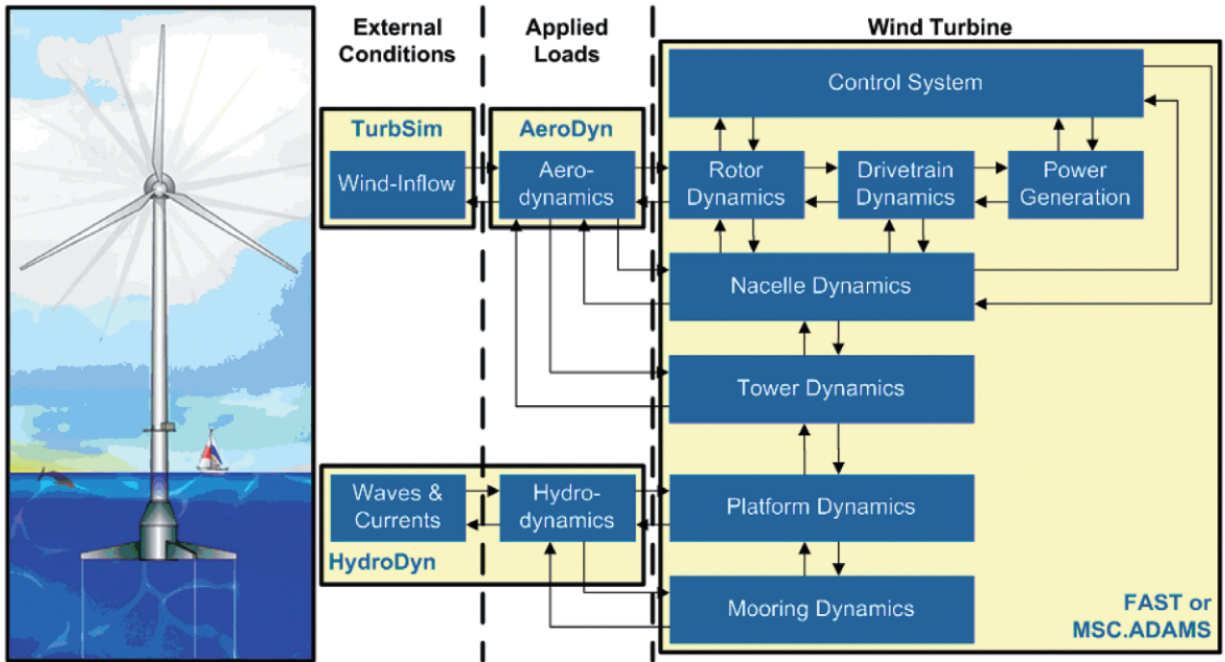


Figure 2.11: Diagram of the OpenFAST modular framework [9].

system. The theory behind the development of the OpenFAST StC submodule is described in an online manual released by NREL [44].

### 2.6.1 Defining the Coordinate System, Position, Velocity, and Acceleration

The primary hanging mass of the TMD is defined in OpenFAST as a particle in space with mass and momentum. An important first step in understanding the dynamics of the TMD is understanding how the coordinate system is defined. The TMD position is defined as the addition of two other position vectors as shown in Fig. 2.12.

Here,  $O$  is the origin of the global reference frame,  $P$  is the origin of the reference frame attached to the FOWT element the TMD is placed in (tower, platform, etc.), and  $TMD$  is the location of the TMD. For the sake of this explanation, it is assumed that  $P$  describes

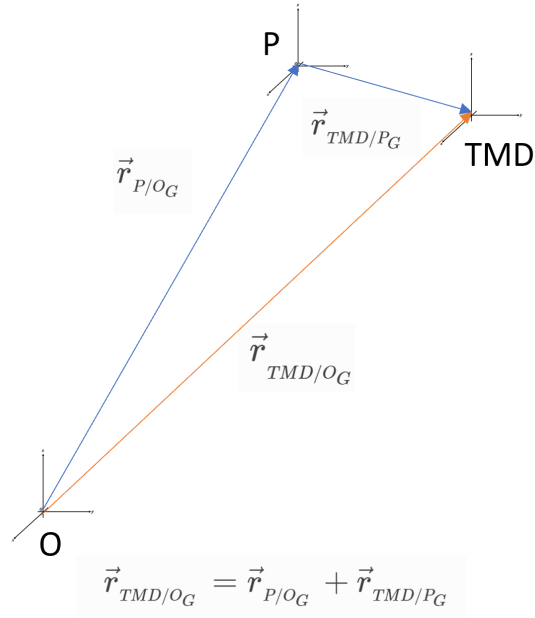


Figure 2.12: Diagram of the body-fixed reference frames and position vectors used to define the TMD position in OpenFAST.

the origin of the platform. The position vector of the TMD,  $\vec{r}_{TMD/O_G}$  is the sum of the vectors  $\vec{r}_{P/O_G}$  and  $\vec{r}_{TMD/P_G}$  which describe the position of the platform relative to the global origin and the position of the TMD with respect to the platform, respectively. Also, here,  $G$  represents the orientation of the global reference frame. Expressing the position vector in terms of the local orientation  $N$  gives,

$$\vec{r}_{TMD/O_n} = \vec{r}_{P/O_n} + \vec{r}_{TMD/P_n} \quad (2.1)$$

and solving for the position of the TMD with respect to the platform gives,

$$\vec{r}_{TMD/P_n} = \vec{r}_{TMD/O_n} - \vec{r}_{P/O_n} \quad (2.2)$$

where,

$$\vec{r}_{TMD/P_N} = \begin{bmatrix} x \\ y \\ z \end{bmatrix}_{TMD/P_N} \quad (2.3)$$

Differentiating Eq. 2.2 gives the velocity of the TMD with respect to the platform in the local coordinate system,

$$\dot{\vec{r}}_{TMD/P_N} = \dot{\vec{r}}_{TMD/O_n} - \dot{\vec{r}}_{P/O_N} - \vec{\omega}_{N/O_N} \times \vec{r}_{TMD/P_N} \quad (2.4)$$

where  $\vec{\omega}_{N/O_N}$  is the angular velocity of the platform in the local orientation,

$$\vec{\omega}_{N/O_N} = \begin{bmatrix} \dot{\theta} \\ \dot{\phi} \\ \dot{\psi} \end{bmatrix}_{N/O_N} \quad (2.5)$$

This term appears because the derivative of the position of the TMD is a function of the relative position of the platform with respect to the global reference frame, as shown in the  $\dot{\vec{r}}_{TMD/O_n} - \dot{\vec{r}}_{P/O_N}$  terms, and a function of the change in the orientation of the platform with respect to the global orientation, hence the  $\vec{\omega}_{N/O_N} \times \vec{r}_{TMD/P_N}$  terms. This is further discussed in Section 2.4.5 in Haug [45]. Differentiating Eq. 2.4,

$$\ddot{\vec{r}}_{TMD/P_N} = \ddot{\vec{r}}_{TMD/O_n} - \ddot{\vec{r}}_{P/O_N} - \vec{\omega}_{N/O_N} \times (\vec{\omega}_{N/O_N} \times \vec{r}_{TMD/P_N}) - \dot{\vec{\omega}}_{N/O_N} \times \vec{r}_{TMD/P_N} - 2\vec{\omega}_{N/O_N} \times \dot{\vec{r}}_{TMD/P_N} \quad (2.6)$$

The terms on the right side are identified in Table 2.3 [44], where  $R_{N/G}$  is the rotation matrix transforming the orientation from G to N.

Here, the acceleration in the inertial reference frame can be replaced with the following force

Table 2.3: Definitions of the terms on the right hand side of Eq. 2.6.

$\ddot{\vec{r}}_{TMD/O_N}$	Acceleration of the TMD in the inertial frame $O_N$
$\ddot{\vec{r}}_{P/O_N} = R_{N/G}\ddot{\vec{r}}_{P/O_G}$	Acceleration of the platform origin with respect to $O_N$
$\vec{\omega}_{N/O_N} = R_{N/G}\vec{\omega}_{N/O_G}$	Angular velocity of platform with respect to $O_N$
$\vec{\omega}_{N/O_N} \times (\vec{\omega}_{N/O_N} \times \vec{r}_{TMD/P_N})$	Centripetal acceleration
$\vec{\alpha}_{N/O_N} \times \vec{r}_{TMD/P_N}$	Tangential acceleration
$2\vec{\omega}_{N/O_N} \times \dot{\vec{r}}_{TMD/P_N}$	Coriolis acceleration

balance,

$$\ddot{\vec{r}}_{TMD/O_N} = \begin{bmatrix} \ddot{x} \\ \ddot{y} \\ \ddot{z} \end{bmatrix}_{TMD/O_N} = \frac{1}{m} \begin{bmatrix} \sum F_X \\ \sum F_Y \\ \sum F_Z \end{bmatrix}_{TMD/O_N} = \frac{1}{m} \vec{F}_{TMD/O_N} \quad (2.7)$$

So substituting this into Eq. 2.6 gives,

$$\ddot{\vec{r}}_{TMD/P_N} = \frac{1}{m} \vec{F}_{TMD/O_N} - \ddot{\vec{r}}_{P/O_N} - \vec{\omega}_{N/O_N} \times (\vec{\omega}_{N/O_N} \times \vec{r}_{TMD/P_N}) - \vec{\alpha}_{N/O_N} \times \vec{r}_{TMD/P_N} - 2\vec{\omega}_{N/O_N} \times \dot{\vec{r}}_{TMD/P_N} \quad (2.8)$$

This provides the basis of understanding for the coordinate system and the definitions of position, velocity, and acceleration as they are used in the StC module of OpenFAST to model TMDs.

## 2.6.2 Developing the Equations of Motion for the Tuned Mass Damper

Now that the coordinate system, position, velocity, and acceleration are defined, the next step is to develop the equations of motion. This primarily involves performing force balance on the TMD and defining the terms from the acceleration equation. Performing a force

balance about the hanging mass  $m$  in Fig. 2.6 with the mass moving in the  $z$ -direction,

$$\vec{F}_{TMD_z/O_N} = \begin{bmatrix} FX_{TMD_z/O_N} + m_z a_{G_z/O_N} \\ FY_{TMD_z/O_N} + m_z a_{G_z/O_N} \\ -c_z \dot{z}_{TMD_z/P_N} - k_z z_{TMD_z/P_N} + m_z a_{G_z/O_N} + F_{ext_z} + F_{StopFrc_z} + F_{zPreLoad} \end{bmatrix} \quad (2.9)$$

where  $F_{ext_z}$ ,  $F_{StopFrc_z}$ , and  $F_{zPreLoad}$  are an external force the user can apply to the mass, a stop force applied to the mass if it moves beyond the user-defined boundaries of displacement, and the preload force which counteracts the static deflection of the spring holding the TMD. The other components from Eq. 2.6 are,

$$\vec{\omega}_{N/O_N} \times (\vec{\omega}_{N/O_N} \times \vec{r}_{TMD/P_N}) = z_{TMD_z/P_N} \begin{bmatrix} \dot{\theta}_{N/O_N} \dot{\psi}_{N/O_N} \\ \dot{\phi}_{N/O_N} \dot{\psi}_{N/O_N} \\ -(\dot{\theta}_{N/O_N}^2 + \dot{\psi}_{N/O_N}^2) \end{bmatrix} \quad (2.10)$$

$$2\vec{\omega}_{N/O_N} \times \dot{\vec{r}}_{TMD/P_N} = \dot{z}_{TMD_z/P_N} \begin{bmatrix} 2\dot{\phi}_{N/O_N} \\ -2\dot{\theta}_{N/O_N} \\ 0 \end{bmatrix} \quad (2.11)$$

$$\vec{\alpha}_{N/O_N} \times \vec{r}_{TMD/P_N} = z_{TMD_z/P_N} \begin{bmatrix} \ddot{\phi}_{N/O_N} \\ -\ddot{\theta}_{N/O_N} \\ 0 \end{bmatrix} \quad (2.12)$$

Because the TMD is restricted to only moving in the  $z$ -direction,

$$r_{TMD_z/P_N} = \begin{bmatrix} 0 \\ 0 \\ z_{TMD_z/P_N} \end{bmatrix} \quad (2.13)$$

Therefore, the acceleration equation takes the form,

$$\ddot{z}_{TMD_z/P_N} = (\dot{\theta}_{N/O_N}^2 + \dot{\psi}_{N/O_N}^2 - \frac{k_z}{m_z})z_{TMD_z/P_N} - (\frac{c_z}{m_z})\dot{z}_{TMD_z/P_N} - \ddot{z}_{P/O_N} + a_{G_z/O_N} + \frac{1}{m_z}(F_{ext_z} + F_{StopFrc_z} + F_{zPreLoad}) \quad (2.14)$$

and the other forces are solved assuming  $\ddot{x}_{TMD_z/P_N} = 0$  and  $\ddot{y}_{TMD_z/P_N} = 0$ ,

$$F_{X_{TMD_z/O_N}} = m_z(-a_{G_x/O_N} + \ddot{x}_{P/O_N} + (\ddot{\phi}_{N/O_N} + \dot{\psi}_{N/O_N}\dot{\phi}_{N/O_N})z_{TMD_z/P_N} + 2\dot{\phi}_{N/O_N}\dot{z}_{TMD_z/P_N}) \quad (2.15)$$

$$F_{Y_{TMD_z/O_N}} = m_z(-a_{G_y/O_N} + \ddot{y}_{P/O_N} + (\ddot{\theta}_{N/O_N} + \dot{\phi}_{N/O_N}\dot{\theta}_{N/O_N})z_{TMD_z/P_N} + 2\dot{\theta}_{N/O_N}\dot{z}_{TMD_z/P_N}) \quad (2.16)$$

This provides the necessary form of the equations to implement them in the State Space approach.

### 2.6.3 State Space Approach to Modeling The Tuned Mass Damper

The State Space approach uses a combination of two equations containing a vector of "states" of the system and matrices of variables that makeup the equations of motion of the system.

Generally they appear in the form,

$$\dot{q} = Aq(t) + Bu(t) \quad (2.17)$$

$$\vec{Y} = Cq(t) + Du(t) \quad (2.18)$$

where  $q$  is the vector of state variables,  $u$  is the vector of inputs, and  $\vec{Y}$  is the vector of outputs. The state vector contains variables that describe the "state" of the system such as the position and velocity of certain degrees of freedom within the system. The matrices  $A$ ,  $B$ ,  $C$ , and  $D$  are representative of the state, input, output, and feedback, respectively.

The State Space approach employs numerical integration methods (Runge-Kutta, Adams-Bashforth, etc.) to advance forward in time and solve for the system states at each time step. In OpenFAST, the state vector,  $q$  has the form,

$$\vec{R}_{TMD/P_N} = \begin{bmatrix} x \\ \dot{x} \\ y \\ \dot{y} \\ z \\ \dot{z} \end{bmatrix}_{TMD/P_N} = \begin{bmatrix} x_{TMD_x/P_N} \\ \dot{x}_{TMD_x/P_N} \\ y_{TMD_y/P_N} \\ \dot{y}_{TMD_y/P_N} \\ z_{TMD_z/P_N} \\ \dot{z}_{TMD_z/P_N} \end{bmatrix} \quad (2.19)$$

and the input state equation is written as,

$$\dot{\vec{R}}_{TMD} = A\vec{R}_{TMD} + B \quad (2.20)$$

The matrix A, Eq. 2.21, represents the coefficients that are in front of each of the state variables in the equations of motion and B, Eq. 2.22, the vector of terms not multiplied by a state variable.

$$A(\vec{u}) = \begin{bmatrix} 0 & 1 & 0 & 0 & 0 & 0 & 0 \\ (\dot{\phi}_{P/O_N}^2 + \dot{\psi}_{P/O_N}^2 - \frac{k_x}{m_x}) & -(\frac{c_x}{m_x}) & 0 & 0 & 0 & 0 & 0 \\ 0 & 0 & 0 & 1 & 0 & 0 & 0 \\ 0 & 0 & (\dot{\theta}_{P/O_N}^2 + \dot{\psi}_{P/O_N}^2 - \frac{k_y}{m_y}) & -(\frac{c_y}{m_y}) & 0 & 0 & 0 \\ 0 & 0 & 0 & 0 & 0 & 0 & 1 \\ 0 & 0 & 0 & 0 & 0 & (\dot{\theta}_{P/O_N}^2 + \dot{\phi}_{P/O_N}^2 - \frac{k_z}{m_z}) & -(\frac{c_z}{m_z}) \end{bmatrix} \quad (2.21)$$

$$B(\vec{u}) = \begin{bmatrix} 0 \\ -\ddot{x}_{P/O_N} + a_{G_x/O_N} + \frac{1}{m_x}(F_{ext_x} + F_{StopFrc}) \\ 0 \\ -\ddot{y}_{P/O_N} + a_{G_y/O_N} + \frac{1}{m_y}(F_{ext_y} + F_{StopFrc}) \\ 0 \\ -\ddot{z}_{P/O_N} + a_{G_z/O_N} + \frac{1}{m_z}(F_{ext_z} + F_{StopFrc} + F_{ZPreLoad}) \end{bmatrix} \quad (2.22)$$

The output equation in OpenFAST takes the form,

$$\vec{Y} = \begin{bmatrix} \vec{F}_{P_G} \\ \vec{M}_{P_G} \end{bmatrix} \quad (2.23)$$

where  $\vec{F}_{P_G}$  is the vector of the net forces acting on the platform from the TMD, and  $\vec{M}_{P_G}$  is the vector of moments acting on the platform. The forces are calculated by summing the forces acting on the platform from the TMD which would be the spring and damper forces as well as the external forces  $F_{ext}$ ,  $F_{StopFrc}$ , and  $F_{PreLoad}$ .

$$\vec{F}_{P_G} = R_{N/G}^T \begin{bmatrix} k_x x_{TMD/P_N} + c_x \dot{x}_{TMD/P_N} - F_{StopFrc_x} - F_{ext_x} - F_{x_{TMD_y/O_N}} - F_{x_{TMD_z/O_N}} \\ k_y y_{TMD/P_N} + c_y \dot{y}_{TMD/P_N} - F_{StopFrc_y} - F_{ext_y} - F_{y_{TMD_x/O_N}} - F_{y_{TMD_z/O_N}} \\ k_z z_{TMD/P_N} + c_z \dot{z}_{TMD/P_N} - F_{StopFrc_z} - F_{ext_z} - F_{z_{TMD_x/O_N}} - F_{z_{TMD_y/O_N}} - F_{ZPreLoad} \end{bmatrix} \quad (2.24)$$

where  $R_{N/G}^T$  is the rotation matrix that transforms between the G and N orientations. The moment vector is determined using the forces perpendicular to the degree of freedom that the TMD is moving in multiplied by the displacement of the TMD in the enabled degree of freedom.

$$\vec{M}_{P_G} = R_{N/G}^T \begin{bmatrix} -(F_{z_{TMD_y/O_N}})y_{TMD/P_N} + (F_{y_{TMD_z/O_N}})z_{TMD/P_N} \\ (F_{z_{TMD_x/O_N}})x_{TMD/P_N} - (F_{x_{TMD_z/O_N}})z_{TMD/P_N} \\ -(F_{y_{TMD_x/O_N}})x_{TMD/P_N} + (F_{x_{TMD_y/O_N}})y_{TMD/P_N} \end{bmatrix} \quad (2.25)$$

With these inputs and outputs defined, the impact of the TMD can be properly modeled in OpenFAST.

# Chapter 3

## System Modeling

### 3.1 Equations of Motion for Tuned Inerter Damper

The first step to obtaining the State Space equations for the TID is to derive the equations of motion. Fig. 3.1 displays a diagram of the TID with the spring, dampers, masses, and degrees of freedom labeled. Here,  $z_p$  is the platform vertical displacement,  $z_b$  is the inerter vertical displacement,  $z_d$  is the hanging mass vertical displacement,  $k_1$  and  $k_2$  are the spring constants,  $b$  is the inerter mass or the inertance, and  $c_1$  is the damping coefficient. In the OpenFAST code, there are additional forces acting between the primary mass of the TID and the platform. These are  $F_{StopFrcz}$ ,  $F_{extz}$ ,  $Fz_{TMDX/ON}$ ,  $Fz_{TMDY/ON}$ , and  $Fz_{PreLoad}$  as discussed in Section 2.6. These forces do not change with this new derivation, so they will not be represented in the following equations until Eq. 3.7. Since this analysis modifies the existing OpenFAST derivation presented in Section 2.6, the derivation presented there is valid here until Eq. 2.13. This discussion will begin from that point moving forward for the TID.

Examining Fig. 3.1 and summing the forces results in,

$$(m_z + b)\ddot{z}_d - b\ddot{z}_b + c_z(\dot{z}_d - \dot{z}_b) + k_z z_d = -m_z \ddot{z}_p \quad (3.1)$$

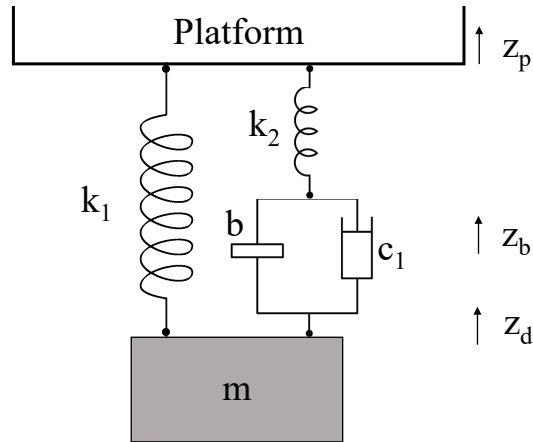


Figure 3.1: Diagram of the Tuned Inerter Damper being studied. The parameters of the system (masses, spring stiffness, and damping coefficients) labeled.

and,

$$k_b z_b = c_z (\dot{z}_d - \dot{z}_b) + b (\ddot{z}_d - \ddot{z}_b) \quad (3.2)$$

Rearranging the terms and solving for the acceleration terms for both the  $z_d$  and  $z_b$  degrees of freedom results in the following equations.

$$\ddot{z}_d = \frac{1}{m_z} (-k_z z_d - k_b z_b) - \ddot{z}_p \quad (3.3)$$

$$\ddot{z}_b = \frac{1}{b} (c_z (\dot{z}_d - \dot{z}_b) - k_b z_b) + \frac{1}{m_z} (-k_z z_d - k_b z_b) - \ddot{z}_p \quad (3.4)$$

These equations are written in the form that can be integrated into the State Space equations.

The next step in deriving the state space equations is to define the state vector.

$$\vec{R}_{TID/P_N} = \begin{bmatrix} x \\ \dot{x} \\ y \\ \dot{y} \\ z_d \\ \dot{z}_d \\ z_b \\ \dot{z}_b \end{bmatrix}_{TID/P_N} \quad (3.5)$$

Here,  $x$ ,  $y$ , and  $z$  represent the displacement in each of the three spacial dimensions, and  $z_b$  is the vertical displacement of the inerter degree of freedom. The dotted terms are the velocities. For this study, the proposed TID only moves vertically, so the equations were only solved for a TID moving in the  $z$ -direction. Future work can build on this to add the ability to model TIDs moving the  $x$  and  $y$  directions as well.

Following the format of the established code, the  $A$  matrix for the State Space equations can be written as,

$$A(\vec{u}) = \begin{bmatrix} 0 & 1 & 0 & 0 & 0 & 0 & 0 & 0 & 0 \\ (\dot{\phi}_{P/O_N}^2 + \dot{\psi}_{P/O_N}^2 - \frac{k_x}{m_x}) & -(\frac{c_x}{m_x}) & 0 & 0 & 0 & 0 & 0 & 0 & 0 \\ 0 & 0 & 0 & 1 & 0 & 0 & 0 & 0 & 0 \\ 0 & 0 & (\dot{\theta}_{P/O_N}^2 + \dot{\psi}_{P/O_N}^2 - \frac{k_y}{m_y}) & -(\frac{c_y}{m_y}) & 0 & 0 & 0 & 0 & 0 \\ 0 & 0 & 0 & 0 & 0 & 0 & 1 & 0 & 0 \\ 0 & 0 & 0 & 0 & 0 & (\dot{\theta}_{P/O_N}^2 + \dot{\phi}_{P/O_N}^2 - \frac{k_z}{m_z}) & 0 & -(\frac{k_b}{m_z}) & 0 \\ 0 & 0 & 0 & 0 & 0 & 0 & 0 & 0 & 1 \\ 0 & 0 & 0 & 0 & 0 & -(\frac{k_z}{m_z}) & (\frac{c_z}{b}) & -(\frac{(m_z+b)k_b}{m_z b}) & -(\frac{c_z}{b}) \end{bmatrix} \quad (3.6)$$

where the  $\dot{\theta}$ ,  $\dot{\psi}$ , and  $\dot{\phi}$  variables represent the angular velocity terms and the terms with the subscript  $P/O_N$  refer to the platform reference frame with respect to the global reference frame. The B matrix can be written as,

$$B(\vec{u}) = \begin{bmatrix} 0 \\ -\ddot{x}_{P/O_N} + a_{G_x/O_N} + \frac{1}{m_x}(F_{ext_x} + F_{StopFrc}) \\ 0 \\ -\ddot{y}_{P/O_N} + a_{G_y/O_N} + \frac{1}{m_y}(F_{ext_y} + F_{StopFrc}) \\ 0 \\ -\ddot{z}_{P/O_N} + a_{G_z/O_N} + \frac{1}{m_z}(F_{ext_z} + F_{StopFrc} + F_{zPreLoad}) \\ 0 \\ -\ddot{z}_{P/O_N} \end{bmatrix} \quad (3.7)$$

where  $a_{G/O_N}$  is the gravity term with respect to that component of the platform reference frame,  $F_{ext}$  represents any prescribed force defined by the user in the input files,  $F_{StopFrc}$  is the stop force applied to the primary mass if it exceeds the specified stop position in the input file, and  $F_{PreLoad}$  is the preload force applied vertically to offset the static deflection of the primary mass due to the force of gravity.

As in Section 2.6, the output equations are written in the form,

$$\vec{Y} = \begin{bmatrix} \vec{F}_{P_G} \\ \vec{M}_{P_G} \end{bmatrix} \quad (3.8)$$

where  $\vec{F}_{P_G}$  is the sum of the forces acting on the platform from the structural controls and  $\vec{M}_{P_G}$  is the net moments acting on the platform from the structural controls.  $\vec{M}_{P_G}$  is the same as the original version of OpenFAST, so it will not be discussed here.  $\vec{F}_{P_G}$  was rederived using Fig. 3.1 and summing the forces acting on the platform. Overall,  $\vec{F}_{P_G}$  can be written

as,

$$\vec{F}_{PG} = R_{N/G}^T \begin{bmatrix} k_x x_{TMD/P_N} + c_x \dot{x}_{TMD/P_N} - F_{StopFrc_x} - F_{ext_x} - F_{x_{TMD_Y/O_N}} - F_{x_{TMD_z/O_N}} \\ k_y y_{TMD/P_N} + c_y \dot{y}_{TMD/P_N} - F_{StopFrc_y} - F_{ext_y} - F_{y_{TMD_X/O_N}} - F_{y_{TMD_z/O_N}} \\ k_z z_{TMD/P_N} + k_b z_{TID/P_N} - F_{StopFrc_z} - F_{ext_z} - F_{z_{TMD_X/O_N}} - F_{z_{TMD_Y/O_N}} - F_{z_{PreLoad}} \end{bmatrix} \quad (3.9)$$

where  $R$  is the rotation matrix that converts the terms from the local (platform) orientation to the global orientation. The other terms in the matrix are written in slightly different terms than used in Eqs. 3.6 and 3.7, but they are easily interpreted and match the form written in the online OpenFAST manual. By plugging in Eqs. 3.6,3.7, and 3.9 to the existing OpenFAST Code, the TID presented in Fig. 3.1 can be modeled within the Structural Control module.

## 3.2 Programming the Tuned Inerter Damper in OpenFAST

Once the equations describing the TID motion were derived, the next step was to modify the existing OpenFAST code to accommodate the new capabilities for modeling the TID. This began with the "StrucCtrl.f90" file. This specific file contains the functions and code that ServoDyn calls to calculate the impact of the structural control methods for each time step. This is where the equations derived in Section 3.1 are input for the program to access. Examples of the input files for the OpenFAST runs are provided in Appendix A.

### 3.2.1 Modifications to StrucCtrl.f90

First, a case where the input specifies that the TID code is to be used was created and designated as "DOFMode\_TID=5," and the extra state variables had to be added to the state vector "x%StC\_x" in the "StC\_Init" subroutine. The same subroutine also sets the initial position and displacements which need to be adjusted to accommodate one additional term each. The next modification was to add an extra term to the stiffness, measured displacement, and measured velocity vectors and then set the values for these vectors as the values set in the input file, shown in Appendix A.2. The code displayed in Appendix B.1 shows the output equations being added to the "StC\_CalcOutput," and only the "m%F\_P(3,i\_pt)" equation changes just like in Eq. 3.9. This subroutine will output the forces and moments created by the TID and send it to ServoDyn. In addition, this subroutine handles setting the measured displacement and velocity as the terms in the state vector from these equations, so these values need to be updated to accommodate the extra terms. The next place where the code needs to be modified is in the "StC\_CalcConstStateDeriv" subroutine where the velocity term in the next time step's  $\dot{q}$  is set at the velocity from the previous time step's  $q$ . In the same subroutine, the input equation Eq. 2.20 is input as shown in Appendix B.2. The equation to calculate  $F_{PreLoad}$  was also modified to include the mass of the inerter  $b$  in the subroutine "Stc\_SetParameters." Lastly, the subroutine "StC\_ParseInputFileInfo" was modified to read the values for "StC\_b\_m" and "StC\_b\_k" as well as the other parameters from the input file, Appendix A.2. These represent the inerter mass,  $b$  and the stiffness  $k_2$ , respectively. This is the last section of code that was modified in "StrucCtrl.f90." Fig. 3.2 summarized the process presented in this section.

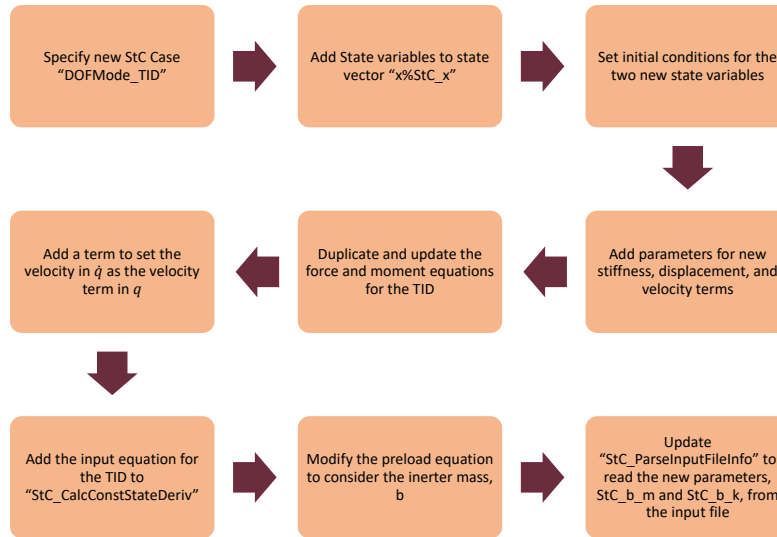


Figure 3.2: Flowchart of the process to modify "StrucCtrl.f90."

### 3.2.2 Modification to ServoDyn.f90

The file "ServoDyn.f90" was also modified to accommodate the changes made to "StrucCtrl.f90." In the "SrvD\_Init\_Jacobian\_x" subroutine, the length of the Jacobian vector had to be increased to consider the extra displacement and velocity states. For this section of the code, there are Jacobian vectors for each section of the FOWT system (each blade, the nacelle, the tower, and the substructure), so two states had to be added to each of these Jacobian vectors. An example of this code is displayed in Appendix B.3. The "SrvD\_Perturb\_x," which perturbs the point of interest (the TID degree of freedom), was modified next to match the dimensions of the Jacobian vectors from "SrvD\_Init\_Jacobian\_x." In the same way, the subroutine "Compute\_dX" which calculates the difference between two input values, was adjusted to match the size of the new state vector as this code is used to calculate the derivatives of the states. A flowchart of the modified sections of code is shown in Fig. 3.3.

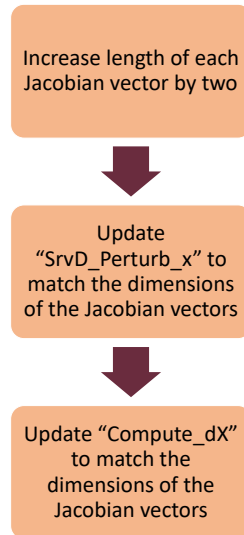


Figure 3.3: Flowchart of the process to modify "ServoDyn.f90."

### 3.2.3 Modifications to StrucCtrl\_Registry.txt

The files ending with "\_Registry.txt" are used to identify the variables that the OpenFAST ".f90" files can use. Therefore, "StrucCtrl\_Registry.txt" dictates which variables can be used in "StrucCtrl.f90." Inside this code, we add the parameters  $M_b$  and  $K_b$  and the input file variables  $StC_b_M$  and  $StC_b_k$ .

### 3.2.4 Modifications to ServoDyn\_IO.f90

The file called "ServoDyn\_IO.f90" formats all of the outputs that ServoDyn can keep track of and display. To allow for the position and velocity of the TID degree of freedom to be tracked, parameters were added to this file so that they can be output by the simulation. This was used to verify that the code operated properly and in the energy harvesting estimation later on in the analysis.

Table 3.1: Initial conditions for the parametric study of the TID parameters to minimize RMS pitch motion.

$\mu$	m (kg)	$k_1$ (N/m)	$c_1$ (N*s/m)	$k_2$ (N/m)	b (kg)
TMD					
0.02	93,800	500 - 10,500	500 - 5,500	-	-
0.05	234,500	5,000 - 15,000	2,000 - 12,000	-	-
0.08	375,200	10,000 - 30,000	10,000 - 30,000	-	-
TID					
0.02	93,800	= $k_{1,opt}$	50 - 300	50 - 300	1,600 - 2,400
0.05	234,500	= $k_{1,opt}$	50 - 750	50 - 750	6,000 - 9,000
0.08	375,200	= $k_{1,opt}$	250 - 1,650	250 - 1,650	2,000 - 14,000

### 3.3 Tuned Inerter Damper Parametric Study

The next step in proving the performance benefits of the TID was to optimize the parameters to determine the best combination to reduce the system motion. There were several possible metrics and methods for the reduction, but this study focused on reducing the root-mean-squared (RMS) value for the platform pitch. To perform the sensitivity analysis, a mass ratio for the TMD and TID was set and the other parameters (stiffnesses, damping, inerter mass) were varied systematically to determine which combination provided the best performance.

For the case where the parameters were tuned to the system's natural frequency, the mass ratios examined were 2%, 5%, and 8% of the whole system combined mass of  $1.40727e + 07$  kg. Using these values, Table 3.1 defines the conditions for the parametric study. For this study, the values were chosen based on preliminary results from a colleague working on a simplified version of this model. To gather data for this study, a program was created to run several OpenFAST simulations. The program swept through the range of data for each parameter, making sure that there was a simulation for each combination of parameters. Later, an analysis to examine tuning the parameters to the dominant wave frequency was completed for a mass ratio of 3%.

### 3.4 Evaluating Energy Harvesting Potential of the TID

As previously discussed, one advantage of the TID configuration presented in this study is that an electrical generator can be used to create the inertance and damping in parallel as shown in Fig. 2.7. This creates an opportunity to harvest additional electricity from the system in addition to the energy generated by the wind turbine. The focus of the vibration absorber was still to reduce the system motion, however, so the parameters of the system were tuned towards that goal instead of for energy harvesting.

For this study, the energy harvesting potential was approximated by the energy dissipated by the dampers within the TID. This is equivalent to the power dissipated by the damper, given as,

$$Power = c_1 * (\dot{z}_b - \dot{z}_d)^2 \quad (3.10)$$

Here, the power was calculated for only one TID. In practice, the whole system energy harvesting potential would be equivalent to the sum of the power of each TID. In order to estimate the electrical energy harvested, the energy harvesting potential would be multiplied by an estimated energy harvesting efficiency,  $\eta$ , which would be the efficiency of the entire energy harvesting system attached to the TID.

# Chapter 4

## Results & Discussion

To evaluate the performance of the TID in comparison to the TMD and no structural control, it is important to use a validated and well documented reference model. For this study, the OC4 Semisubmersible Floating System [10], which is already in OpenFAST and is well documented, acted as the reference model, shown in Fig. 4.1. The proposed system would place one vibration absorber, TMD or TID, in each of the three outer vertical columns of the platform. A diagram of the platform is shown in Fig. 4.2 This would allow for ease of access for maintenance and the possibility for retrofitting existing FOWT turbines.

An important point to understand is that adding the TMD and TID impacted the dynamics of the platform not only because they absorbed the vibrations but also because they added mass to the system. This changed the system's center of mass as well as the system's moment of inertia. This can impact the characteristics of the system's oscillation. To address this issue, the mass added to the system in the vibration absorbers was offset by removing ballast water from the system. This approach did not perfectly address this issue since the moment of inertia still changed, but it did make them more comparable and realistic to what would be done in deploying this type of system. Fig. 4.3 displays a comparison between the results of a heave free decay test if the added mass of the absorbers was not addressed. As shown, it was important to ensure the platform mass was properly conserved for better accuracy in simulations.

In addition, OpenFAST has some parameters that needed to be updated to fit the specific

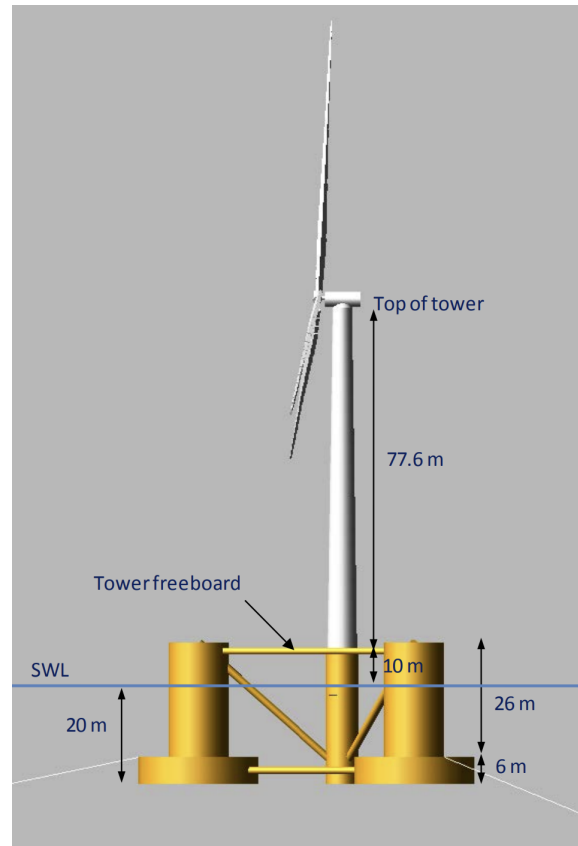


Figure 4.1: Diagram of the OC4 semisubmersible floating system used as the reference model for this study [10].

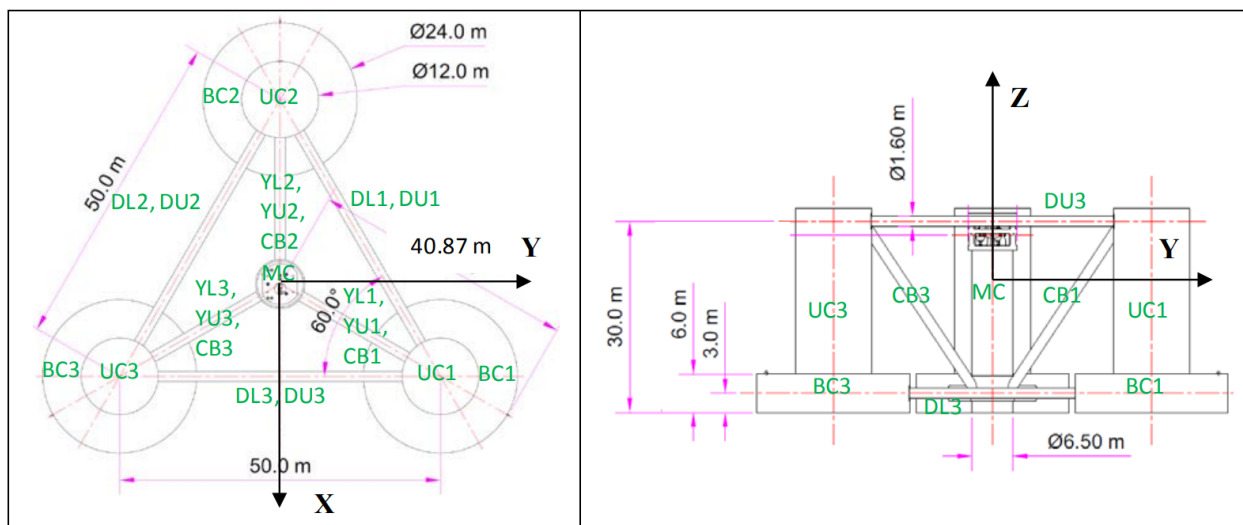


Figure 4.2: Diagram of the semisubmersible platform for the DeepCwind platform used in the OC4 analysis [10].

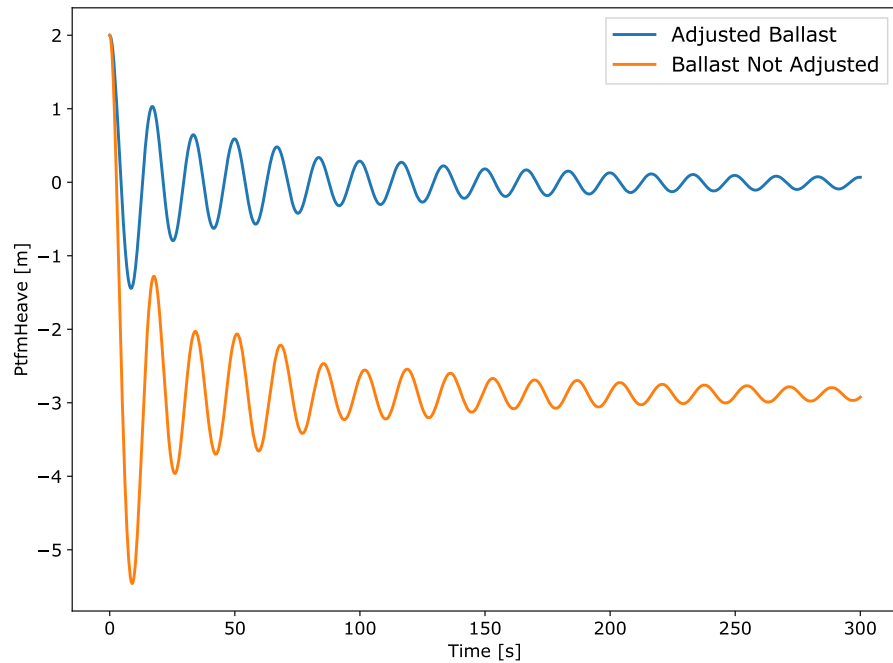


Figure 4.3: Comparison between OpenFAST results when the added mass from the absorber is and is not offset in the ballast water levels.

system being tested to ensure the most accuracy. One example of this was the  $DT\_UJac$  parameter defined in the .fst file. This parameter controls the amount of time between calls to get the Jacobian matrix that is used to solve the relationship between the forces and loads in the Elastodyn module. It is recommended that for floating systems, the value for  $DT\_UJac$  should be equal to  $\frac{1}{10}f_n$  where  $f_n$  is the natural frequency for the rotational degrees of freedom of the system [44]. Fig. 4.4 provides an example of what can happen when  $DT\_UJac$  is not set properly when using the StC module. As shown, the baseline system with no structural control behaves as expected, but the system with structural control when  $DT\_UJac$  is not set properly does not reflect accurate behavior of the system. The results of the simulation were not accurate because the system pitch motion should settle at approximately zero. However, fixing this issue caused the system to settle about the same location as the baseline.

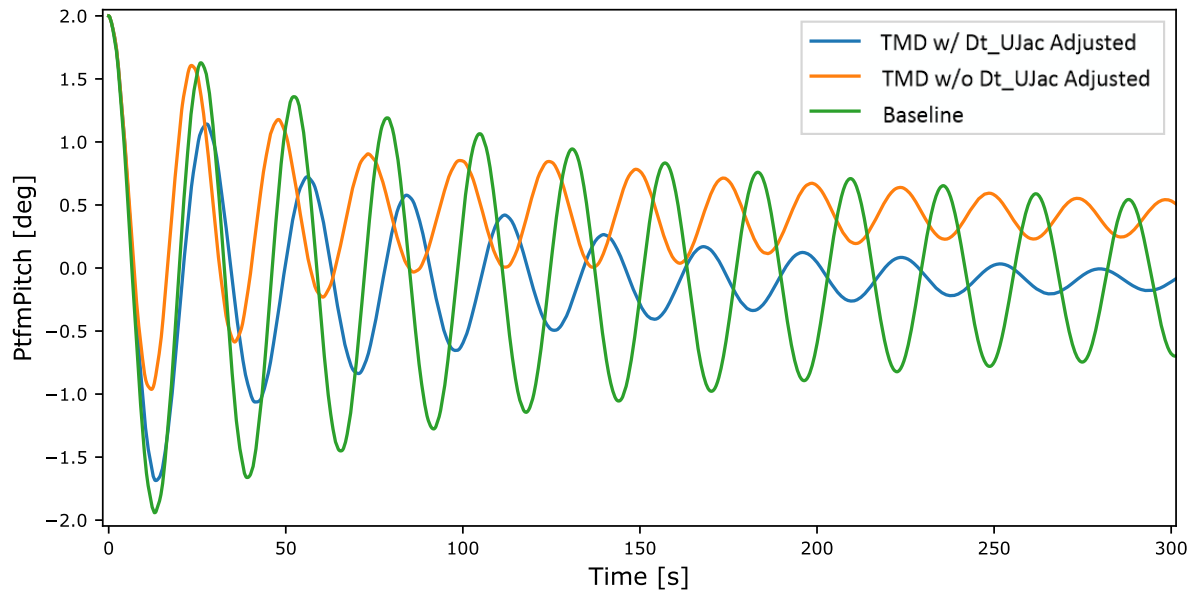


Figure 4.4: Time-domain data from OpenFAST for a pitch free decay test to display the settling position discrepancy.

## 4.1 Model Validation

The first step in evaluating the performance of the TID code, was to ensure that the model acted similar to what the theory presented. For this analysis, the values did not need to be the optimized values from the parametric study. Instead, values from a colleague's optimization results were used. These values came from a simplified model of the same OC4 semisubmersible platform, so they are expected to be somewhat realistic but not the ideal values for this model. Figs. 4.5 and 4.7 display the time-domain results from a heave and pitch free decay test, respectively, and Figs. 4.6 and 4.8 display the frequency-domain results from the same tests.

Examining the results from the time-domain plots, Figs. 4.5 and 4.7, the reduction in platform motion is visible especially in the pitch motion of Fig. 4.7 where the TID outperforms the TMD. The frequency-domain plots make it easier to compare the results as there is a

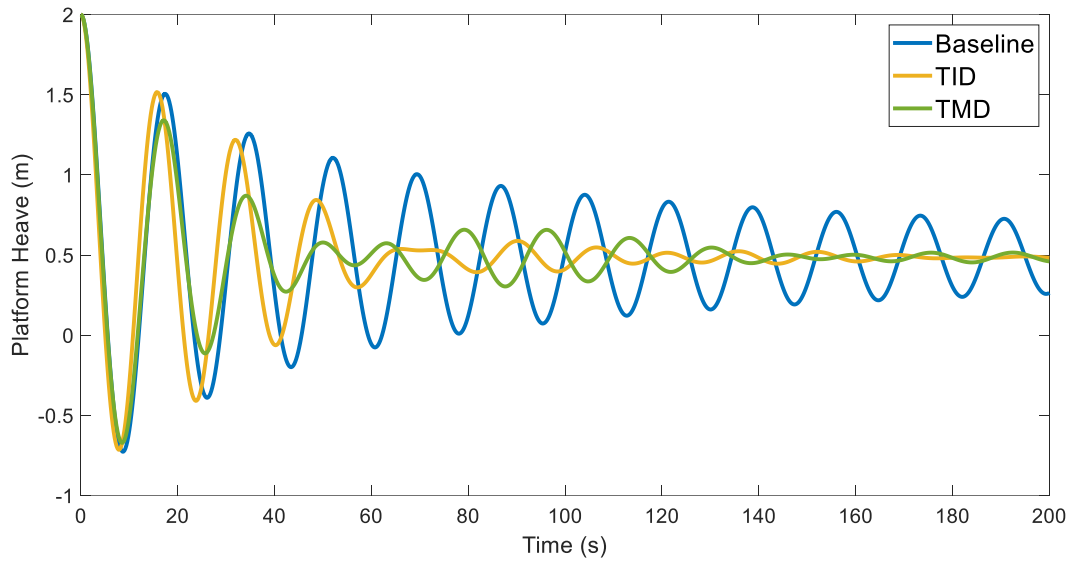


Figure 4.5: Time domain results for the heave free decay test at an 8% mass ratio.

clear reduction on the pitch displayed in Fig. 4.8 when comparing the TID to the TMD, and the results in Fig. 4.6 show that the overall reduction is similar between the TMD and TID. In addition, the shape of the frequency-domain results in Fig. 4.6 show good agreement with the plots from Figs. 2.8 and 2.9. Because the parameters used in these simulations were not the same as the optimized ones from the parametric study, it was determined that the results of the model match the theoretical values well enough to call the model validated even though the magnitude of the reduction was not the same. The following analysis will focus more on recreating the magnitude of the reduction seen in the literature by using values optimized for the OpenFAST model.

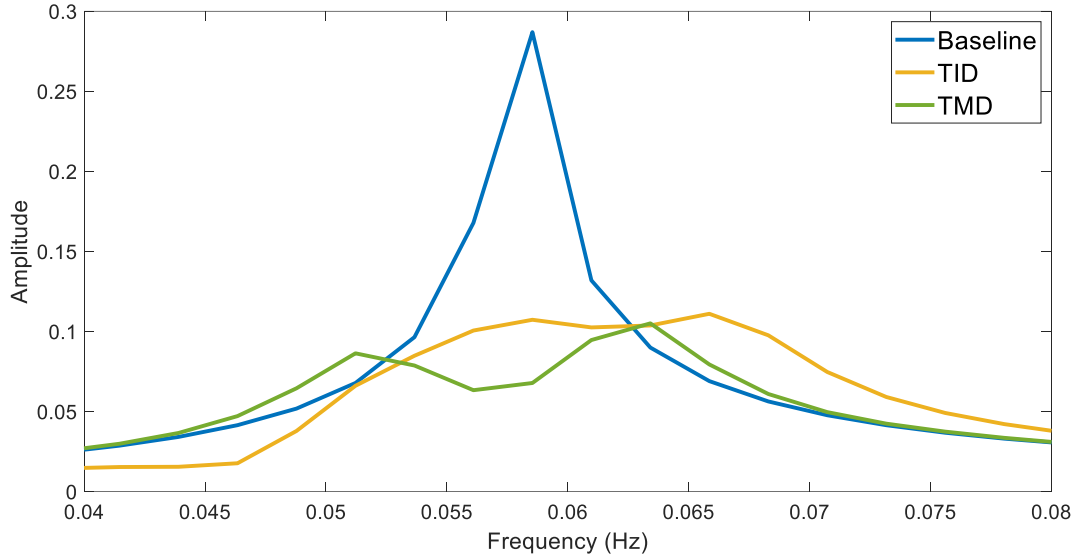


Figure 4.6: Frequency domain results for the heave free decay test at an 8% mass ratio.

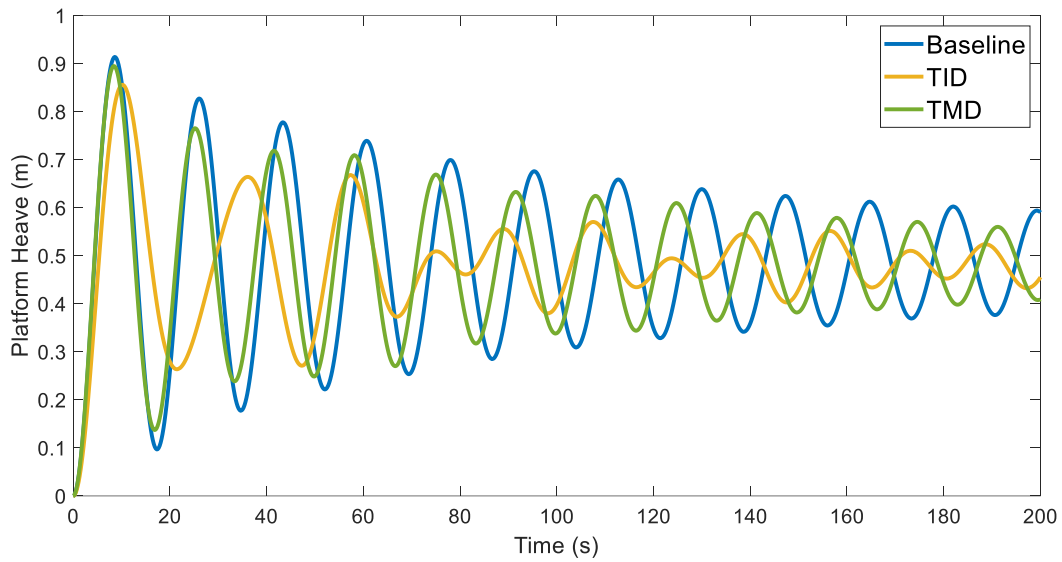


Figure 4.7: Time domain results for the pitch free decay test at an 8% mass ratio.

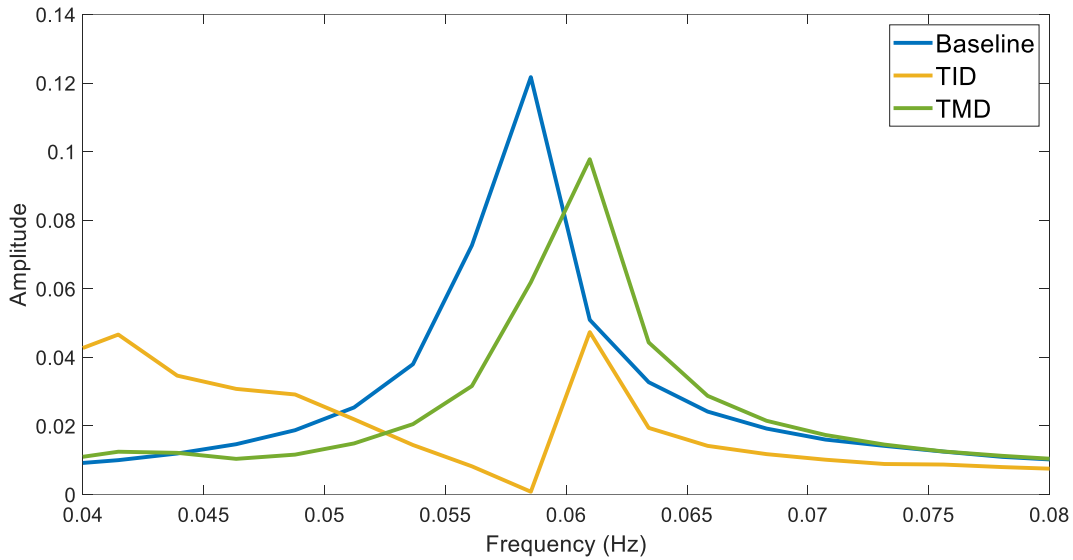


Figure 4.8: Frequency domain results for the pitch free decay test at an 8% mass ratio.

## 4.2 Tuned Inerter Damper Parametric Study

### 4.2.1 Pitch Free Decay

As discussed previously, it was important to investigate which parameters provided the best performance of the vibration absorbers. To this end, a parametric study was performed where simulations were run using a range of parameters and the performance was compared between these different configurations. This was done for both the TMD and the TID. The optimized vibration absorber parameters are listed in Table 4.1, where  $\mu$  is the mass ratio of the primary hanging mass relative to the mass of the whole FOWT. Multiplying the total system mass by the mass ratio provides the total mass added with the TMDs and TIDs. Therefore, the mass  $m$  is equal to one-third of the total system mass multiplied by the mass ratio. The parameters were tuned to dampen the vibrations of the system at its natural frequency to avoid resonance.

Table 4.1: Optimized values from the parametric study to minimize the impact of pitch motion for the pitch free decay test.

$\mu$	m (kg)	$k_1$ (N/m)	$c_1$ (N*s/m)	$k_2$ (N/m)	b (kg)
TMD					
0.02	93,800	5,000	1,750	-	-
0.05	234,500	12,500	7,500	-	-
0.08	375,200	19,000	15,000	-	-
TID					
0.02	93,800	5,500	75	125	2,000
0.05	234,500	12,500	250	350	6,000
0.08	375,200	20,000	250	450	8,000

It was found that the stiffness of the primary spring,  $k_1$ , of both the TMD and TID were very close, so it was assumed that these values are equal for the study. This enabled the simulations to be run faster and examine the impact of other parameters first. Figs. 4.9, 4.10, and 4.11 display plots of the RMS pitch value as a function of the primary stiffness,  $k_1$ , and damping,  $c_1$ , for the TMD.

Figs. 4.12, 4.13, and 4.14 display surfaces of the RMS pitch for each mass ratio of the TID. Examining the plots reveals that all of the RMS pitch values appear to confirm the results presented in Table 4.1. These results will be validated by running simulations for a pitch free decay case and various wind and wave cases.

### 4.2.2 JONSWAP Wave Spectrum

In order to examine the impact of the tuning the system parameters to the most dominant input frequency, an additional study was done to tune the parameters of the TMD and TID to input waves. For this test, a JONSWAP wave spectrum was generated for waves with a significant wave height of 3 meters and period of 10 seconds. The goal, again, was to minimize the system pitch by systematically varying the system parameters. Here, only a

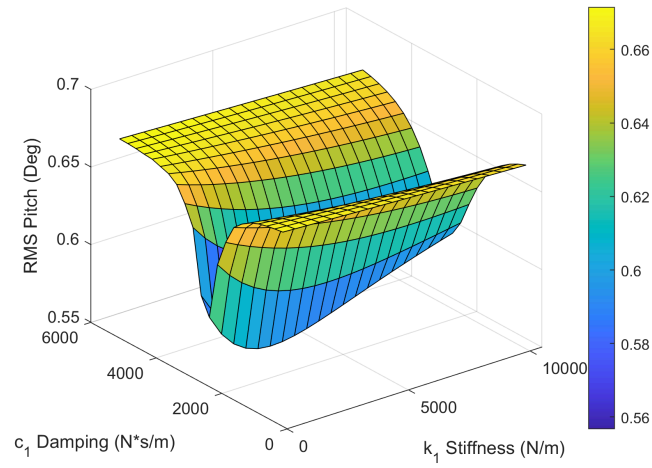


Figure 4.9: RMS pitch values as a function of the stiffness and damping values in the TMD for a 2% mass ratio

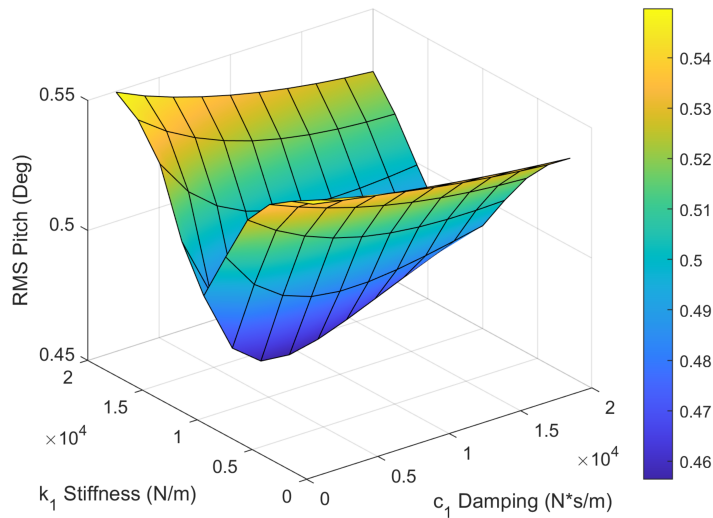


Figure 4.10: RMS pitch values as a function of the stiffness and damping values in the TMD for a 5% mass ratio.

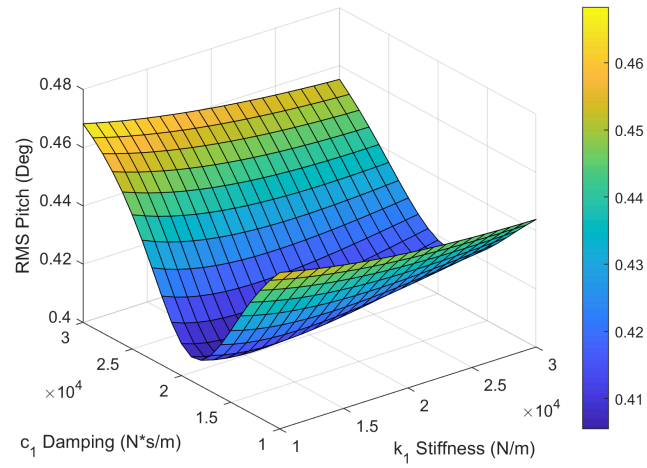


Figure 4.11: RMS pitch values as a function of the stiffness and damping values in the TMD for an 8% mass ratio.

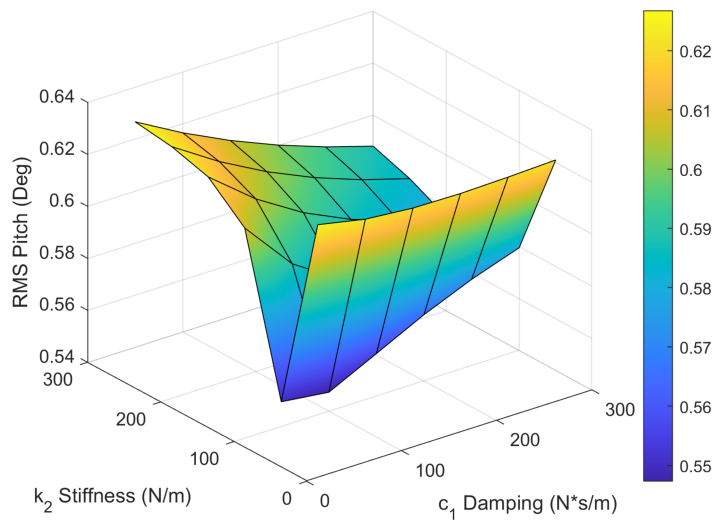


Figure 4.12: RMS pitch values as a function of the stiffness and damping values in the TID for a 2% mass ratio

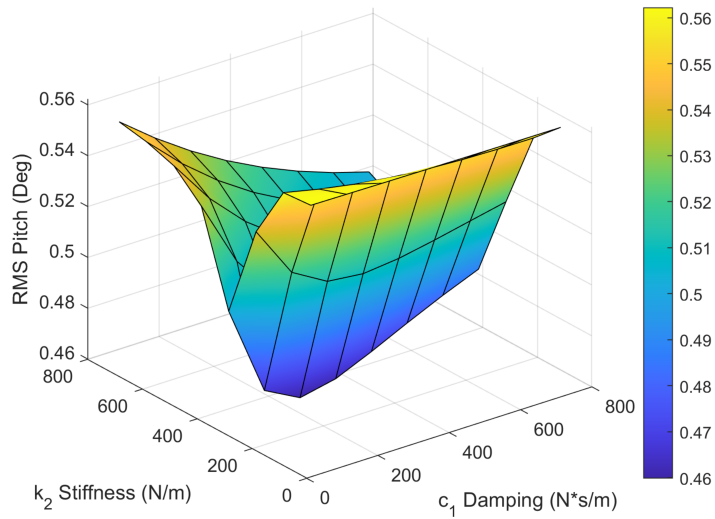


Figure 4.13: RMS pitch values as a function of the stiffness and damping values in the TID for a 5% mass ratio.

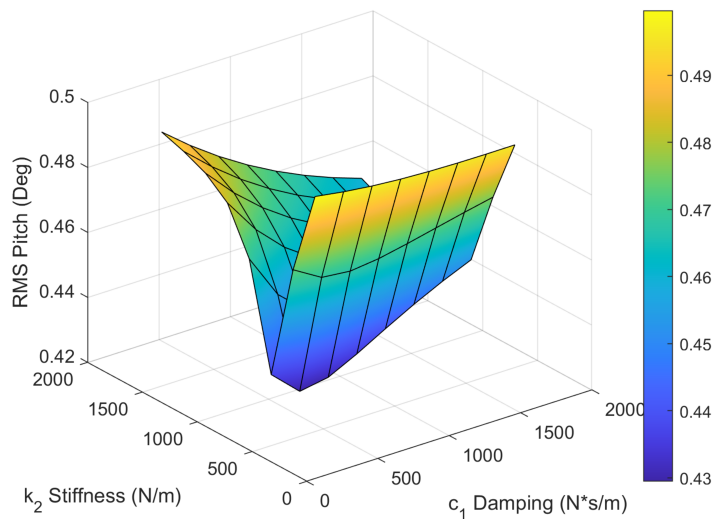


Figure 4.14: RMS pitch values as a function of the stiffness and damping values in the TID for an 8% mass ratio.

Table 4.2: Optimized values from the parametric study to minimize the impact of pitch motion for the JONSWAP wave spectrum.

$\mu$	m (kg)	$k_1$ (N/m)	$c_1$ (N*s/m)	$k_2$ (N/m)	b (kg)
TMD					
0.03	140,700	70,000	2,000	-	-
TID					
0.03	140,700	65,000	3,000	20500	500

mass ratio of 3% was examined, and, again, a 3% mass ratio means that each TMD or TID contains mass equivalent to 1% of the total system mass. The final results from this analysis are presented in Table 4.2.

### 4.3 Pitch Free Decay Tests

Free decay testing is an important benchmark test in evaluating the performance of the vibration absorbers because it minimizes the external factors influencing the system's motion. In a test with wind or waves, those external factors greatly influence the results of the simulation. In a free decay test, the only factors influencing the motion of the system are the system's hydrodynamics and the influence of the vibration absorber. The pitch free decay test was performed using the optimal pitch parameters presented in Table 4.1. The results of the whole study are presented in Table 4.3, and the results for the 2, 5, and 8 percent mass ratio can be seen in Figs. 4.15, 4.16, and 4.17. In addition, a Fourier Transform of the 2, 5, and 8 percent mass ratio cases appears in Figs. 4.18, 4.19, and 4.20.

Examining the data, it appears that the TMD performed slightly better than the TID. Examining the amplitude of the frequency domain plots, especially at the pitch natural frequency of 0.039 Hz, the TMD and TID are very comparable in performance. The TID appears to have a smaller amplitude at the natural frequency when compared to the TMD.

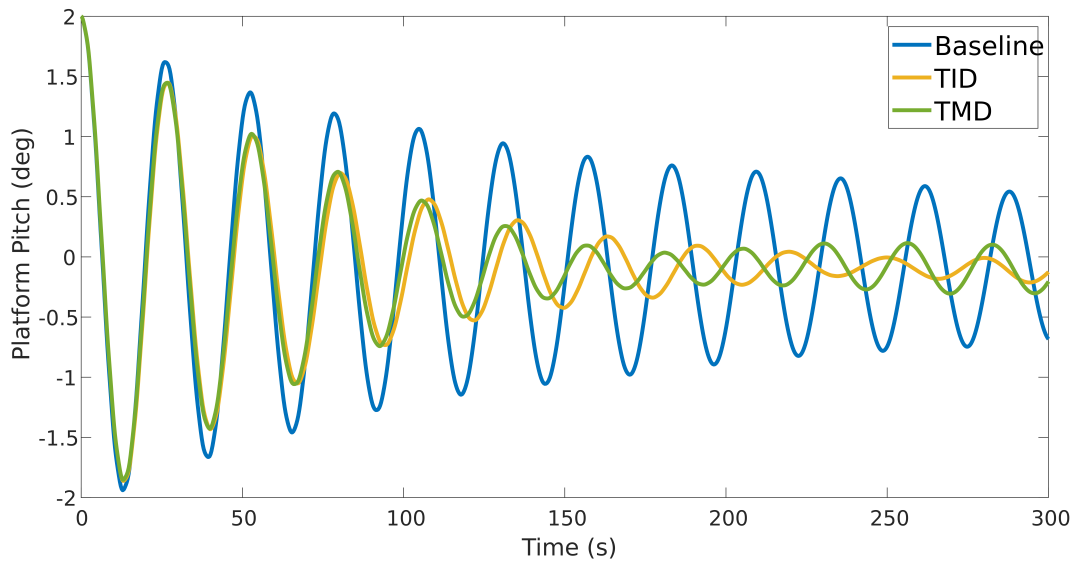


Figure 4.15: Time domain results for the 2 percent mass ratio case for the TMD and TID compared to the baseline free decay test.

Looking at the numerical data in Table 4.3, it appears that the performance of the TMD and TID are heavily dependant on the mass ratio and are sensitive to changes in the stiffness and damping values. Therefore, the results may be slightly different if a more precise optimization were run. One consideration for this conclusion, though, is that the system will hardly be operating under free decay conditions. Therefore, it is necessary to run more simulations that consider external inputs.

## 4.4 Wave Only Tests

The first step to test the system's response to realistic conditions is to ensure that the floating platform is properly interacting with incoming waves. To accomplish this, a JONSWAP wave spectrum was used to examine the system's response to a wave with a period of 10 seconds and a significant height of 3 meters. As previously mentioned, a similar optimization to the free decay tests was run to ensure that the system parameters would be properly tuned.

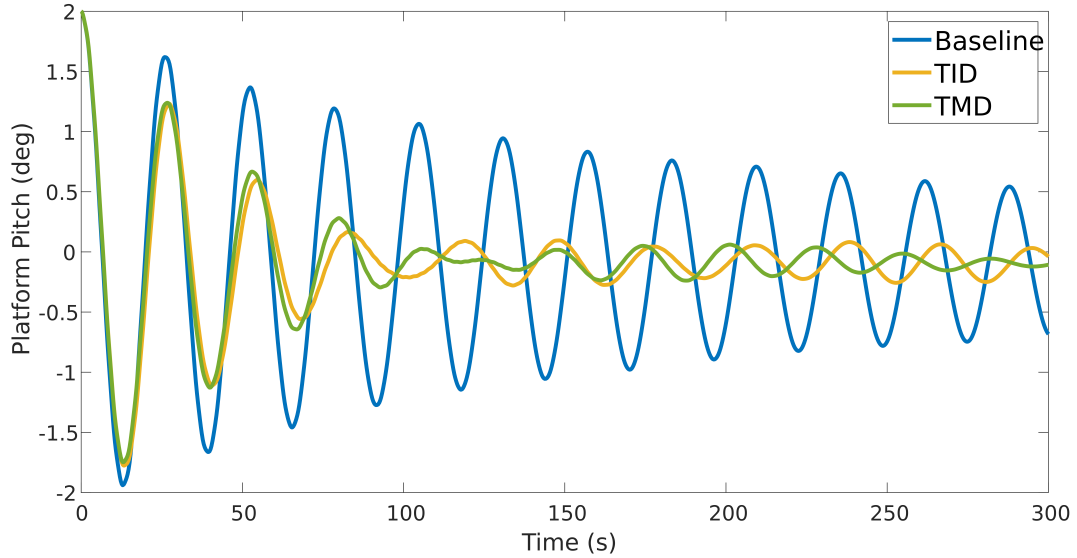


Figure 4.16: Time domain results for the 5 percent mass ratio case for the TMD and TID compared to the baseline free decay test.

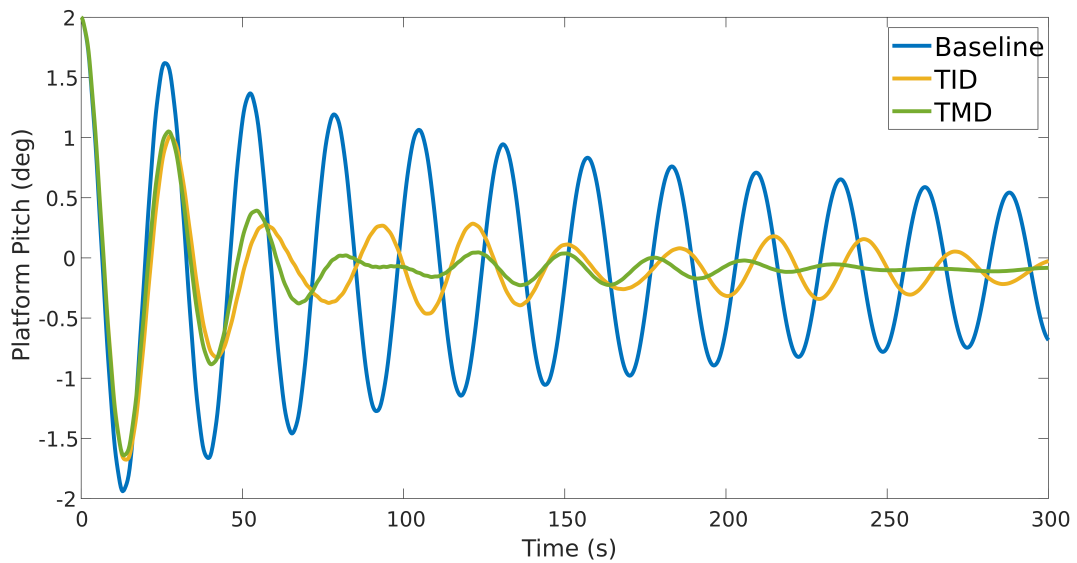


Figure 4.17: Time domain results for the 8 percent mass ratio case for the TMD and TID compared to the baseline free decay test.

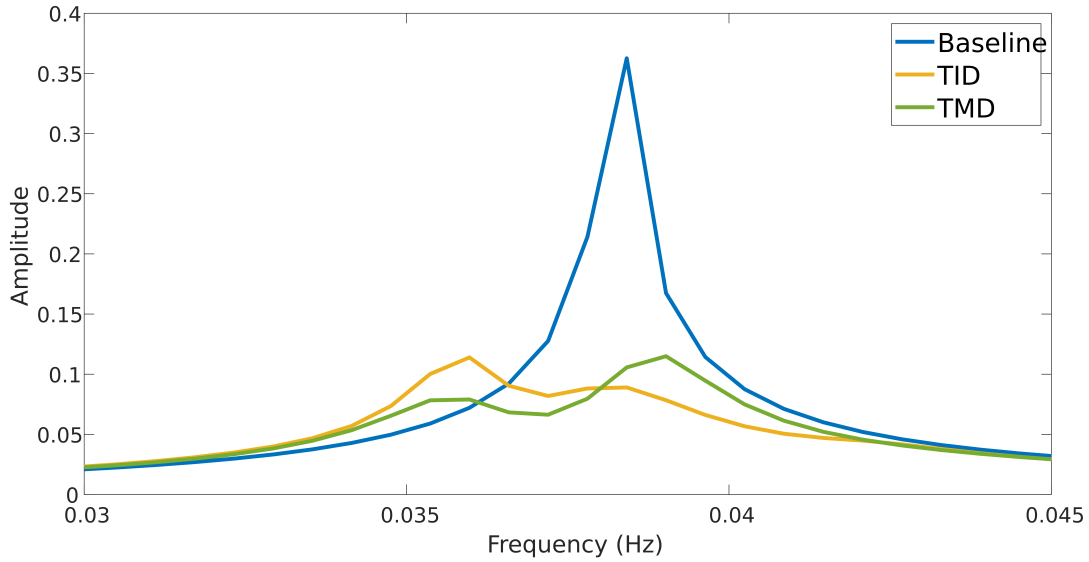


Figure 4.18: Frequency domain results for the 2 percent mass ratio case for the baseline, TMD, and TID free decay test.

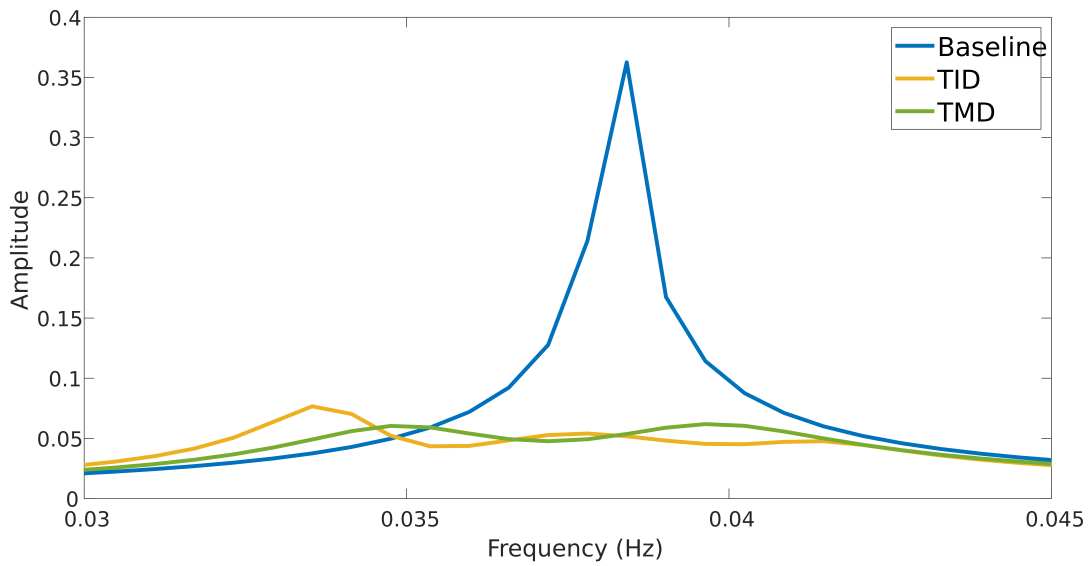


Figure 4.19: Frequency domain results for the 5 percent mass ratio case for the baseline, TMD, and TID free decay test.

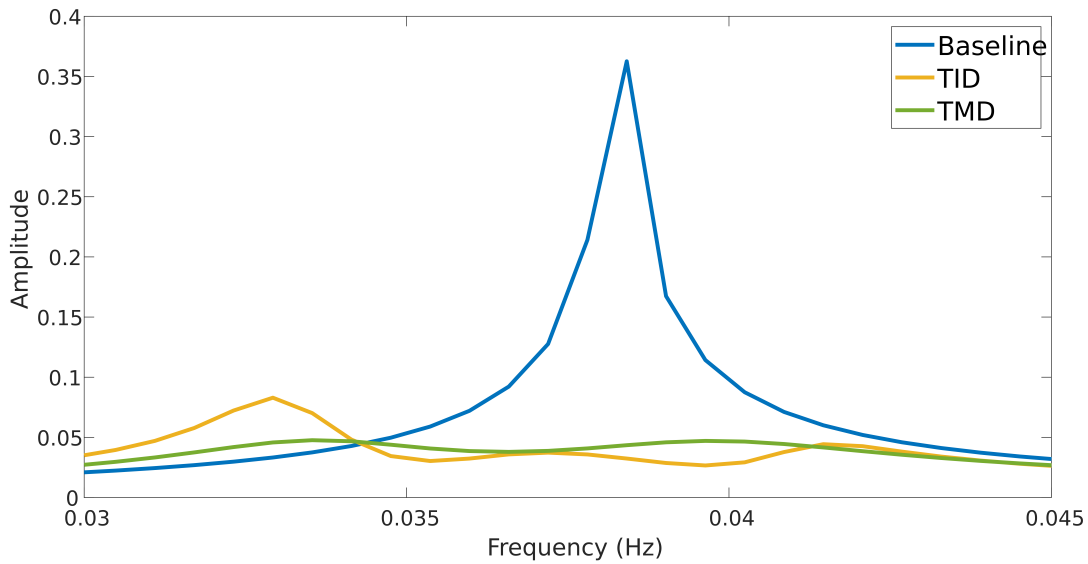


Figure 4.20: Frequency domain results for the 8 percent mass ratio case for the baseline, TMD, and TID free decay test.

From this analysis, the parameters for the TMD and TID were determined and are included in Table 4.2.

The time domain results of this test are shown in Fig. 4.21. Examining these results, it appears that the TMD and TID clearly reduce the system pitch. For this analysis, the first 800 seconds of the simulation were ignored to ensure that the system reached steady state. In addition, the frequency domain results are presented in Fig. 4.22. These results help to show that the TMD and TID reduce the system pitch, especially close to the primary wave frequency 0.1 Hz. These results show that the TMD and TID both do a good job of reducing the system pitch at the predetermined wave frequency. In addition, more precise optimization is expected to increase the observable benefits of the TMD and TID.

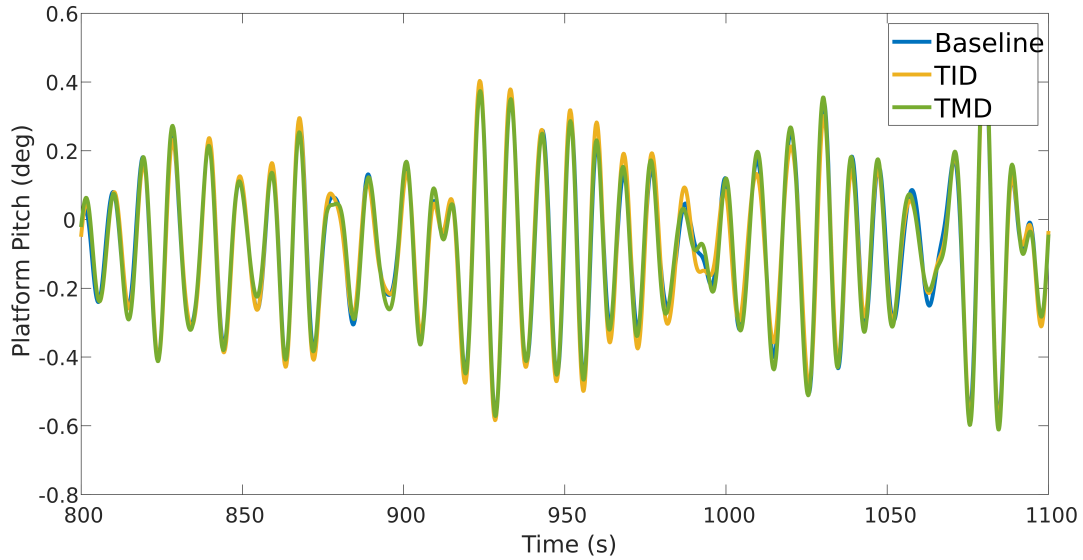


Figure 4.21: Time domain results for the baseline, TMD, and TID using a mass ratio of 3% with a JONSWAP wave with a period of 10 seconds and height of 3 meters.

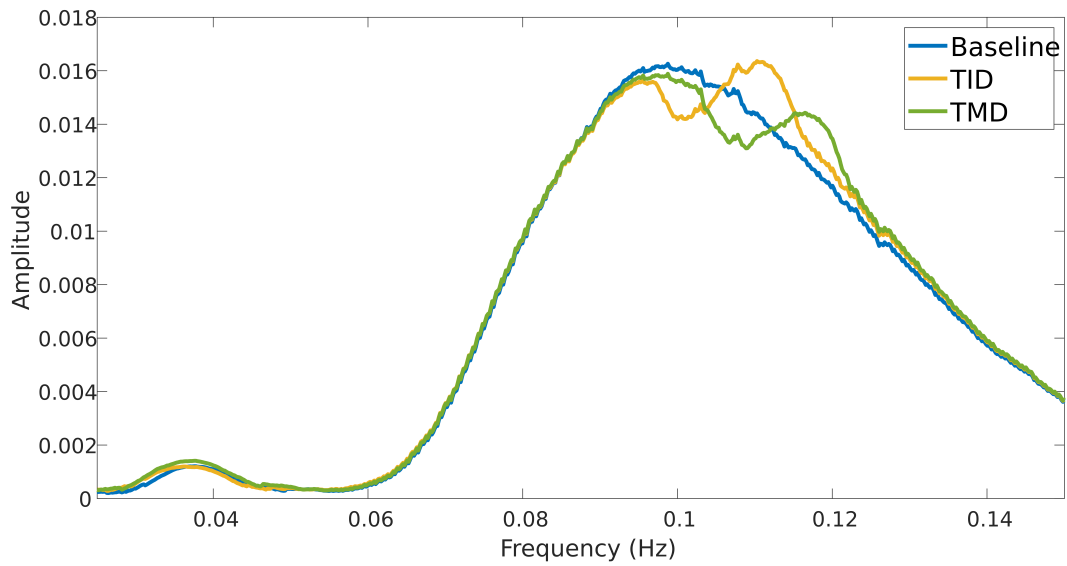


Figure 4.22: Frequency domain results for the baseline, TMD, and TID using a mass ratio of 3% with a JONSWAP wave with a period of 10 seconds and height of 3 meters.

Table 4.3: Final results for pitch free decay test.

Case	RMS Pitch (Degrees)	Percent Reduction
Baseline	0.3996	-
TMD		
$\mu=0.02$	0.2525	36.805
$\mu=0.05$	0.2093	47.614
$\mu=0.08$	0.1913	52.132
TID		
$\mu=0.02$	0.2541	36.403
$\mu=0.05$	0.2131	46.671
$\mu=0.08$	0.2050	48.69

## 4.5 Wave and Wind Tests

The next step in testing is looking at the impact of the vibration absorbers with wind and wave inputs. For this analysis, a wind speed of 9 meters per second was used. In addition, the same wave case as the previous section, JONSWAP wave with a period of 10 seconds and significant wave height of 3 meters, was used. Another aspect of this analysis was examining the impact of the wind and wave input acting at different angles as shown in Fig. 4.23. The wind and waves will not always be acting the same direction, so the angle between them  $\beta$  will change. For this study, only a  $\beta$  of 0 and 30 degrees were examined. In addition, as shown in Fig. 4.23, the wind always acts directly in alignment with the x-axis and the waves will change their angle of incidence.

Based on the results, the angle of incidence does not significantly impact the performance of the TMD or TID. This occurred because the three TMDs and TIDs are arranged in an equilateral triangle about the central tower. Therefore, the masses are spaced equally and respond symmetrically no matter what angle the inputs come from. The results shown in Figs. 4.24 and 4.25 show that the platform pitch is not visibly reduced by adding the TMD or TID when the wind and the wave cases are being run at the same time. This may be

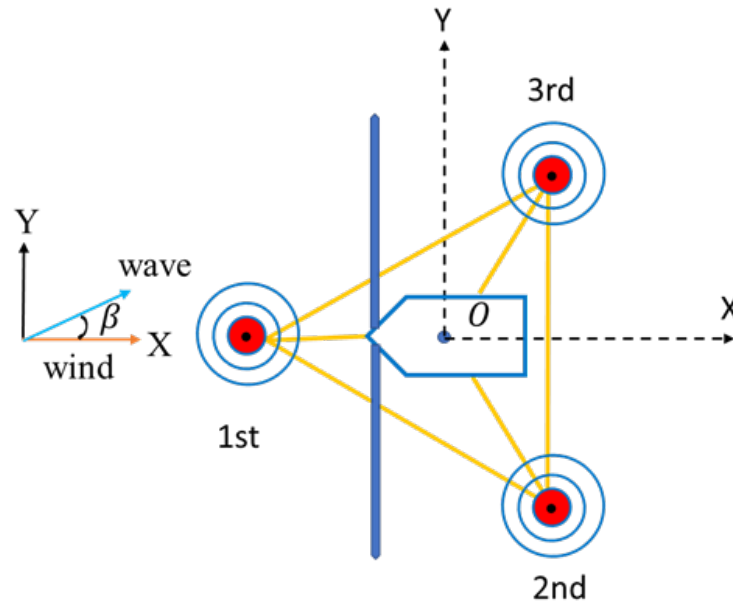


Figure 4.23: Diagram of the wind and wave alignment approach used.

because the influence of the wind is significantly higher than the impact of the waves on the system's motion. In addition, when the system is pitched to a large degree because of the wind, the mooring lines apply more force to the platform and reduce the impact of the wave motion. Both of these explanations account for why the impact of the TMD and TID are shown when only testing in waves but not when testing both wind and waves. Because of this, it is inconclusive at the moment what impact the TMD and TID have on the system under both wind and wave excitation.

## 4.6 Energy Harvesting Potential of the Tuned Inerter Damper

As previously discussed, one benefit of the TID configuration used in this study is that the inerter setup can be simplified to include an electrical generator in place of the inerter

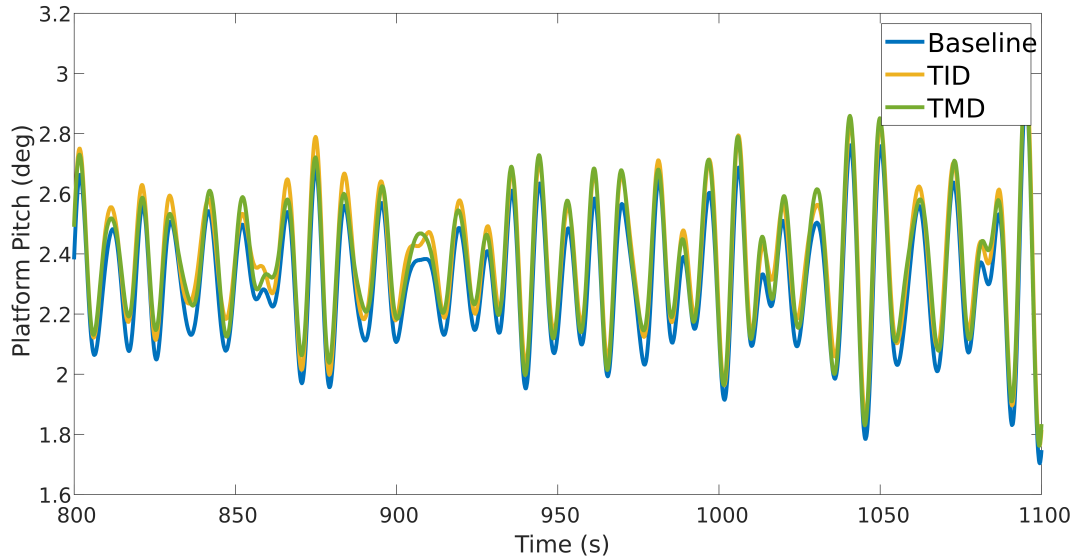


Figure 4.24: Time domain results for the baseline, TMD, and TID using a mass ratio of 3% with a JONSWAP wave with a period of 10 seconds and height of 3 meters and a 9 meter per second wind input with an angle of incidence of 0 degrees.

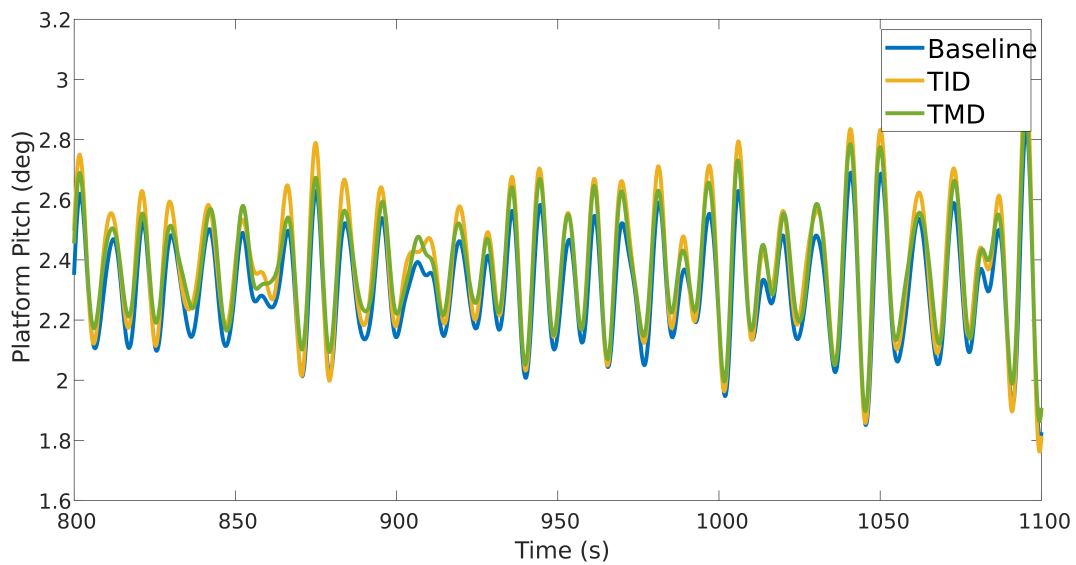


Figure 4.25: Time domain results for the baseline, TMD, and TID using a mass ratio of 3% with a JONSWAP wave with a period of 10 seconds and height of 3 meters and a 9 meter per second wind input with an angle of incidence of 30 degrees.

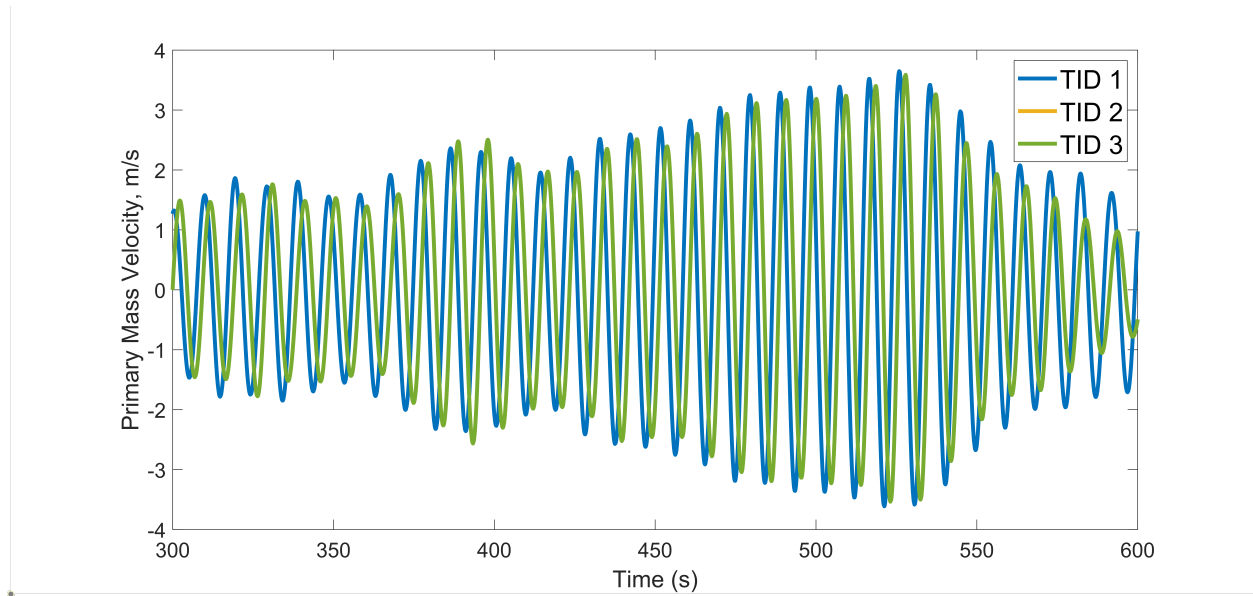


Figure 4.26: Velocity plot of the primary (m) mass in the TID in column 1 of the platform with a JONSWAP wave input of 10 s and 3 m.

and damper in parallel. This means that the TID has the potential to harvest additional electricity from the motion of the TID degree of freedom. Eq. 3.10 can be used to estimate the energy harvesting potential if the velocity of the TID is known. With the added capabilities presented in Section 3.2, the position and velocity of each TID was able to be tracked. Figs. 4.26 and 4.27 shows an example of this motion. Here the velocities of the three TIDs was tracked. In order to estimate the energy harvesting potential, the relative velocity between the primary and secondary masses would be plugged into Eq. 3.10 and multiplied by an electrical efficiency to account for any energy losses in converting the kinetic energy into electricity.

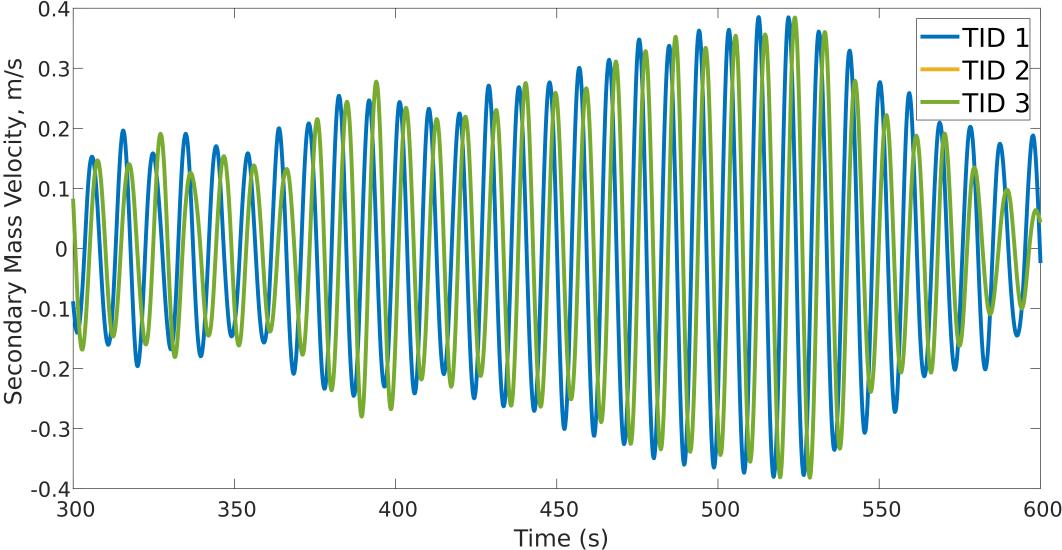


Figure 4.27: Velocity plot of the secondary (b) mass in the TID in column 1 of the platform with a JONSWAP wave input of 10 s and 3 m.

# Chapter 5

## Conclusions & Future Work

This study presented the results of building on the capabilities of the well-proven floating offshore wind turbine modeling software OpenFAST to allow it to include an inerter-based vibration absorber in the system's structural control. The results for the wind and wave simulations as well as the free decay tests show that the theory presented and the code modifications displayed operate as expected. The parameters for the vibration absorber were separately tuned to the system's natural frequency and the primary frequency of the incoming waves using a parametric study, and the performance of these configurations was displayed and shown to improve the performance of the system.

The overall findings of this study show that the TID code developed for OpenFAST operates as expected and shows that the TID does improve the on performance of the TMD in reducing the platform motion in certain cases. In addition, the TIDs were shown to be able to generate a usable amount of electricity based on the vibrational energy that they dissipated. There are a few limitations to this study, however.

First, it is important to mention that the results presented here are still for a model and will not entirely represent how the system will act in the real world. Factors such as friction, damage to the system, or other factors outside the scope of the model may cause the system to operate differently than what the results presented here may show. In addition, OpenFAST receives regular updates, so there may be future versions of OpenFAST that produce different results or fix bugs present in this version of OpenFAST (OpenFAST v3.2.1). In addition,

the

Next, the analysis discussed here is tailored toward a specific application of the updated OpenFAST code. A more generalized code could be created using the methods presented here, but, for the sake of this project, the TID was only modeled for the z-direction. In addition, this research focuses on three TIDs located within the semisubmersible platform. As discussed in Section 2, there are other studies that examined placing the TIDs in different locations within the system. Future work may want to examine using a general purpose version of this model to analyze placing TIDs of different orientations in other locations of the system. In addition, with this methodology, it should be possible to create versions of OpenFAST that can model other systems as long as the equations can be written in the same way as those in Section 2.6 and 3.

In addition, the system that the model represents is currently a passive system. This means that the system operates as-is and there are no external inputs to the system. An active control scheme for this type of system would control certain parameters to achieve optimal performance in multiple scenarios. This appears to be a good fit for the results of this type of system since the performance of the vibration absorber was heavily dependant on the operating conditions. For example, if the system is tuned to dampen the vibrations at the system's natural frequency, vibrations due to waves and wind will still impact the system negatively. If the system was able to actively tune itself to the dominant frequency, then it could address the largest contributor to the vibration at that time.

Work is being done to validate that the system will operate as expected in real world, scaled tests. a 1:50 scale model of the semisubmersible platform with functional TMDs and TIDs that can be placed in the platform is in development and will be tested soon. These results should help validate the model presented here. Overall, the system that this model is built for is still a concept and is not yet in practical development. The real system will need find

a way to replicate the model as closely as possible if the results from Section [4.2](#).

# Bibliography

- [1] “Windexchange,” 2023.
- [2] G. DNV, “Electrifying the future,” *DNV GL, Høvik*, 2014.
- [3] M. Borg and M. Collu, “A comparison between the dynamics of horizontal and vertical axis offshore floating wind turbines,” *Philosophical Transactions of the Royal Society A: Mathematical, Physical and Engineering Sciences*, vol. 373, no. 2035, p. 20140076, 2015.
- [4] W. Musial, “Offshore wind market report: 2022 edition,” report, US Department of Energy, 2022.
- [5] C. Coudurier, O. Lepreux, and N. Petit, “Modelling of a tuned liquid multi-column damper. application to floating wind turbine for improved robustness against wave incidence,” *Ocean Engineering*, vol. 165, pp. 277–292, 2018.
- [6] Y. Hu and M. Z. Chen, “Performance evaluation for inerter-based dynamic vibration absorbers,” *International Journal of Mechanical Sciences*, vol. 99, pp. 297–307, 2015.
- [7] Z. Zhang and C. Høeg, “Inerter-enhanced tuned mass damper for vibration damping of floating offshore wind turbines,” *Ocean Engineering*, vol. 223, p. 108663, 2021.
- [8] K. S. Banister, A. Weinstein, and D. Roddier, “Windwavefloat: Combining offshore wind turbines and wec in a single structure,”
- [9] M. A. Lackner and M. A. Rotea, “Structural control of floating wind turbines,” *Mechanics*, vol. 21, no. 4, pp. 704–719, 2011. Cited By :171 Export Date: 16 February 2022.

- [10] A. Robertson, J. Jonkman, M. Masciola, H. Song, A. Goupee, A. Coulling, and C. Luan, “Definition of the semisubmersible floating system for phase ii of oc4,” report, National Renewable Energy Lab.(NREL), Golden, CO (United States), 2014.
- [11] T. Stehly and P. Duffy, “2021 cost of wind energy review,” report, National Renewable Energy Laboratory, 2022.
- [12] M. Barooni, T. Ashuri, D. Velioglu Sogut, S. Wood, and S. Ghaderpour Taleghani, “Floating offshore wind turbines: Current status and future prospects,” *Energies*, vol. 16, no. 1, p. 2, 2022.
- [13] W. Musial, S. Butterfield, and B. Ram, “Energy from offshore wind,” in *Offshore Technology Conference*, Offshore Technology Conference.
- [14] L. A. Lara-Valencia, Y. Farbiarz-Farbiarz, and Y. Valencia-González, “Design of a tuned mass damper inerter (tmdi) based on an exhaustive search optimization for structural control of buildings under seismic excitations,” *Shock and Vibration*, vol. 2020, pp. 1–19, 2020.
- [15] F. Qian, Y. Luo, H. Sun, W. C. Tai, and L. Zuo, “Optimal tuned inerter dampers for performance enhancement of vibration isolation,” *Engineering Structures*, vol. 198, p. 109464, 2019.
- [16] X. Tong, X. Zhao, and A. Karcanias, “Passive vibration control of an offshore floating hydrostatic wind turbine model,” *Wind Energy*, vol. 21, no. 9, pp. 697–714, 2018. Cited By :10 Export Date: 8 December 2021.
- [17] X. Wei and X. Zhao, “Vibration suppression of a floating hydrostatic wind turbine model using bidirectional tuned liquid column mass damper,” *Wind Energy*, vol. 23, no. 10, pp. 1887–1904, 2020. Cited By :3 Export Date: 8 December 2021.

- [18] A. R. Henderson and D. Witcher, “Floating offshore wind energy—a review of the current status and an assessment of the prospects,” *Wind Engineering*, vol. 34, no. 1, pp. 1–16, 2010.
- [19] M. Leimeister, A. Kolios, and M. Collu, “Critical review of floating support structures for offshore wind farm deployment,” in *Journal of Physics: Conference Series*, vol. 1104, p. 012007, IOP Publishing.
- [20] F. Vorpahl, H. Schwarze, T. Fischer, M. Seidel, and J. Jonkman, “Offshore wind turbine environment, loads, simulation, and design,” *Wiley Interdisciplinary Reviews: Energy and Environment*, vol. 2, no. 5, pp. 548–570, 2013. Export Date: 19 April 2023; Cited By: 79; Correspondence Address: F. Vorpahl; Fraunhofer Institute for Wind Energy and Energy Systems Technology IWES, Bremerhaven, Germany; email: fabian.vorpahl@iwes.fraunhofer.de.
- [21] W. Weijtjens, N. Noppe, T. Verbelen, C. Devriendt, and A. Iliopoulos, *Fatigue life assessment of three offshore wind turbines*, pp. 742–747. CRC Press, 2016.
- [22] J. Li, W. Shi, L. Zhang, C. Michailides, and X. Li, “Wind–wave coupling effect on the dynamic response of a combined wind–wave energy converter,” *Journal of Marine Science and Engineering*, vol. 9, no. 10, 2021. Export Date: 3 November 2021.
- [23] R. Biswal and A. Mehmanparast, “Fatigue damage analysis of offshore wind turbine monopile weldments,” *Procedia Structural Integrity*, vol. 17, pp. 643–650, 2019.
- [24] A. Saenz-Aguirre, A. Ulazia, G. Ibarra-Berastegi, and J. Saenz, “Floating wind turbine energy and fatigue loads estimation according to climate period scaled wind and waves,” *Energy Conversion and Management*, vol. 271, p. 116303, 2022.
- [25] J. Gao, B. Sweetman, and S. Tang, “Multiaxial fatigue assessment of floating offshore

- wind turbine blades operating on compliant floating platforms,” *Ocean Engineering*, vol. 261, p. 111921, 2022.
- [26] S. Park, M. Glade, and M. A. Lackner, “Multi-objective optimization of orthogonal tlcds for reducing fatigue and extreme loads of a floating offshore wind turbine,” *Engineering Structures*, vol. 209, 2020. Cited By :10 Export Date: 8 December 2021.
- [27] W. Yu and P. W. Cheng, “Verification of a passive tuned liquid multi-column damper for floating wind turbine,” in *The 30th International Ocean and Polar Engineering Conference*, OnePetro.
- [28] M. Ghassempour, G. Failla, and F. Arena, “Vibration mitigation in offshore wind turbines via tuned mass damper,” *Engineering Structures*, vol. 183, pp. 610–636, 2019. Ghassempour, Mina Failla, Giuseppe Arena, Felice Arena, Felice/0000-0002-0517-1859 1873-7323.
- [29] M. L. Brodersen, A. S. Bjorke, and J. Hogsberg, “Active tuned mass damper for damping of offshore wind turbine vibrations,” *Wind Energy*, vol. 20, no. 5, pp. 783–796, 2017. Brodersen, Mark L. Bjorke, Ann-Sofie Hogsberg, Jan Hogsberg, Jan Becker/V-6894-2018 Hogsberg, Jan Becker/0000-0002-1098-3245 1099-1824.
- [30] J. Yang, E. M. He, and Y. Q. Hu, “Dynamic modeling and vibration suppression for an offshore wind turbine with a tuned mass damper in floating platform,” *Applied Ocean Research*, vol. 83, pp. 21–29, 2019. Yang, J. He, E. M. Hu, Y. Q. 1879-1549.
- [31] M. Hussan, M. S. Rahman, F. Sharmin, K. Dookie, and D. Jeongyun, “Multiple tuned mass damper for multi-mode vibration reduction of offshore wind turbine under seismic excitation,” *Ocean Engineering*, vol. 160, pp. 449–60, 2018. 18089366 multimode vibration reduction offshore wind turbine seismic excitation wind energy production

industry dynamic structural responses static wind wave loads root mean square fast Fourier transforms response surface methodology seismic hazard wind turbine structure design multimode control strategy.

- [32] R. Zhang, Z. Zhao, and K. Dai, “Seismic response mitigation of a wind turbine tower using a tuned parallel inerter mass system,” *Engineering Structures*, vol. 180, pp. 29–39, 2019.
- [33] Y. Hu, M. Z. Chen, Z. Shu, and L. Huang, “Analysis and optimisation for inerter-based isolators via fixed-point theory and algebraic solution,” *Journal of Sound and Vibration*, vol. 346, pp. 17–36, 2015.
- [34] Y. Shen, L. Chen, X. Yang, D. Shi, and J. Yang, “Improved design of dynamic vibration absorber by using the inerter and its application in vehicle suspension,” *Journal of Sound and Vibration*, vol. 361, pp. 148–158, 2016.
- [35] Y. Hu, J. Wang, M. Z. Chen, Z. Li, and Y. Sun, “Load mitigation for a barge-type floating offshore wind turbine via inerter-based passive structural control,” *Engineering Structures*, vol. 177, pp. 198–209, 2018.
- [36] Y. Li, S. Park, J. Z. Jiang, M. Lackner, S. Neild, and I. Ward, “Vibration suppression for monopile and spar-buoy offshore wind turbines using the structure-immittance approach,” *Wind Energy*, vol. 23, no. 10, pp. 1966–1985, 2020.
- [37] H. Zhu, C. Hu, M. Sueyoshi, and S. Yoshida, “Integration of a semisubmersible floating wind turbine and wave energy converters: an experimental study on motion reduction,” *Journal of Marine Science and Technology (Japan)*, vol. 25, no. 3, pp. 667–674, 2020.
- Export Date: 9 November 2021.

- [38] A. Aubault, M. Alves, A. n. Sarmiento, D. Roddier, and A. Peiffer, “Modeling of an oscillating water column on the floating foundation windfloat,” in *International Conference on Offshore Mechanics and Arctic Engineering*, vol. 44373, pp. 235–246.
- [39] A. Peiffer, D. Roddier, and A. Aubault, “Design of a point absorber inside the windfloat structure,” in *International Conference on Offshore Mechanics and Arctic Engineering*, vol. 44373, pp. 247–255.
- [40] J. M. Jonkman and P. D. Sclavounos, “Development of fully coupled aeroelastic and hydrodynamic models for offshore wind turbines,” vol. 16, pp. 11922–11942. Cited By :83 Export Date: 12 April 2022 Correspondence Address: Jonkman, J.M.; National Renewable Energy Laboratory (NREL), Golden, CO 80401-3393, United States.
- [41] J. M. Jonkman, “Dynamics of offshore floating wind turbines-model development and verification,” *Wind Energy*, vol. 12, no. 5, pp. 459–492, 2009. Cited By :286 Export Date: 8 December 2021.
- [42] A. J. Coulling, A. J. Goupee, A. N. Robertson, J. M. Jonkman, and H. J. Dagher, “Validation of a fast semi-submersible floating wind turbine numerical model with deepwind test data,” *Journal of Renewable and Sustainable Energy*, vol. 5, no. 2, 2013. Cited By :178 Export Date: 3 November 2021.
- [43] A. Jain, A. N. Robertson, J. M. Jonkman, A. J. Goupee, R. W. Kimball, and A. H. P. Swift, “Fast code verification of scaling laws for deepwind floating wind system tests,” in *Proceedings of the International Offshore and Polar Engineering Conference*, pp. 355–365. Cited By :40 Export Date: 3 November 2021.
- [44] W. La Cava and M. A. Lackner, “Theory manual for the tuned mass damper module in openfast.”

- [45] E. J. Haug, *Computer aided kinematics and dynamics of mechanical systems*, vol. 1. Allyn and Bacon Boston, 1989.

# Appendices

# Appendix A

## OpenFAST Input Files

### A.1 Main OpenFAST Input File

```

----- OpenFAST example INPUT FILE -----
FAST Certification Test #25: NREL 5.0 MW Baseline Wind Turbine with OC4-DeepCwind semi
configuration, for use in offshore analysis
----- SIMULATION CONTROL -----
True          Echo          - Echo input data to <RootName>.ech (flag)
"FATAL"       AbortLevel    - Error level when simulation should abort (string)
{"WARNING", "SEVERE", "FATAL"}
    1640      TMax          - Total run time (s)
    0.0125    DT           - Recommended module time step (s)
    2         InterpOrder   - Interpolation order for input/output time history (-)
{1=linear, 2=quadratic}
    0         NumCrctn      - Number of correction iterations (-) {0=explicit
calculation, i.e., no corrections}
    2.57      DT_UJac       - Time between calls to get Jacobians (s)
    1E+06     UJacSc1Fact   - Scaling factor used in Jacobians (-)
----- FEATURE SWITCHES AND FLAGS -----
    1         CompElast     - Compute structural dynamics (switch) {1=ElastoDyn;
2=ElastoDyn + BeamDyn for blades}
    0         CompInflow    - Compute inflow wind velocities (switch) {0=still air;
1=InflowWind; 2=external from OpenFOAM}
    0         CompAero      - Compute aerodynamic loads (switch) {0=None; 1=AeroDyn
v14; 2=AeroDyn v15}
    1         CompServo     - Compute control and electrical-drive dynamics (switch)
{0=None; 1=ServoDyn}
    1         CompHydro     - Compute hydrodynamic loads (switch) {0=None; 1=HydroDyn}
    0         CompSub       - Compute sub-structural dynamics (switch) {0=None;
1=SubDyn; 2=External Platform MCKF}
    3         CompMooring   - Compute mooring system (switch) {0=None; 1=MAP++;
2=FEAMooring; 3=MoorDyn; 4=OrcaFlex}
    0         CompIce       - Compute ice loads (switch) {0=None; 1=IceFloe; 2=IceDyn}
    0         MHK           - MHK turbine type (switch) {0=Not an MHK turbine; 1=Fixed
MHK turbine; 2=Floating MHK turbine}
----- ENVIRONMENTAL CONDITIONS -----
    9.80665   Gravity       - Gravitational acceleration (m/s^2)
    1.225     AirDens        - Air density (kg/m^3)
    1025      WtrDens        - Water density (kg/m^3)
    1.464E-05 KinVisc       - Kinematic viscosity of working fluid (m^2/s)
    335       SpdSound       - Speed of sound in working fluid (m/s)
    103500    Patm           - Atmospheric pressure (Pa) [used only for an MHK turbine
cavitation check]
    1700      Pvap           - Vapour pressure of working fluid (Pa) [used only for an
MHK turbine cavitation check]
    200       WtrDpth        - Water depth (m)
    0         MSL2SWL       - Offset between still-water level and mean sea level (m)
[positive upward]
----- INPUT FILES -----
"NRELOffshrBslne5MW_OC4DeepCwindSemi_ElastoDyn.dat"  EDFile          - Name of file
containing ElastoDyn input parameters (quoted string)
"unused"      BDBldFile(1)  - Name of file containing BeamDyn input parameters for
blade 1 (quoted string)
"unused"      BDBldFile(2)  - Name of file containing BeamDyn input parameters for
blade 2 (quoted string)
"unused"      BDBldFile(3)  - Name of file containing BeamDyn input parameters for
blade 3 (quoted string)
"../5MW_Baseline/NRELOffshrBslne5MW_InflowWind_steady12mps.dat"  InflowFile      -
Name of file containing inflow wind input parameters (quoted string)
"NRELOffshrBslne5MW_OC3Hywind_AeroDyn15.dat"      AeroFile         - Name of file
containing aerodynamic input parameters (quoted string)

```

```

"ServoDyn_with_StC.dat"   ServoFile       - Name of file containing control and
electrical-drive input parameters (quoted string)
"NRELOffshshrBslime5MW_OC4DeepCwindSemi_HydroDyn.dat"   HydroFile       - Name of file
containing hydrodynamic input parameters (quoted string)
"unused"      SubFile           - Name of file containing sub-structural input parameters
(quoted string)
"NRELOffshshrBslime5MW_OC4DeepCwindSemi_MoorDyn.dat"   MooringFile      - Name of file
containing mooring system input parameters (quoted string)
"unused"      IceFile           - Name of file containing ice input parameters (quoted
string)
----- OUTPUT -----
True          SumPrint         - Print summary data to "<RootName>.sum" (flag)
              1  SttsTime        - Amount of time between screen status messages (s)
              99999 ChkptTime     - Amount of time between creating checkpoint files for
potential restart (s)
              0.0125 DT_Out      - Time step for tabular output (s) (or "default")
              0  TStart         - Time to begin tabular output (s)
              0  OutFileFmt      - Format for tabular (time-marching) output file (switch)
{1: text file [<RootName>.out], 2: binary file [<RootName>.outb], 3: both}
True          TabDelim         - Use tab delimiters in text tabular output file? (flag)
{uses spaces if false}
"ES10.3E2"    OutFmt           - Format used for text tabular output, excluding the time
channel. Resulting field should be 10 characters. (quoted string)
----- LINEARIZATION -----
False         Linearize        - Linearization analysis (flag)
False         CalcSteady       - Calculate a steady-state periodic operating point before
linearization? [unused if Linearize=False] (flag)
              3  TrimCase       - Controller parameter to be trimmed {1:yaw; 2:torque;
3:pitch} [used only if CalcSteady=True] (-)
              0.001 TrimTol     - Tolerance for the rotational speed convergence [used only
if CalcSteady=True] (-)
              0.01  TrimGain     - Proportional gain for the rotational speed error (>0)
[used only if CalcSteady=True] (rad/(rad/s) for yaw or pitch; Nm/(rad/s) for torque)
              0  Twr_Kdmp       - Damping factor for the tower [used only if
CalcSteady=True] (N/(m/s))
              0  Bld_Kdmp       - Damping factor for the blades [used only if
CalcSteady=True] (N/(m/s))
              2  NLinTimes      - Number of times to linearize (-) [>=1] [unused if
Linearize=False]
              30,      60  LinTimes - List of times at which to linearize (s) [1
to NLinTimes] [used only when Linearize=True and CalcSteady=False]
              1  LinInputs      - Inputs included in linearization (switch) {0=none;
1=standard; 2=all module inputs (debug)} [unused if Linearize=False]
              1  LinOutputs     - Outputs included in linearization (switch) {0=none;
1=from OutList(s); 2=all module outputs (debug)} [unused if Linearize=False]
False         LinOutJac        - Include full Jacobians in linearization output (for
debug) (flag) [unused if Linearize=False; used only if LinInputs=LinOutputs=2]
False         LinOutMod        - Write module-level linearization output files in addition
to output for full system? (flag) [unused if Linearize=False]
----- VISUALIZATION -----
              0  WrVTK          - VTK visualization data output: (switch) {0=none;
1=initialization data only; 2=animation; 3=mode shapes}
              3  VTK_type       - Type of VTK visualization data: (switch) {1=surfaces;
2=basic meshes (lines/points); 3=all meshes (debug)} [unused if WrVTK=0]
False         VTK_fields       - Write mesh fields to VTK data files? (flag) {true/false}
[unused if WrVTK=0]
              10  VTK_fps       - Frame rate for VTK output (frames per second){will use
closest integer multiple of DT} [used only if WrVTK=2 or WrVTK=3]

```

## A.2 StC Input File

```

----- STRUCTURAL CONTROL (StC) INPUT FILE -----
Input file for tuned mass damper, module by Matt Lackner, Meghan Glade, and Semyung Park
(UMass)
----- SIMULATION CONTROL -----
True          Echo          - Echo input data to <RootName>.ech (flag)
----- StC DEGREES OF FREEDOM -----
          5  StC_DOF_MODE - DOF mode (switch) {0: No StC or TLCD DOF; 1: StC_X_DOF,
StC_Y_DOF, and/or StC_Z_DOF (three independent StC DOFs); 2: StC_XY_DOF (Omni-Directional
StC); 3: TLCD; 4: Prescribed force/moment time series}; 5: TID
false       StC_X_DOF      - DOF on or off for StC X (flag) [Used only when
StC_DOF_MODE=1]
false       StC_Y_DOF      - DOF on or off for StC Y (flag) [Used only when
StC_DOF_MODE=1]
true        StC_Z_DOF      - DOF on or off for StC Z (flag) [Used only when
StC_DOF_MODE=1]
----- StC LOCATION ----- [relative
to the reference origin of component attached to]
          14.435 StC_P_X      - At rest X position of StC (m)
           -25  StC_P_Y      - At rest Y position of StC (m)
            0   StC_P_Z      - At rest Z position of StC (m)
----- StC INITIAL CONDITIONS ----- [used
only when StC_DOF_MODE=1 or 2]
            0   StC_X_DSP      - StC X initial displacement (m) [relative to at rest
position]
            0   StC_Y_DSP      - StC Y initial displacement (m) [relative to at rest
position]
            0   StC_Z_DSP      - StC Z initial displacement (m) [relative to at rest
position; used only when StC_DOF_MODE=1 and StC_Z_DOF=TRUE]
"gravity"   StC_Z_PreLd      - StC Z pre-load (N) {"gravity" to offset for gravity load;
"none" or 0 to turn off} [used only when StC_DOF_MODE=1 and StC_Z_DOF=TRUE]
----- StC CONFIGURATION ----- [used
only when StC_DOF_MODE=1 or 2]
           10  StC_X_PSP      - Positive stop position (maximum X mass displacement) (m)
          -10  StC_X_NSP      - Negative stop position (minimum X mass displacement) (m)
           10  StC_Y_PSP      - Positive stop position (maximum Y mass displacement) (m)
          -10  StC_Y_NSP      - Negative stop position (minimum Y mass displacement) (m)
          10000 StC_Z_PSP      - Positive stop position (maximum Z mass displacement) (m)
[used only when StC_DOF_MODE=1 and StC_Z_DOF=TRUE]
          -10000 StC_Z_NSP      - Negative stop position (minimum Z mass displacement) (m)
[used only when StC_DOF_MODE=1 and StC_Z_DOF=TRUE]
----- StC MASS, STIFFNESS, & DAMPING ----- [used
only when StC_DOF_MODE=1 or 2]
            0   StC_X_M        - StC X mass (kg) [must equal StC_Y_M for StC_DOF_MODE = 2]
            0   StC_Y_M        - StC Y mass (kg) [must equal StC_X_M for StC_DOF_MODE = 2]
          375200 StC_Z_M        - StC Z mass (kg) [used only when StC_DOF_MODE=1 and
StC_Z_DOF=TRUE]
          19016 StC_b_M         - StC Inerter mass (kg) [used only when StC_DOF_MODE=5 and
StC_Z_DOF=TRUE]
            0   StC_XY_M        - StC XY mass (kg) [used only when StC_DOF_MODE=2]
            0   StC_X_K         - StC X stiffness (N/m)
            0   StC_Y_K         - StC Y stiffness (N/m)
          28554 StC_Z_K         - StC Z stiffness (N/m) [used only when StC_DOF_MODE=1 and
StC_Z_DOF=TRUE]
          1618 StC_b_K          - StC b stiffness (N/m) [used only when StC_DOF_MODE=1 and
StC_Z_DOF=TRUE]
            0   StC_X_C         - StC X damping (N/(m/s))
            0   StC_Y_C         - StC Y damping (N/(m/s))

```

1522 StC\_Z\_C - StC Z damping (N/(m/s)) [used only when StC\_DOF\_MODE=1 and StC\_Z\_DOF=TRUE or StC\_DOF\_MODE=5]  
 0 StC\_X\_KS - Stop spring X stiffness (N/m)  
 0 StC\_Y\_KS - Stop spring Y stiffness (N/m)  
 1500 StC\_Z\_KS - Stop spring Z stiffness (N/m) [used only when StC\_DOF\_MODE=1 and StC\_Z\_DOF=TRUE]  
 0 StC\_X\_CS - Stop spring X damping (N/(m/s))  
 0 StC\_Y\_CS - Stop spring Y damping (N/(m/s))  
 1000 StC\_Z\_CS - Stop spring Z damping (N/(m/s)) [used only when StC\_DOF\_MODE=1 and StC\_Z\_DOF=TRUE]

----- StC USER-DEFINED SPRING FORCES ----- [used only when StC\_DOF\_MODE=1 or 2]

False Use\_F\_TBL - Use spring force from user-defined table (flag)  
 17 NKInpSt - Number of spring force input stations

----- StC SPRING FORCES TABLE ----- [used only when StC\_DOF\_MODE=1 or 2]

X (m)	F_X (N)	Y (m)	F_Y (N)	Z (m)	F_Z (N)
-6.000000E+00	-4.800000E+06	-6.000000E+00	-4.800000E+06	-6.000000E+00	-
4.800000E+06					
-5.000000E+00	-2.400000E+06	-5.000000E+00	-2.400000E+06	-5.000000E+00	-
2.400000E+06					
-4.500000E+00	-1.200000E+06	-4.500000E+00	-1.200000E+06	-4.500000E+00	-
1.200000E+06					
-4.000000E+00	-6.000000E+05	-4.000000E+00	-6.000000E+05	-4.000000E+00	-
6.000000E+05					
-3.500000E+00	-3.000000E+05	-3.500000E+00	-3.000000E+05	-3.500000E+00	-
3.000000E+05					
-3.000000E+00	-1.500000E+05	-3.000000E+00	-1.500000E+05	-3.000000E+00	-
1.500000E+05					
-2.500000E+00	-1.000000E+05	-2.500000E+00	-1.000000E+05	-2.500000E+00	-
1.000000E+05					
-2.000000E+00	-6.500000E+04	-2.000000E+00	-6.500000E+04	-2.000000E+00	-
6.500000E+04					
0.000000E+00	0.000000E+00	0.000000E+00	0.000000E+00	0.000000E+00	
0.000000E+00					
2.000000E+00	6.500000E+04	2.000000E+00	6.500000E+04	2.000000E+00	
6.500000E+04					
2.500000E+00	1.000000E+05	2.500000E+00	1.000000E+05	2.500000E+00	
1.000000E+05					
3.000000E+00	1.500000E+05	3.000000E+00	1.500000E+05	3.000000E+00	
1.500000E+05					
3.500000E+00	3.000000E+05	3.500000E+00	3.000000E+05	3.500000E+00	
3.000000E+05					
4.000000E+00	6.000000E+05	4.000000E+00	6.000000E+05	4.000000E+00	
6.000000E+05					
4.500000E+00	1.200000E+06	4.500000E+00	1.200000E+06	4.500000E+00	
1.200000E+06					
5.000000E+00	2.400000E+06	5.000000E+00	2.400000E+06	5.000000E+00	
2.400000E+06					
6.000000E+00	4.800000E+06	6.000000E+00	4.800000E+06	6.000000E+00	
4.800000E+06					

----- StructCtrl CONTROL ----- [used only when StC\_DOF\_MODE=1 or 2]

0 StC\_CMODE - Control mode (switch) {0:none; 1: Semi-Active Control Mode; 4: Active Control Mode through Simulink (not available); 5: Active Control Mode through Bladed interface}

0 StC\_CChan - Control channel group (1:10) for stiffness and damping (StC\_[XYZ]\_K, StC\_[XYZ]\_C, and StC\_[XYZ]\_Brake) (specify additional channels for blade instances of StC active control -- one channel per blade) [used only when StC\_DOF\_MODE=1 or 2, and StC\_CMODE=4 or 5]

1 StC\_SA\_MODE - Semi-Active control mode {1: velocity-based ground hook control; 2: Inverse velocity-based ground hook control; 3: displacement-based ground hook control 4: Phase difference Algorithm with Friction Force 5: Phase difference Algorithm with Damping Force} (-)

0 StC\_X\_C\_HIGH - StC X high damping for ground hook control  
 0 StC\_X\_C\_LOW - StC X low damping for ground hook control  
 0 StC\_Y\_C\_HIGH - StC Y high damping for ground hook control  
 0 StC\_Y\_C\_LOW - StC Y low damping for ground hook control  
 0 StC\_Z\_C\_HIGH - StC Z high damping for ground hook control [used only when StC\_DOF\_MODE=1 and StC\_Z\_DOF=TRUE]  
 0 StC\_Z\_C\_LOW - StC Z low damping for ground hook control [used only when StC\_DOF\_MODE=1 and StC\_Z\_DOF=TRUE]

0 StC\_X\_C\_BRAKE - StC X high damping for braking the StC (Don't use it now. should be zero)  
 0 StC\_Y\_C\_BRAKE - StC Y high damping for braking the StC (Don't use it now. should be zero)  
 0 StC\_Z\_C\_BRAKE - StC Z high damping for braking the StC (Don't use it now. should be zero) [used only when StC\_DOF\_MODE=1 and StC\_Z\_DOF=TRUE]

----- TLCD ----- [used only when StC\_DOF\_MODE=3]

7.9325 L\_X - X TLCD total length (m)  
 6.5929 B\_X - X TLCD horizontal length (m)  
 2.0217 area\_X - X TLCD cross-sectional area of vertical column (m<sup>2</sup>)  
 0.913 area\_ratio\_X - X TLCD cross-sectional area ratio (vertical column area divided by horizontal column area) (-)  
 2.5265 headLossCoeff\_X - X TLCD head loss coeff (-)  
 1000 rho\_X - X TLCD liquid density (kg/m<sup>3</sup>)  
 3.5767 L\_Y - Y TLCD total length (m)  
 2.1788 B\_Y - Y TLCD horizontal length (m)  
 1.2252 area\_Y - Y TLCD cross-sectional area of vertical column (m<sup>2</sup>)  
 2.7232 area\_ratio\_Y - Y TLCD cross-sectional area ratio (vertical column area divided by horizontal column area) (-)  
 0.6433 headLossCoeff\_Y - Y TLCD head loss coeff (-)  
 1000 rho\_Y - Y TLCD liquid density (kg/m<sup>3</sup>)

----- PRESCRIBED TIME SERIES ----- [used only when StC\_DOF\_MODE=4]

1 PrescribedForcesCoord- Prescribed forces are in global or local coordinates (switch) {1: global; 2: local}  
 "TimeForceSeries.dat" PrescribedForcesFile - Time series force and moment (7 columns of time, FX, FY, FZ, MX, MY, MZ)

-----

### A.3 ServoDyn Input File

```

----- SERVODYN v1.05.* INPUT FILE -----
NREL 5.0 MW Baseline Wind Turbine for Use in Offshore Analysis. Properties from Dutch
Offshore Wind Energy Converter (DOWEC) 6MW Pre-Design (10046_009.pdf) and REpower 5M 5MW
(5m_uk.pdf)
----- SIMULATION CONTROL -----
False      Echo      - Echo input data to <RootName>.ech (flag)
"DEFAULT"  DT      - Communication interval for controllers (s) (or "default")
----- PITCH CONTROL -----
      0  PCMode      - Pitch control mode {0: none, 3: user-defined from routine
PitchCntrl, 4: user-defined from Simulink/Labview, 5: user-defined from Bladed-style DLL}
(switch)
      0  TPCOn      - Time to enable active pitch control (s) [unused when
PCMode=0]
      9999.9  TPitManS(1) - Time to start override pitch maneuver for blade 1 and end
standard pitch control (s)
      9999.9  TPitManS(2) - Time to start override pitch maneuver for blade 2 and end
standard pitch control (s)
      9999.9  TPitManS(3) - Time to start override pitch maneuver for blade 3 and end
standard pitch control (s) [unused for 2 blades]
      8  PitManRat(1) - Pitch rate at which override pitch maneuver heads toward
final pitch angle for blade 1 (deg/s)
      8  PitManRat(2) - Pitch rate at which override pitch maneuver heads toward
final pitch angle for blade 2 (deg/s)
      8  PitManRat(3) - Pitch rate at which override pitch maneuver heads toward
final pitch angle for blade 3 (deg/s) [unused for 2 blades]
      90  BlPitchF(1) - Blade 1 final pitch for pitch maneuvers (degrees)
      90  BlPitchF(2) - Blade 2 final pitch for pitch maneuvers (degrees)
      90  BlPitchF(3) - Blade 3 final pitch for pitch maneuvers (degrees) [unused
for 2 blades]
----- GENERATOR AND TORQUE CONTROL -----
      0  VSContrl    - Variable-speed control mode {0: none, 1: simple VS, 3: user-
defined from routine UserVSCont, 4: user-defined from Simulink/Labview, 5: user-defined
from Bladed-style DLL} (switch)
      2  GenModel    - Generator model {1: simple, 2: Thevenin, 3: user-defined
from routine UserGen} (switch) [used only when VSContrl=0]
      94.4  GenEff     - Generator efficiency [ignored by the Thevenin and user-
defined generator models] (%)
True      GenTiStr   - Method to start the generator {T: timed using TimGenOn, F:
generator speed using SpdGenOn} (flag)
True      GenTiStp   - Method to stop the generator {T: timed using TimGenOf, F:
when generator power = 0} (flag)
      9999.9  SpdGenOn - Generator speed to turn on the generator for a startup (HSS
speed) (rpm) [used only when GenTiStr=False]
      0  TimGenOn    - Time to turn on the generator for a startup (s) [used only
when GenTiStr=True]
      9999.9  TimGenOf - Time to turn off the generator (s) [used only when
GenTiStp=True]
----- SIMPLE VARIABLE-SPEED TORQUE CONTROL -----
      9999.9  VS_RtGnSp - Rated generator speed for simple variable-speed generator
control (HSS side) (rpm) [used only when VSContrl=1]
      9999.9  VS_RtTq   - Rated generator torque/constant generator torque in Region 3
for simple variable-speed generator control (HSS side) (N-m) [used only when VSContrl=1]
      9999.9  VS_Rgn2K   - Generator torque constant in Region 2 for simple variable-
speed generator control (HSS side) (N-m/rpm^2) [used only when VSContrl=1]
      9999.9  VS_SlPc    - Rated generator slip percentage in Region 2 1/2 for simple
variable-speed generator control (%) [used only when VSContrl=1]
----- SIMPLE INDUCTION GENERATOR -----

```

```

    9999.9  SIG_SlPc    - Rated generator slip percentage (%) [used only when
VSContrl=0 and GenModel=1]
    9999.9  SIG_SySp    - Synchronous (zero-torque) generator speed (rpm) [used only
when VSContrl=0 and GenModel=1]
    9999.9  SIG_RtTq    - Rated torque (N-m) [used only when VSContrl=0 and
GenModel=1]
    9999.9  SIG_PORT    - Pull-out ratio (Tpullout/Trated) (-) [used only when
VSContrl=0 and GenModel=1]
----- THEVENIN-EQUIVALENT INDUCTION GENERATOR -----
    9999.9  TEC_Freq    - Line frequency [50 or 60] (Hz) [used only when VSContrl=0
and GenModel=2]
    9998    TEC_NPo1    - Number of poles [even integer > 0] (-) [used only when
VSContrl=0 and GenModel=2]
    9999.9  TEC_SRes    - Stator resistance (ohms) [used only when VSContrl=0 and
GenModel=2]
    9999.9  TEC_RRes    - Rotor resistance (ohms) [used only when VSContrl=0 and
GenModel=2]
    9999.9  TEC_VLL    - Line-to-line RMS voltage (volts) [used only when VSContrl=0
and GenModel=2]
    9999.9  TEC_SLR    - Stator leakage reactance (ohms) [used only when VSContrl=0
and GenModel=2]
    9999.9  TEC_RLR    - Rotor leakage reactance (ohms) [used only when VSContrl=0
and GenModel=2]
    9999.9  TEC_MR     - Magnetizing reactance (ohms) [used only when VSContrl=0 and
GenModel=2]
----- HIGH-SPEED SHAFT BRAKE -----
    0      HSSBrMode    - HSS brake model {0: none, 1: simple, 3: user-defined from
routine UserHSSBr, 4: user-defined from Simulink/Labview, 5: user-defined from Bladed-
style DLL} (switch)
    9999.9  THSSBrDp    - Time to initiate deployment of the HSS brake (s)
    0.6     HSSBrDT     - Time for HSS-brake to reach full deployment once initiated
(sec) [used only when HSSBrMode=1]
    28116.2 HSSBrTqF    - Fully deployed HSS-brake torque (N-m)
----- NACELLE-YAW CONTROL -----
    0      YCMode      - Yaw control mode {0: none, 3: user-defined from routine
UserYawCont, 4: user-defined from Simulink/Labview, 5: user-defined from Bladed-style
DLL} (switch)
    9999.9  TYCOOn     - Time to enable active yaw control (s) [unused when YCMode=0]
    0      YawNeut     - Neutral yaw position--yaw spring force is zero at this yaw
(degrees)
    9.02832E+09 YawSpr    - Nacelle-yaw spring constant (N-m/rad)
    1.916E+07  YawDamp   - Nacelle-yaw damping constant (N-m/(rad/s))
    9999.9  TYawManS   - Time to start override yaw maneuver and end standard yaw
control (s)
    0.3     YawManRat   - Yaw maneuver rate (in absolute value) (deg/s)
    0      NacYawF     - Final yaw angle for override yaw maneuvers (degrees)
----- AERODYNAMIC FLOW CONTROL -----
    0      AfCmode     - Airfoil control mode {0: none, 1: cosine wave cycle, 4:
user-defined from Simulink/Labview, 5: user-defined from Bladed-style DLL} (switch)
    0      AfC_Mean    - Mean level for cosine cycling or steady value (-) [used only
with AfCmode==1]
    0      AfC_Amp     - Amplitude for for cosine cycling of flap signal (-) [used
only with AfCmode==1]
    0      AfC_Phase   - Phase relative to the blade azimuth (0 is vertical) for for
cosine cycling of flap signal (deg) [used only with AfCmode==1]
----- STRUCTURAL CONTROL -----
    0      NumBStC     - Number of blade structural controllers (integer)

```

```

"unused"      BStCfiles   - Name of the files for blade structural controllers (quoted
strings) [unused when NumBStC==0]
0             NumNStC    - Number of nacelle structural controllers (integer)
"unused"      NStCfiles   - Name of the files for nacelle structural controllers (quoted
strings) [unused when NumNStC==0]
0             NumTStC    - Number of tower structural controllers (integer)
"unused"      TStCfiles   - Name of the files for tower structural controllers (quoted
strings) [unused when NumTStC==0]
3             NumSStC    - Number of substructure structural controllers (integer)
"StC-Sub-Zdof-1.dat" "StC-Sub-Zdof-2.dat" "StC-Sub-Zdof-3.dat" SStCfiles - Name of
the files for substructure structural controllers (quoted strings) [unused when
NumSStC==0]
----- CABLE CONTROL -----
0             CCmode     - Cable control mode {0: none, 4: user-defined from
Simulink/Labview, 5: user-defined from Bladed-style DLL} (switch)
----- BLADED INTERFACE ----- [used
only with Bladed Interface]
"./5MW_Baseline/ServoData/DISCON_OC3Hywind.dll" DLL_FileName - Name/location of the
dynamic library {.dll [Windows] or .so [Linux]} in the Bladed-DLL format (-) [used only
with Bladed Interface]
"DISCON.IN"   DLL_InFile  - Name of input file sent to the DLL (-) [used only with
Bladed Interface]
"DISCON"      DLL_ProcName - Name of procedure in DLL to be called (-) [case sensitive;
used only with DLL Interface]
"default"     DLL_DT      - Communication interval for dynamic library (s) (or
"default") [used only with Bladed Interface]
false         DLL_Ramp    - Whether a linear ramp should be used between DLL_DT time
steps [introduces time shift when true] (flag) [used only with Bladed Interface]
9999.9        BPCutoff    - Cutoff frequency for low-pass filter on blade pitch from DLL
(Hz) [used only with Bladed Interface]
0             NacYaw_North - Reference yaw angle of the nacelle when the upwind end
points due North (deg) [used only with Bladed Interface]
0             Ptch_Cntrl  - Record 28: Use individual pitch control {0: collective
pitch; 1: individual pitch control} (switch) [used only with Bladed Interface]
0             Ptch_SetPnt - Record 5: Below-rated pitch angle set-point (deg) [used
only with Bladed Interface]
0             Ptch_Min    - Record 6: Minimum pitch angle (deg) [used only with Bladed
Interface]
0             Ptch_Max    - Record 7: Maximum pitch angle (deg) [used only with Bladed
Interface]
0             PtchRate_Min - Record 8: Minimum pitch rate (most negative value allowed)
(deg/s) [used only with Bladed Interface]
0             PtchRate_Max - Record 9: Maximum pitch rate (deg/s) [used only with
Bladed Interface]
0             Gain_OM     - Record 16: Optimal mode gain (Nm/(rad/s)^2) [used only with
Bladed Interface]
0             GenSpd_MinOM - Record 17: Minimum generator speed (rpm) [used only with
Bladed Interface]
0             GenSpd_MaxOM - Record 18: Optimal mode maximum speed (rpm) [used only with
Bladed Interface]
0             GenSpd_Dem   - Record 19: Demanded generator speed above rated (rpm) [used
only with Bladed Interface]
0             GenTrq_Dem   - Record 22: Demanded generator torque above rated (Nm) [used
only with Bladed Interface]
0             GenPwr_Dem   - Record 13: Demanded power (W) [used only with Bladed
Interface]
----- BLADED INTERFACE TORQUE-SPEED LOOK-UP TABLE -----

```

0 DLL\_NumTrq - Record 26: No. of points in torque-speed look-up table {0 = none and use the optimal mode parameters; nonzero = ignore the optimal mode PARAMETERS by setting Record 16 to 0.0} (-) [used only with Bladed Interface]

GenSpd\_TLU GenTrq\_TLU  
(rpm) (Nm)

----- OUTPUT -----  
True SumPrint - Print summary data to <RootName>.sum (flag) (currently unused)  
2 OutFile - Switch to determine where output will be placed: {1: in module output file only; 2: in glue code output file only; 3: both} (currently unused)  
True TabDelim - Use tab delimiters in text tabular output file? (flag) (currently unused)  
"ES10.3E2" OutFmt - Format used for text tabular output (except time). Resulting field should be 10 characters. (quoted string) (currently unused)  
0 TStart - Time to begin tabular output (s) (currently unused)  
OutList - The next line(s) contains a list of output parameters. See OutListParameters.xlsx for a listing of available output channels, (-)  
"GenPwr" - Electrical generator power  
"GenTq" - Electrical generator torque  
"SStC1\_XQ"  
"SStC1\_XQD"  
"SStC1\_YQ"  
"SStC1\_YQD"  
"SStC1\_ZQ"  
"SStC1\_ZQD"  
"SStC1\_bQ"  
"SStC1\_bQD"  
"SStC1\_Fxi"  
"SStC1\_Fyi"  
"SStC1\_Fzi"  
"SStC1\_Mxi"  
"SStC1\_Myi"  
"SStC1\_Mzi"  
"SStC1\_Fx1"  
"SStC1\_Fy1"  
"SStC1\_Fz1"  
"SStC1\_Mx1"  
"SStC1\_My1"  
"SStC1\_Mz1"  
"SStC2\_XQ"  
"SStC2\_XQD"  
"SStC2\_YQ"  
"SStC2\_YQD"  
"SStC2\_ZQ"  
"SStC2\_ZQD"  
"SStC2\_bQ"  
"SStC2\_bQD"  
"SStC2\_Fxi"  
"SStC2\_Fyi"  
"SStC2\_Fzi"  
"SStC2\_Mxi"  
"SStC2\_Myi"  
"SStC2\_Mzi"  
"SStC2\_Fx1"  
"SStC2\_Fy1"  
"SStC2\_Fz1"  
"SStC2\_Mx1"  
"SStC2\_My1"

"SStC2\_Mz1"  
"SStC3\_XQ"  
"SStC3\_XQD"  
"SStC3\_YQ"  
"SStC3\_YQD"  
"SStC3\_ZQ"  
"SStC3\_ZQD"  
"SStC3\_bQ"  
"SStC3\_bQD"  
"SStC3\_Fxi"  
"SStC3\_Fyi"  
"SStC3\_Fzi"  
"SStC3\_Mxi"  
"SStC3\_Myi"  
"SStC3\_Mzi"  
"SStC3\_Fx1"  
"SStC3\_Fy1"  
"SStC3\_Fz1"  
"SStC3\_Mx1"  
"SStC3\_My1"  
"SStC3\_Mz1"

END of input file (the word "END" must appear in the first 3 columns of this last OutList line)

-----

## A.4 Elastodyn Input File

----- ELASTODYN for OpenFAST INPUT FILE -----  
 NREL 5.0 MW Baseline Wind Turbine for Use in Offshore Analysis. Properties from Dutch Offshore Wind Energy Converter (DOWEC) 6MW Pre-Design (10046\_009.pdf) and REpower 5M 5MW (5m\_uk.pdf).

----- SIMULATION CONTROL -----  
 False Echo - Echo input data to "<RootName>.ech" (flag)  
 3 Method - Integration method: {1: RK4, 2: AB4, or 3: ABM4} (-)  
 "DEFAULT" DT - Integration time step (s)

----- DEGREES OF FREEDOM -----  
 False FlapDOF1 - First flapwise blade mode DOF (flag)  
 False FlapDOF2 - Second flapwise blade mode DOF (flag)  
 False EdgeDOF - First edgewise blade mode DOF (flag)  
 False TeetDOF - Rotor-teeter DOF (flag) [unused for 3 blades]  
 False DrTrDOF - Drivetrain rotational-flexibility DOF (flag)  
 False GenDOF - Generator DOF (flag)  
 False YawDOF - Yaw DOF (flag)  
 True TwFADOF1 - First fore-aft tower bending-mode DOF (flag)  
 True TwFADOF2 - Second fore-aft tower bending-mode DOF (flag)  
 True TwSSDOF1 - First side-to-side tower bending-mode DOF (flag)  
 True TwSSDOF2 - Second side-to-side tower bending-mode DOF (flag)  
 True PtfmSgDOF - Platform horizontal surge translation DOF (flag)  
 True PtfmSwDOF - Platform horizontal sway translation DOF (flag)  
 True PtfmHvDOF - Platform vertical heave translation DOF (flag)  
 True PtfmRDOF - Platform roll tilt rotation DOF (flag)  
 True PtfmPDOF - Platform pitch tilt rotation DOF (flag)  
 True PtfmYDOF - Platform yaw rotation DOF (flag)

----- INITIAL CONDITIONS -----  
 0 OopDefl - Initial out-of-plane blade-tip displacement (meters)  
 0 IPDefl - Initial in-plane blade-tip deflection (meters)  
 0 BlPitch(1) - Blade 1 initial pitch (degrees)  
 0 BlPitch(2) - Blade 2 initial pitch (degrees)  
 0 BlPitch(3) - Blade 3 initial pitch (degrees) [unused for 2 blades]  
 0 TeetDefl - Initial or fixed teeter angle (degrees) [unused for 3 blades]  
 0 Azimuth - Initial azimuth angle for blade 1 (degrees)  
 0 RotSpeed - Initial or fixed rotor speed (rpm)  
 0 NacYaw - Initial or fixed nacelle-yaw angle (degrees)  
 0 TTDspFA - Initial fore-aft tower-top displacement (meters)  
 0 TTDspSS - Initial side-to-side tower-top displacement (meters)  
 0 PtfmSurge - Initial or fixed horizontal surge translational displacement  
 of platform (meters)  
 0 PtfmSway - Initial or fixed horizontal sway translational displacement  
 of platform (meters)  
 0 PtfmHeave - Initial or fixed vertical heave translational displacement of  
 platform (meters)  
 0 PtfmRoll - Initial or fixed roll tilt rotational displacement of  
 platform (degrees)  
 2 PtfmPitch - Initial or fixed pitch tilt rotational displacement of  
 platform (degrees)  
 0 PtfmYaw - Initial or fixed yaw rotational displacement of platform  
 (degrees)

----- TURBINE CONFIGURATION -----  
 3 NumBl - Number of blades (-)  
 63 TipRad - The distance from the rotor apex to the blade tip (meters)  
 1.5 HubRad - The distance from the rotor apex to the blade root (meters)  
 -2.5 PreCone(1) - Blade 1 cone angle (degrees)  
 -2.5 PreCone(2) - Blade 2 cone angle (degrees)  
 -2.5 PreCone(3) - Blade 3 cone angle (degrees) [unused for 2 blades]

0	HubCM	- Distance from rotor apex to hub mass [positive downwind]
(meters)		
0	UndSling	- Undersling length [distance from teeter pin to the rotor apex] (meters) [unused for 3 blades]
0	Delta3	- Delta-3 angle for teetering rotors (degrees) [unused for 3 blades]
0	AzimB1Up	- Azimuth value to use for I/O when blade 1 points up (degrees)
-5.0191	OverHang	- Distance from yaw axis to rotor apex [3 blades] or teeter pin [2 blades] (meters)
1.912	ShftGagL	- Distance from rotor apex [3 blades] or teeter pin [2 blades] to shaft strain gages [positive for upwind rotors] (meters)
-5	ShftTilt	- Rotor shaft tilt angle (degrees)
1.9	NacCMxn	- Downwind distance from the tower-top to the nacelle CM (meters)
0	NacCMyn	- Lateral distance from the tower-top to the nacelle CM (meters)
1.75	NacCMzn	- Vertical distance from the tower-top to the nacelle CM (meters)
-3.09528	NcIMUxn	- Downwind distance from the tower-top to the nacelle IMU (meters)
0	NcIMUyn	- Lateral distance from the tower-top to the nacelle IMU (meters)
2.23336	NcIMUzn	- Vertical distance from the tower-top to the nacelle IMU (meters)
1.96256	Twr2Shft	- Vertical distance from the tower-top to the rotor shaft (meters)
87.6	TowerHt	- Height of tower above ground level [onshore] or MSL [offshore] (meters)
10	TowerBsHt	- Height of tower base above ground level [onshore] or MSL [offshore] (meters)
0	PtfmCMxt	- Downwind distance from the ground level [onshore] or MSL [offshore] to the platform CM (meters)
0	PtfmCMyt	- Lateral distance from the ground level [onshore] or MSL [offshore] to the platform CM (meters)
-8.6588	PtfmCMzt	- Vertical distance from the ground level [onshore] or MSL [offshore] to the platform CM (meters)
0	PtfmRefzt	- Vertical distance from the ground level [onshore] or MSL [offshore] to the platform reference point (meters)
----- MASS AND INERTIA -----		
0	TipMass(1)	- Tip-brake mass, blade 1 (kg)
0	TipMass(2)	- Tip-brake mass, blade 2 (kg)
0	TipMass(3)	- Tip-brake mass, blade 3 (kg) [unused for 2 blades]
56780	HubMass	- Hub mass (kg)
115926	HubIner	- Hub inertia about rotor axis [3 blades] or teeter axis [2 blades] (kg m <sup>2</sup> )
534.116	GenIner	- Generator inertia about HSS (kg m <sup>2</sup> )
240000	NacMass	- Nacelle mass (kg)
2.60789E+06	NacYIner	- Nacelle inertia about yaw axis (kg m <sup>2</sup> )
0	YawBrMass	- Yaw bearing mass (kg)
3852180	PtfmMass	- Platform mass (kg)
2.56193E+09	PtfmRIner	- Platform inertia for roll tilt rotation about the platform CM (kg m <sup>2</sup> )
2.56193E+09	PtfmPIner	- Platform inertia for pitch tilt rotation about the platform CM (kg m <sup>2</sup> )
4.24265E+09	PtfmYIner	- Platform inertia for yaw rotation about the platform CM (kg m <sup>2</sup> )
----- BLADE -----		
17	BldNodes	- Number of blade nodes (per blade) used for analysis (-)

```

"../5MW_Baseline/NRELOffshrBslne5MW_Blade.dat"    BldFile(1) - Name of file containing
properties for blade 1 (quoted string)
"../5MW_Baseline/NRELOffshrBslne5MW_Blade.dat"    BldFile(2) - Name of file containing
properties for blade 2 (quoted string)
"../5MW_Baseline/NRELOffshrBslne5MW_Blade.dat"    BldFile(3) - Name of file containing
properties for blade 3 (quoted string) [unused for 2 blades]
-----
      0 TeetMod      - Rotor-teeter spring/damper model {0: none, 1: standard, 2:
user-defined from routine UserTeet} (switch) [unused for 3 blades]
      0 TeetDmpP     - Rotor-teeter damper position (degrees) [used only for 2
blades and when TeetMod=1]
      0 TeetDmp      - Rotor-teeter damping constant (N-m/(rad/s)) [used only for 2
blades and when TeetMod=1]
      0 TeetCDmp     - Rotor-teeter rate-independent Coulomb-damping moment (N-m)
[used only for 2 blades and when TeetMod=1]
      0 TeetSStP     - Rotor-teeter soft-stop position (degrees) [used only for 2
blades and when TeetMod=1]
      0 TeetHStP     - Rotor-teeter hard-stop position (degrees) [used only for 2
blades and when TeetMod=1]
      0 TeetSSSp     - Rotor-teeter soft-stop linear-spring constant (N-m/rad) [used
only for 2 blades and when TeetMod=1]
      0 TeetHSSp     - Rotor-teeter hard-stop linear-spring constant (N-m/rad) [used
only for 2 blades and when TeetMod=1]
-----
      100 GBoxEff     - Gearbox efficiency (%)
      97  GBRatio     - Gearbox ratio (-)
8.67637E+08 DTTorSpr  - Drivetrain torsional spring (N-m/rad)
6.215E+06  DTTorDmp  - Drivetrain torsional damper (N-m/(rad/s))
-----
      False Furling   - Read in additional model properties for furling turbine
(flag) [must currently be FALSE]
"unused"   FurlFile  - Name of file containing furling properties (quoted string)
[unused when Furling=False]
-----
      20 TwrNodes    - Number of tower nodes used for analysis (-)
"NRELOffshrBslne5MW_OC4DeepCwindSemi_ElastoDyn_Tower.dat" TwrFile  - Name of file
containing tower properties (quoted string)
-----
      True  SumPrint  - Print summary data to "<RootName>.sum" (flag)
      2    OutFile   - Switch to determine where output will be placed: {1: in
module output file only; 2: in glue code output file only; 3: both} (currently unused)
      True  TabDelim  - Use tab delimiters in text tabular output file? (flag)
(currently unused)
"ES10.3E2" OutFmt    - Format used for text tabular output (except time). Resulting
field should be 10 characters. (quoted string) (currently unused)
      0    TStart    - Time to begin tabular output (s) (currently unused)
      1    DecFact   - Decimation factor for tabular output {1: output every time
step} (-) (currently unused)
      1    NTwGages  - Number of tower nodes that have strain gages for output [0 to
9] (-)
      10   TwrGagNd  - List of tower nodes that have strain gages [1 to TwrNodes] (-
) [unused if NTwGages=0]
      1    NBlGages  - Number of blade nodes that have strain gages for output [0 to
9] (-)
      9    BldGagNd  - List of blade nodes that have strain gages [1 to BldNodes] (-
) [unused if NBlGages=0]
      OutList - The next line(s) contains a list of output parameters. See
OutListParameters.xlsx for a listing of available output channels, (-)

```

"Azimuth" - Blade 1 azimuth angle  
"RotSpeed" - Low-speed shaft speed  
"GenSpeed" - High-speed shaft speed  
"OoPDefl1" - Blade 1 out-of-plane deflection  
"IPDefl1" - Blade 1 in-plane deflection  
"TwstDefl1" - Blade 1 tip twist  
"BldPitch1" - Blade 1 pitch angle  
"TTDspFA" - Tower fore-aft deflection  
"TTDspSS" - Tower side-to-side deflection  
"TTDspTwst" - Tower top twist  
"PtfmSurge" - Platform translational surge displacement  
"PtfmSway" - Platform translational sway displacement  
"PtfmHeave" - Platform translational heave displacement  
"PtfmRoll" - Platform rotational roll displacement  
"PtfmPitch" - Platform rotational pitch displacement  
"PtfmYaw" - Platform rotational yaw displacement  
END of input file (the word "END" must appear in the first 3 columns of this last OutList line)  
-----

## A.5 HydroDyn Input File

```

----- HydroDyn Input File -----
NREL 5.0 MW offshore baseline floating platform HydroDyn input properties for the OC4
Semi-submersible.
False          Echo          - Echo the input file data (flag)
----- ENVIRONMENTAL CONDITIONS -----
"default"     WtrDens          - Water density (kg/m^3)
"default"     WtrDpth          - Water depth (meters)
"default"     MSL2SWL         - Offset between still-water level and mean sea level
(meters) [positive upward; unused when WaveMod = 6; must be zero if PotMod=1 or 2]
----- WAVES -----
0 WaveMod      - Incident wave kinematics model {0: none=still water, 1:
regular (periodic), 1P#: regular with user-specified phase, 2: JONSWAP/Pierson-Moskowitz
spectrum (irregular), 3: White noise spectrum (irregular), 4: user-defined spectrum from
routine UserWaveSpctrm (irregular), 5: Externally generated wave-elevation time series,
6: Externally generated full wave-kinematics time series [option 6 is invalid for
PotMod/=0]} (switch)
0 WaveStMod    - Model for stretching incident wave kinematics to
instantaneous free surface {0: none=no stretching, 1: vertical stretching, 2:
extrapolation stretching, 3: Wheeler stretching} (switch) [unused when WaveMod=0 or when
PotMod/=0]
4600 WaveTMax  - Analysis time for incident wave calculations (sec)
[unused when WaveMod=0; determines WaveDOmega=2Pi/WaveTMax in the IFFT]
0.2 WaveDT     - Time step for incident wave calculations (sec)
[unused when WaveMod=0; 0.1<=WaveDT<=1.0 recommended; determines WaveOmegaMax=Pi/WaveDT
in the IFFT]
3 WaveHs       - Significant wave height of incident waves (meters)
[used only when WaveMod=1, 2, or 3]
10 WaveTp      - Peak-spectral period of incident waves (sec)
[used only when WaveMod=1 or 2]
"DEFAULT"     WavePkShp       - Peak-shape parameter of incident wave spectrum (-) or
DEFAULT (string) [used only when WaveMod=2; use 1.0 for Pierson-Moskowitz]
0.314159 WvLowCOff - Low cut-off frequency or lower frequency limit of the
wave spectrum beyond which the wave spectrum is zeroed (rad/s) [unused when WaveMod=0, 1,
or 6]
1.570796 WvHiCOff - High cut-off frequency or upper frequency limit of the
wave spectrum beyond which the wave spectrum is zeroed (rad/s) [unused when WaveMod=0, 1,
or 6]
0 WaveDir      - Incident wave propagation heading direction
(degrees) [unused when WaveMod=0 or 6]
0 WaveDirMod   - Directional spreading function {0: none, 1: COS2S}
(-) [only used when WaveMod=2,3, or 4]
1 WaveDirSpread - Wave direction spreading coefficient ( > 0 )
(-) [only used when WaveMod=2,3, or 4 and WaveDirMod=1]
1 WaveNDir     - Number of wave directions
(-) [only used when WaveMod=2,3, or 4 and WaveDirMod=1; odd number only]
0 WaveDirRange - Range of wave directions (full range: WaveDir +/-
1/2*WaveDirRange) (degrees) [only used when WaveMod=2,3,or 4 and WaveDirMod=1]
123456789 WaveSeed(1) - First random seed of incident waves [-2147483648 to
2147483647] (-) [unused when WaveMod=0, 5, or 6]
RANLUX WaveSeed(2) - Second random seed of incident waves [-2147483648 to
2147483647] for intrinsic pRNG, or an alternative pRNG: "RanLux" (-) [unused
when WaveMod=0, 5, or 6]
FALSE WaveNDamp - Flag for normally distributed amplitudes
(flag) [only used when WaveMod=2, 3, or 4]
"" WvKinFile    - Root name of externally generated wave data file(s)
(quoted string) [used only when WaveMod=5 or 6]
1 NWaveElev    - Number of points where the incident wave elevations can
be computed (-) [maximum of 9 output locations]

```

```

    0 WaveElevxi - List of xi-coordinates for points where the incident
wave elevations can be output (meters) [NWaveElev points, separated by commas or white
space; unused if NWaveElev = 0]
    0 WaveElevyi - List of yi-coordinates for points where the incident
wave elevations can be output (meters) [NWaveElev points, separated by commas or white
space; unused if NWaveElev = 0]
----- 2ND-ORDER WAVES ----- [unused
with WaveMod=0 or 6]
FALSE WvDiffQTF - Full difference-frequency 2nd-order wave kinematics
(flag)
FALSE WvSumQTF - Full summation-frequency 2nd-order wave kinematics
(flag)
    0 WvLowCOFFD - Low frequency cutoff used in the difference-
frequencies (rad/s) [Only used with a difference-frequency method]
    1.256637 WvHiCOFFD - High frequency cutoff used in the difference-
frequencies (rad/s) [Only used with a difference-frequency method]
    0.618319 WvLowCOFFS - Low frequency cutoff used in the summation-frequencies
(rad/s) [Only used with a summation-frequency method]
    3.141593 WvHiCOFFS - High frequency cutoff used in the summation-frequencies
(rad/s) [Only used with a summation-frequency method]
----- CURRENT ----- [unused
with WaveMod=6]
    0 CurrMod - Current profile model {0: none=no current, 1: standard,
2: user-defined from routine UserCurrent} (switch)
    0 CurrSSV0 - Sub-surface current velocity at still water level
(m/s) [used only when CurrMod=1]
"DEFAULT" CurrSSDir - Sub-surface current heading direction (degrees) or
DEFAULT (string) [used only when CurrMod=1]
    20 CurrNSRef - Near-surface current reference depth
(meters) [used only when CurrMod=1]
    0 CurrNSV0 - Near-surface current velocity at still water level
(m/s) [used only when CurrMod=1]
    0 CurrNSDir - Near-surface current heading direction
(degrees) [used only when CurrMod=1]
    0 CurrDIV - Depth-independent current velocity
(m/s) [used only when CurrMod=1]
    0 CurrDIDir - Depth-independent current heading direction
(degrees) [used only when CurrMod=1]
----- FLOATING PLATFORM ----- [unused
with WaveMod=6]
    1 PotMod - Potential-flow model {0: none=no potential flow, 1:
frequency-to-time-domain transforms based on WAMIT output, 2: fluid-impulse theory (FIT)}
(switch)
    1 ExctnMod - Wave-excitation model {0: no wave-excitation
calculation, 1: DFT, 2: state-space} (switch) [only used when PotMod=1; STATE-SPACE
REQUIRES *.ssxctn INPUT FILE]
    1 RdtMod - Radiation memory-effect model {0: no memory-effect
calculation, 1: convolution, 2: state-space} (switch) [only used when PotMod=1; STATE-
SPACE REQUIRES *.ss INPUT FILE]
    60 RdtTMax - Analysis time for wave radiation kernel calculations
(sec) [only used when PotMod=1 and RdtMod=1; determines RdtDOmega=Pi/RdtTMax in the
cosine transform; MAKE SURE THIS IS LONG ENOUGH FOR THE RADIATION IMPULSE RESPONSE
FUNCTIONS TO DECAY TO NEAR-ZERO FOR THE GIVEN PLATFORM!]
    0.0125 RdtDT - Time step for wave radiation kernel calculations (sec)
[only used when PotMod=1 and ExctnMod>1 or RdtMod>0; DT<=RdtDT<=0.1 recommended;
determines RdtDOmegaMax=Pi/RdtDT in the cosine transform]
    1 NBody - Number of WAMIT bodies to be used (-) [>=1; only used
when PotMod=1. If NBodyMod=1, the WAMIT data contains a vector of size 6*NBody x 1 and

```

matrices of size  $6 \times N_{Body}$  x  $6 \times N_{Body}$ ; if  $N_{BodyMod} > 1$ , there are  $N_{Body}$  sets of WAMIT data each with a vector of size  $6 \times 1$  and matrices of size  $6 \times 6$

1  $N_{BodyMod}$  - Body coupling model {1: include coupling terms between each body and  $N_{Body}$  in HydroDyn equals  $N_{BODY}$  in WAMIT, 2: neglect coupling terms between each body and  $N_{BODY}=1$  with  $X_{BODY}=0$  in WAMIT, 3: Neglect coupling terms between each body and  $N_{BODY}=1$  with  $X_{BODY}=/0$  in WAMIT} (switch) [only used when  $PotMod=1$ ]

"../5MW\_Baseline/HydroData/marin\_semi" PotFile - Root name of potential-flow model data; WAMIT output files containing the linear, nondimensionalized, hydrostatic restoring matrix (.hst), frequency-dependent hydrodynamic added mass matrix and damping matrix (.1), and frequency- and direction-dependent wave excitation force vector per unit wave amplitude (.3) (quoted string) [1 to  $N_{Body}$  if  $N_{BodyMod} > 1$ ] [MAKE SURE THE FREQUENCIES INHERENT IN THESE WAMIT FILES SPAN THE PHYSICALLY-SIGNIFICANT RANGE OF FREQUENCIES FOR THE GIVEN PLATFORM; THEY MUST CONTAIN THE ZERO- AND INFINITE-FREQUENCY LIMITS!]

1 WAMITULEN - Characteristic body length scale used to redimensionalize WAMIT output (meters) [1 to  $N_{Body}$  if  $N_{BodyMod} > 1$ ] [only used when  $PotMod=1$ ]

0.0 PtfmRefxt - The xt offset of the body reference point(s) from (0,0,0) (meters) [1 to  $N_{Body}$ ] [only used when  $PotMod=1$ ]

0.0 PtfmRefyt - The yt offset of the body reference point(s) from (0,0,0) (meters) [1 to  $N_{Body}$ ] [only used when  $PotMod=1$ ]

0.0 PtfmRefzt - The zt offset of the body reference point(s) from (0,0,0) (meters) [1 to  $N_{Body}$ ] [only used when  $PotMod=1$ . If  $N_{BodyMod}=2$ ,  $PtfmRefzt=0.0$ ]

0.0 PtfmRefztRot - The rotation about zt of the body reference frame(s) from xt/yt (degrees) [1 to  $N_{Body}$ ] [only used when  $PotMod=1$ ]

13917 PtfmVol0 - Displaced volume of water when the body is in its undisplaced position ( $m^3$ ) [1 to  $N_{Body}$ ] [only used when  $PotMod=1$ ; USE THE SAME VALUE COMPUTED BY WAMIT AS OUTPUT IN THE .OUT FILE!]

0.0 PtfmCOBxt - The xt offset of the center of buoyancy (COB) from (0,0) (meters) [1 to  $N_{Body}$ ] [only used when  $PotMod=1$ ]

0.0 PtfmCOByt - The yt offset of the center of buoyancy (COB) from (0,0) (meters) [1 to  $N_{Body}$ ] [only used when  $PotMod=1$ ]

----- 2ND-ORDER FLOATING PLATFORM FORCES ----- [unused with  $WaveMod=0$  or 6, or  $PotMod=0$  or 2]

0 MnDrift - Mean-drift 2nd-order forces computed  
{0: None; [7, 8, 9, 10, 11, or 12]: WAMIT file to use} [Only one of MnDrift, NewmanApp, or DiffQTF can be non-zero. If  $N_{Body} > 1$ ,  $MnDrift /= 8$ ]

0 NewmanApp - Mean- and slow-drift 2nd-order forces computed with Newman's approximation {0: None; [7, 8, 9, 10, 11, or 12]: WAMIT file to use} [Only one of MnDrift, NewmanApp, or DiffQTF can be non-zero. If  $N_{Body} > 1$ ,  $NewmanApp /= 8$ . Used only when  $WaveDirMod=0$ ]

0 DiffQTF - Full difference-frequency 2nd-order forces computed with full QTF {0: None; [10, 11, or 12]: WAMIT file to use} [Only one of MnDrift, NewmanApp, or DiffQTF can be non-zero]

0 SumQTF - Full summation -frequency 2nd-order forces computed with full QTF {0: None; [10, 11, or 12]: WAMIT file to use}

----- PLATFORM ADDITIONAL STIFFNESS AND DAMPING ----- [unused with  $PotMod=0$  or 2]

0 AddF0 - Additional preload (N, N-m) [If  $N_{BodyMod}=1$ , one size  $6 \times N_{Body}$  x 1 vector; if  $N_{BodyMod} > 1$ ,  $N_{Body}$  size  $6 \times 1$  vectors]

0

0

0

0

0

0 0 0 0 0 0

AddCLin - Additional linear stiffness (N/m, N/rad, N-m/m, N-m/rad)  
[If  $N_{BodyMod}=1$ , one size  $6 \times N_{Body}$  x  $6 \times N_{Body}$  matrix; if  $N_{BodyMod} > 1$ ,  $N_{Body}$  size  $6 \times 6$  matrices]

0	0	0	0	0	0
0	0	0	0	0	0
0	0	0	0	0	0
0	0	0	0	0	0
0	0	0	0	0	0
0	0	0	0	0	0

AddBLin - Additional linear damping(N/(m/s), N/(rad/s), N-m/(m/s), N-m/(rad/s))  
 [If NBodyMod=1, one size 6\*NBody x 6\*NBody matrix; if NBodyMod>1, NBody size 6 x 6 matrices]

0	0	0	0	0	0
0	0	0	0	0	0
0	0	0	0	0	0
0	0	0	0	0	0
0	0	0	0	0	0
0	0	0	0	0	0

AddBQuad - Additional quadratic drag(N/(m/s)^2, N/(rad/s)^2, N-m(m/s)^2, N-m/(rad/s)^2)  
 [If NBodyMod=1, one size 6\*NBody x 6\*NBody matrix; if NBodyMod>1, NBody size 6 x 6 matrices]

0	0	0	0	0	0
0	0	0	0	0	0
0	0	0	0	0	0
0	0	0	0	0	0
0	0	0	0	0	0
0	0	0	0	0	0

----- AXIAL COEFFICIENTS -----

2		NAXCoef		- Number of axial coefficients (-)	
AxCoefID	AxCd	AxCa	AxCp		
(-)	(-)	(-)	(-)		
1	0.00	0.00	1.00		
2	9.60	0.00	1.00		

----- MEMBER JOINTS -----

44 NJoints - Number of joints (-) [must be exactly 0 or at least 2]

JointID	Jointxi	Jointyi	Jointzi	JointAxID	JointOvrlp	[JointOvrlp= 0: do nothing at joint, 1: eliminate overlaps by calculating super member]
(-)	(m)	(m)	(m)	(-)	(switch)	
1	0.00000	0.00000	-20.00000	1	0	
2	0.00000	0.00000	10.00000	1	0	
3	14.43376	25.00000	-14.00000	1	0	
4	14.43376	25.00000	12.00000	1	0	
5	-28.86751	0.00000	-14.00000	1	0	
6	-28.86751	0.00000	12.00000	1	0	
7	14.43376	-25.00000	-14.00000	1	0	
8	14.43376	-25.00000	12.00000	1	0	
9	14.43375	25.00000	-20.00000	2	0	
10	-28.86750	0.00000	-20.00000	2	0	
11	14.43375	-25.00000	-20.00000	2	0	
12	9.23760	22.00000	10.00000	1	0	
13	-23.67130	3.00000	10.00000	1	0	
14	-23.67130	-3.00000	10.00000	1	0	
15	9.23760	-22.00000	10.00000	1	0	
16	14.43375	-19.00000	10.00000	1	0	
17	14.43375	19.00000	10.00000	1	0	
18	4.04145	19.00000	-17.00000	1	0	
19	-18.47520	6.00000	-17.00000	1	0	
20	-18.47520	-6.00000	-17.00000	1	0	
21	4.04145	-19.00000	-17.00000	1	0	
22	14.43375	-13.00000	-17.00000	1	0	
23	14.43375	13.00000	-17.00000	1	0	

24	1.62500	2.81500	10.00000	1	0
25	11.43376	19.80385	10.00000	1	0
26	-3.25000	0.00000	10.00000	1	0
27	-22.87000	0.00000	10.00000	1	0
28	1.62500	-2.81500	10.00000	1	0
29	11.43376	-19.80385	10.00000	1	0
30	1.62500	2.81500	-17.00000	1	0
31	8.43376	14.60770	-17.00000	1	0
32	-3.25000	0.00000	-17.00000	1	0
33	-16.87000	0.00000	-17.00000	1	0
34	1.62500	-2.81500	-17.00000	1	0
35	8.43376	-14.60770	-17.00000	1	0
36	1.62500	2.81500	-16.20000	1	0
37	11.43376	19.80385	9.13000	1	0
38	-3.25000	0.00000	-16.20000	1	0
39	-22.87000	0.00000	9.13000	1	0
40	1.62500	-2.81500	-16.20000	1	0
41	11.43376	-19.80385	9.13000	1	0
42	14.43376	25.00000	-19.94000	1	0
43	-28.86751	0.00000	-19.94000	1	0
44	14.43376	-25.00000	-19.94000	1	0

----- MEMBER CROSS-SECTION PROPERTIES -----  
 4 NPropSets - Number of member property sets (-)

PropSetID	PropD	PropThck	
(-)	(m)	(m)	
1	6.50000	0.03000	! Main Column
2	12.00000	0.06000	! Upper Columns
3	24.00000	0.06000	! Base Columns
4	1.60000	0.01750	! Pontoons

----- SIMPLE HYDRODYNAMIC COEFFICIENTS (model 1) -----

SimplCd	SimplCdMG	SimplCa	SimplCaMG	SimplCp	SimplCpMG	SimplAxCd
SimplAxCdMG	SimplAxCa	SimplAxCaMG	SimplAxCp	SimplAxCpMG		
(-)	(-)	(-)	(-)	(-)	(-)	(-)
0.00	0.00	0.00	0.00	0.00	1.00	0.00
0.00	0.00	0.00	1.00	1.00	1.00	1.00

----- DEPTH-BASED HYDRODYNAMIC COEFFICIENTS (model 2) -----

Dpth	DpthCd	DpthCdMG	DpthCa	DpthCaMG	DpthCp	DpthCpMG	DpthAxCd
DpthAxCdMG	DpthAxCa	DpthAxCaMG	DpthAxCp	DpthAxCpMG			
(m)	(-)	(-)	(-)	(-)	(-)	(-)	(-)
(-)	(-)	(-)	(-)	(-)	(-)	(-)	(-)

----- MEMBER-BASED HYDRODYNAMIC COEFFICIENTS (model 3) -----

MemberID	MemberCd1	MemberCd2	MemberCdMG1	MemberCdMG2	MemberCa1	MemberCa2
MemberCa2	MemberCaMG1	MemberCaMG2	MemberCp1	MemberCp2	MemberCpMG1	MemberCpMG2
MemberAxCa2	MemberAxCaMG1	MemberAxCaMG2	MemberAxCp1	MemberAxCp2	MemberAxCpMG1	MemberAxCpMG2
MemberAxCpMG2						
(-)	(-)	(-)	(-)	(-)	(-)	(-)
(-)	(-)	(-)	(-)	(-)	(-)	(-)
(-)	(-)	(-)	(-)	(-)	(-)	(-)
(-)	(-)	(-)	(-)	(-)	(-)	(-)
1	0.56	0.56	0.00	0.00	0.00	0.00
0.00	0.00	0.00	0.00	0.00	0.00	0.00
0.00	0.00	0.00	0.00	0.00	0.00	0.00
0.00	0.00	0.00	0.00	0.00	0.00	0.00

! Main Column



0.00	0.00	0.00	0.00	0.00	0.00	0.00
0.00	0.00	0.00	0.00	0.00	! Delta Pontoon, Lower 3	
14	0.63	0.63	0.00	0.00	0.00	0.00
0.00	0.00	0.00	0.00	0.00	0.00	0.00
0.00	0.00	0.00	0.00	0.00	0.00	0.00
0.00	0.00	0.00	0.00	0.00	! Y Pontoon, Upper 1	
15	0.63	0.63	0.00	0.00	0.00	0.00
0.00	0.00	0.00	0.00	0.00	0.00	0.00
0.00	0.00	0.00	0.00	0.00	0.00	0.00
0.00	0.00	0.00	0.00	0.00	! Y Pontoon, Upper 2	
16	0.63	0.63	0.00	0.00	0.00	0.00
0.00	0.00	0.00	0.00	0.00	0.00	0.00
0.00	0.00	0.00	0.00	0.00	0.00	0.00
0.00	0.00	0.00	0.00	0.00	! Y Pontoon, Upper 3	
17	0.63	0.63	0.00	0.00	0.00	0.00
0.00	0.00	0.00	0.00	0.00	0.00	0.00
0.00	0.00	0.00	0.00	0.00	0.00	0.00
0.00	0.00	0.00	0.00	0.00	! Y Pontoon, Lower 1	
18	0.63	0.63	0.00	0.00	0.00	0.00
0.00	0.00	0.00	0.00	0.00	0.00	0.00
0.00	0.00	0.00	0.00	0.00	0.00	0.00
0.00	0.00	0.00	0.00	0.00	! Y Pontoon, Lower 2	
19	0.63	0.63	0.00	0.00	0.00	0.00
0.00	0.00	0.00	0.00	0.00	0.00	0.00
0.00	0.00	0.00	0.00	0.00	0.00	0.00
0.00	0.00	0.00	0.00	0.00	! Y Pontoon, Lower 3	
20	0.63	0.63	0.00	0.00	0.00	0.00
0.00	0.00	0.00	0.00	0.00	0.00	0.00
0.00	0.00	0.00	0.00	0.00	0.00	0.00
0.00	0.00	0.00	0.00	0.00	! Cross Brace 1	
21	0.63	0.63	0.00	0.00	0.00	0.00
0.00	0.00	0.00	0.00	0.00	0.00	0.00
0.00	0.00	0.00	0.00	0.00	0.00	0.00
0.00	0.00	0.00	0.00	0.00	! Cross Brace 2	
22	0.63	0.63	0.00	0.00	0.00	0.00
0.00	0.00	0.00	0.00	0.00	0.00	0.00
0.00	0.00	0.00	0.00	0.00	0.00	0.00
0.00	0.00	0.00	0.00	0.00	! Cross Brace 3	

----- MEMBERS -----

MemberID	MJointID1	MJointID2	MPropSetID1	MPropSetID2	MDivSize	MCoefMod	PropPot
25	NMembers						- Number of members (-)
[MCoefMod=1: use simple coeff table, 2: use depth-based coeff table, 3: use member-based coeff table] [ PropPot/=0 if member is modeled with potential-flow theory]							
(-)	(-)	(-)	(-)	(-)	(m)	(switch)	(flag)
1	1	2	1	1	1.0000	3	TRUE
! Main Column							
2	3	4	2	2	1.0000	3	TRUE
! Upper Column 1							
3	5	6	2	2	1.0000	3	TRUE
! Upper Column 2							
4	7	8	2	2	1.0000	3	TRUE
! Upper Column 3							
5	42	3	3	3	1.0000	3	TRUE
! Base Column 1							
6	43	5	3	3	1.0000	3	TRUE
! Base Column 2							
7	44	7	3	3	1.0000	3	TRUE
! Base Column 3							

23	9	42	3	3	1.0000	3	TRUE
! Base column cap 1							
24	10	43	3	3	1.0000	3	TRUE
! Base column cap 2							
25	11	44	3	3	1.0000	3	TRUE
! Base column cap 3							
8	12	13	4	4	1.0000	3	TRUE
! Delta Pontoon, Upper 1							
9	14	15	4	4	1.0000	3	TRUE
! Delta Pontoon, Upper 2							
10	16	17	4	4	1.0000	3	TRUE
! Delta Pontoon, Upper 3							
11	18	19	4	4	1.0000	3	TRUE
! Delta Pontoon, Lower 1							
12	20	21	4	4	1.0000	3	TRUE
! Delta Pontoon, Lower 2							
13	22	23	4	4	1.0000	3	TRUE
! Delta Pontoon, Lower 3							
14	24	25	4	4	1.0000	3	TRUE
! Y Pontoon, Upper 1							
15	26	27	4	4	1.0000	3	TRUE
! Y Pontoon, Upper 2							
16	28	29	4	4	1.0000	3	TRUE
! Y Pontoon, Upper 3							
17	30	31	4	4	1.0000	3	TRUE
! Y Pontoon, Lower 1							
18	32	33	4	4	1.0000	3	TRUE
! Y Pontoon, Lower 2							
19	34	35	4	4	1.0000	3	TRUE
! Y Pontoon, Lower 3							
20	36	37	4	4	1.0000	3	TRUE
! Cross Brace 1							
21	38	39	4	4	1.0000	3	TRUE
! Cross Brace 2							
22	40	41	4	4	1.0000	3	TRUE
! Cross Brace 3							

----- FILLED MEMBERS -----  
 2 NFillGroups - Number of filled member groups (-) [If FillDens =  
 DEFAULT, then FillDens = WtrDens; FillFSLoc is related to MSL2SWL]

FillNumM	FillMList	FillFSLoc	FillDens
(-)	(-)	(m)	(kg/m^3)
3	2 3 4	-9.47	1025
3	5 6 7	-14.89	1025

----- MARINE GROWTH -----  
 0 NMGDepths - Number of marine-growth depths specified (-)

MGDpth	MGThck	MGDens
(m)	(m)	(kg/m^3)

----- MEMBER OUTPUT LIST -----  
 0 NMOutputs - Number of member outputs (-) [must be < 10]  
 MemberID NOutLoc NodeLocs [NOutLoc < 10; node locations are normalized distance from  
 the start of the member, and must be >=0 and <= 1] [unused if NMOutputs=0]  
 (-) (-) (-)

----- JOINT OUTPUT LIST -----  
 0 NJOutputs - Number of joint outputs [Must be < 10]  
 0 JOutLst - List of JointIDs which are to be output (-)[unused if  
 NJOutputs=0]

----- OUTPUT -----  
 True HDSum - Output a summary file [flag]

False            OutAll            - Output all user-specified member and joint loads (only at each member end, not interior locations) [flag]  
2    OutSwTch            - Output requested channels to: [1=Hydrodyn.out, 2=GlueCode.out, 3=both files]  
"E15.7e2"            OutFmt            - Output format for numerical results (quoted string) [not checked for validity!]  
"A11"            OutSFmt            - Output format for header strings (quoted string) [not checked for validity!]

----- OUTPUT CHANNELS -----  
"Wave1Elev"            - Wave elevation at the platform reference point (0, 0)

"HydroFxi"

"HydroFyi"

"HydroFzi"

"HydroMxi"

"HydroMyi"

"HydroMzi"

"B1Surge"

"B1Sway"

"B1Heave"

"B1Roll"

"B1Pitch"

"B1Yaw"

END of output channels and end of file. (the word "END" must appear in the first 3 columns of this line)

# Appendix B

## OpenFAST Modified Subroutines

### B.1 Calc\_Output

## B.2 Calc\_ConstStateDerivative

## B.3 SrvD\_\_Init\_\_Jacobian